NUMERICAL MODELLING OF LIQUID CONTAINING STRUCTURE UNDER DYNAMIC LOADING

A THESIS
SUBMITTED TO THE FACULTY OF GRADUATE AND POSTDOCTORAL STUDIES IN PARTIAL FULFILLMENT OF THE REQUIREMENTS FOR THE

DEGREE OF MASTER OF APPLIED SCIENCE IN CIVIL ENGINEERING

By

ADEL BARAKATI

ACADEMIC ADVISORS:

Dr. ABDOLMAJID MOHAMMADIAN (University of Ottawa)

Dr. REZA KIANOUSH (Ryerson University)

Department of Civil Engineering
UNIVERSITY OF OTTAWA
OTTAWA, ONTARIO,
CANADA

The M.A.Sc. in Civil Engineering is a joint program with Carleton University administered by the Ottawa-Carleton Institute for Civil Engineering

uOttawa

L'Université canadienne
Canada's university

Abstract

Liquid containing tanks (LCTs) are used in water distribution systems and in the industry for storing water, toxic and flammable liquids and are expected to be functional after severe earthquakes. The failure of a large tank during seismic excitation has implications far beyond the economic value of the tanks and their contents. Then seismic design becomes a high necessity for this type of structure.

However, tanks differ from buildings in two ways: first, during seismic excitation, the liquid inside the tank exerts a hydrodynamic force on tank walls, base, and roof in addition to the hydrostatic forces. Second, LCTs are generally required to remain watertight. Many current standards and guidelines such as ACI 350.3-06, ACI 371R-08, ASCE7, API650, EUROCODE8 and NZSEE 1986 code, cover seismic designs which are based primarily on theoretical analysis. This analysis is still not enough to fully describe the behavior of this structure under seismic oscillation noting that the theoretical analysis is based on a linear model and two dimensional spaces. So the focus of this study is to measure two important dynamic parameters which are the natural period and the maximum sloshing height of the water under harmonic motion by conducting an experimental investigation and computational fluid dynamic (CFD) simulation. OpenFoam is the numerical tool chosen in this study. There is currently no study done with this tool to measure the behavior of the water inside a square tank neither under seismic motion nor harmonic oscillation.

Finally, a comparison between the experimental, the analytical and the numerical results will be presented to confirm the level of validity of each method. Then a conclusion is made to summarize this research and to propose future works.

Résumé

Les réservoirs de stockage des liquides sont utilisés dans les systèmes de distribution d'eau potable et dans les industries pour le stockage de l'eau, des liquides toxiques et des liquides inflammables. Ces réservoirs sont conçus d'être fonctionnelle après les sévères tremblements de terre. La défaillance d'un grand réservoir lors de l'excitation sismique a des implications au-delà de la valeur économique des réservoirs et de leurs contenus. Pour cela, la conception parasismique devient d'une haute nécessité pour ce type de structure.

Cependant, les réservoirs diffèrent de la structure d'édifices en deux points: premièrement, lors de l'excitation sismique, le liquide à l'intérieur du réservoir exerce une force hydrodynamique sur les murs, sur la base et sur le toit du réservoir. Deuxièmement, ces réservoirs sont généralement moins ductiles et ont une faible redondance par rapport aux structures des bâtiments. Plusieurs codes de conception reliée à ce type de structure telle que ACI 350,3 -06, ACI 371R-08, ASCE7, API650, EUROCODE8 et NZSEE 1986, couvrent la conception parasismique de ce type de structures, qui sont basées principalement sur l'analyse théorique. Malheureusement cette analyse n'est pas toujours suffisante pour décrire efficacement le comportement de ces structures au cours des oscillations sismique. Puisque généralement l'analyse théorique est basée sur le modèle linéaire et l'espace de deux dimensions. Donc, l'objectif de cette étude dynamique est de mesurer deux paramètres importants, qui sont la période naturelle et la hauteur maximale de ballottement de l'eau sous l'action d'un certain mouvement harmonique du réservoir. Cette étude consiste à mener une investigation expérimentale et une simulation numérique. OpenFoam était l'outil numérique choisi dans cette

étude. Il n'y a actuellement aucune étude faite avec cet outil pour mesurer le comportement de l'eau dans un réservoir à base carré sous l'action d'un mouvement séismique ou harmonique.

Enfin, une comparaison entre les résultats théoriques, expérimentaux, et numériques sera présentée pour confirmer le niveau de validité de chaque méthode. Ensuite, une conclusion est élaborée pour résumer cette recherche et proposer des recommandations relatives à des recherches futures.

Remerciements

Tout d'abord, je tiens à remercier mon Dieu qui m'a donné l'occasion, la puissance et la patience de terminer ce travail et me garder en bonne santé.

Je veux aussi présenter mes reconnaissances particulières à mon superviseur Dr. Majid Mohammadian pour son aide et son soutien tout au long de ma carrière universitaire. Dr Mohammadian était toujours là quand j'ai besoin de son aide. Merci de m'aider et de me donner de votre précieuse temps pour terminer ma thèse.

Je suis également reconnaissant aussi envers Dr. Reza Kianouch Université de Ryerson pour ses commentaires et ses importants conseils.

Mes sincères remerciements aussi pour ma famille: mes parents, ma femme, mes enfants mes frères et mes sœurs pour leur encouragement et leur grand soutien.

Enfin, je tiens également à remercier tous mes enseignants, mes collègues et les personnels du département de génie civil à l'Université d'Ottawa, où j'ai passé une belle et importante partie de ma vie.

Acknowledgments

Firstly, I want to thank my God who has given me the opportunity, the power and the patience to finish this work and has kept me in good health.

I would like also to give special gratitude and thanks to my supervisor, Dr. Majid Mohammadian, for his help and support all along my academic career. Dr. Mohammadian has always been there when I need his help. Thank you for giving me your valuable time and assistance to help me complete my thesis.

I am also grateful to Dr. Reza Kianouch of Ryerson University for his important comments and advice.

My sincere thanks also to my family: my parents, my wife, my children, my sisters and my brothers for their encouragements and great support.

Finally, I also want to thank all my teachers, my colleagues and the staff in the Civil Engineering Department at University of Ottawa, where I have spent an important part of my life.

Table of Contents

List of Tables

List of Figures

List of Symbols

a	Acceleration on the fluid element $[m/s^2]$;
A	Maximum amplitude of the shaking table displacement $[m]$;
C_c	Period-dependent seismic response coefficients;
D_{max}	Freeboard (sloshing height) measured from the liquid surface at rest $[m]$;
$D_{\max(Analytical)}$	Sloshing height measured analytically $[m]$;
$D_{\max(Experimental)}$	Sloshing height measured experimentally $[m]$;
$D_{\max(Numerical)}$	Sloshing height measured numerically $[m]$;
e	Internal energy $[J]$;
f	Frequency of oscillation of the tank $[Hz]$;
F	Force on the fluid element $[N]$;
g	The acceleration of gravity $[m/s^2]$;
h	Height level of the water $[m]$;
I	Importance factor;
L	Length of the square tank $[m]$;
m	Masse of the fluid element $[kg]$;
p	Fluid pressure $[MPa]$;
S	Site profile coefficient;
t	Time $[s]$;
T	Oscillation period of the table $[s]$;
T_c	Natural period of the first (convective) mode of sloshing $[s]$;
u	Component of vector velocity field in $\vec{\imath}$ direction
v	Component of vector velocity field in $\vec{\jmath}$ direction
w	Component of vector velocity field in $\vec{k}$ direction
ω	Circular frequency of the shaking table $[rd/s]$;
ρ	Density of fluid $[kg/m^3]$;
μ	Dynamic viscosity $[N.s/m^2]$;
$\Delta_{R(A/E)}$	The relative error between the experimental and the analytical results Concerning D_{max} at the naturel period of oscillation;

$\Delta_{R\ (A/N)}$	Relative error between the experimental and the analytical results concerning D_{max}at the naturel period of oscillation;
$\Delta_{R\ (N/E)}$	Relative error between the numerical and the experimental results Concerning D_{max};

Chapter 1. Introduction

1.1. Background

As known from catastrophic events, liquid storage tanks have frequently collapsed or been heavily damaged during earthquakes all over the word. Damage or collapse of the tanks causes some unwanted events such as shortage of drinking water, uncontrolled fires and spillage of dangerous fluids (Figure 1.1). For this reason, many theoretical and experimental investigations of the dynamic behaviour of different types of liquid storage tanks have been conducted to seek possible improvements in the design of such tanks to resist earthquake excitation.

Figure 1.1 Refinery tanks in Ichira Chiba earthquake and tsunami (Japan 2011- 9.0 magnitude quake).

Liquid storage tanks are common structures in the field of civil engineering. Their number is increasing continually in the word. In civil engineering, these facilities are especially

employed in water distribution systems for municipal use for storing drinking water, most of which are used as fire-fighting systems, compressed gases (gas tank) or for oil, fuel, and ethanol storage facilities. In industry, and particularly in heavy industry, they are also used to store various kinds of liquids which can be dangerous, such as toxic or flammable products. Tanks also are used in petroleum plants and nuclear power plants and are classified as equipment requiring high seismic safety. In most cases, LCTs are required to maintain their design integrity under the influence of any disaster such as an earthquake.

During many earthquakes, a number of large tanks were severely damaged or collapsed. Thus it is vital that these structures be preserved, in order to prevent them from spreading their valuable or dangerous content, causing uncontrollable chain reactions that can cause more damage than the earthquakes themselves. Therefore, in an earthquake, some unwanted events may happen such as shortage of water or uncontrolled fires. In these cases, some reservoirs such as water reservoirs play a crucial role in the organization of first aid in the after-quake period, especially when we deal with the safety of people and their lives and with environmental protection. Many studies have been conducted since the early 1930s.The objective of these studies is to understand the dynamic comportment of the liquid containing tank in order to design it well and to limit the tank damages observed during earthquakes. Failure mechanisms reported on storage containing structures depend on different factors, and the design of these tanks will depend on the same factors. These factors include the configuration, the construction material and the supporting system. Any of these factors themselves depend on various parameters. Configuration of the tank usually depends on the usage purpose and can be circular, rectangular, square, cone-shaped or other shapes. The most common construction materials are steel and concrete. Concrete tanks can be cast-in-place, prestressed or post-tensioned. Furthermore the

method of construction also matters. The next contributing factor is the supporting system, as the tank can be elevated, anchored or unanchored into the foundation. It is worth mentioning here that LCTs are designed for serviceability, and leakage beyond the limit will be considered as a failure of the structure. Different types of failures can happen to liquid storage tanks; we can identify them by the type of material of the tanks. This is why the design depends on the tank material. The seismic design of tanks varies from that of buildings in part due to the sloshing effect of the contained fluid. Furthermore, cracking, which may be permitted in the design of buildings, is avoided in liquid containing structures to prevent leakage. Many methods of seismic analysis of tanks are currently used by researchers and have been adopted by a number of industry standards. This report provides experimental studies and theoretical backgrounds related to the liquid containing structure done in this field. Many current standards and guides such as ACI 350.3-06 and ACI 371R-08 covert seismic design. This report will also present some of these design procedures, which are based on the simplified methods evolved from earlier analytical work by Housner 1960, A.S. Veletsos 1977-1984, M.A. Haroun 1981 and Shivakuinar 1997, and others. Of these, the best known is Housner's pioneering work, published in the early1960s by the Atomic Energy Commission. Housner's method will be adopted by many codes in the world and by a number of industry standards.

1.2. Objectives and Scope of Study

Seismic design of liquid storage tanks requires knowledge of many parameters related to the dynamic response of these types of structures. Several studies already exist in this field, but much remains to be done to properly design these structures. Also, several methods have been proposed to calculate the dynamic parameters of such systems.

In general, a better understanding of the behavior of these systems and calculating their dynamic parameter can be adequately achieved by using two different approaches. The first approach involves theoretical investigation through analytical and numerical techniques. The second approach is to use experimental investigation.

The first objective of this study is to investigate some parameters that have very important effects on seismic design of LCTs. These parameters are the natural period (or the fundamental period) and the maximum sloshing height.

A series of forced vibration tests using a shaking table were conducted to illustrate and to check the effectiveness of the theoretical analysis for determining the two parameters (natural period and sloshing height). Also, it should be noted that these experimental tests and analytical analysis were done under the following assumptions:

- A small-scale model was used in this experiment.
- The tank was a closed square tank with fixed base and filled with water.
- The excitation was harmonic.
- The water was assumed to be perfect homogeneous liquid and incompressible.
- The analytical solution is based only on two dimensional analysis.

The combined use of these two methods (analytical and experimental) allows for obtaining a realistic approximation of the two parameters (naturel period and sloshing height). Once the data were collected, the OpenFoam model was used as a numerical tool to analyse the same system. If the comparison between the numerical, the theoretical and the measured results shows good agreement, we can confirm the validity of OpenFoam for determination and justification of these response parameters found by the analytical solution. Consequently, we can extend our study by

using OpenFoam to analyse more complicated excitation motions such as recorded earthquake time history or different shapes of tanks.

Furthermore the numerical model allows us to obtain results based on 3D and nonlinear analysis, which represent more realistic results. It also allows us to justify the accuracy of the analytical method in terms of resonance period and maximum sloshing height of a tank filled with a liquid (water).

In general, this study provides methods and basic information on dynamic behavior of LCTs. Such information can be used first for engineering judgment for design applications or to develop practical codes. Equally, such results can be used for research and scientific application because of the lack of sufficient data in this field of study.

1.3. Structure of the Thesis

This thesis is divided into five chapters.

Chapter 1 (the current chapter) presents an introduction to the topic, and a general overview of the behavior LCTs under seismic loading was discussed. The scope and the objectives of work are presented as well.

Chapter 2 (literature review) summarizes some of the previous research studies related to the dynamic analysis of LCTs under some specific conditions. It is divided into sections to present different types of analyses used in this field of research. The main methods of analysis described in these subsections were the numerical methods, the analytical methods and the experimental methods.

Chapter 3 presents the experimental set up, the results of the experiments, discussions and the conclusion. Special attention in this chapter was paid to studying the natural period and the sloshing behavior of the LCTs. In the discussion part, a comparison was presented between analytical and experimental results.

Chapter 4 presents the OpenFoam software to stimulate the behavior of the square tank and its related dynamic parameters such as the natural period and the liquid sloshing under harmonic oscillation. A comparison between model simulations, laboratory experiments, and analytical results is presented in this chapter.

Finally, Chapter 5 presents a summary and final conclusions obtained in this project as well as recommendations for future studies.

Chapter 2. Literature Review

2.1. Introduction

The analysis of the dynamic response of liquid containing structures under earthquake loading is associated with the fluid structure interaction domain of research. Since this domain is quite large, liquid containing structures are designed and analyzed by taking into consideration the fundamentals of liquid sloshing theory as the primary concern. Many studies have been conducted to present liquid sloshing effects in storage tanks using different methods of analysis. Among these methods, there are experimental, numerical and analytical techniques. Usually analytical solutions are restricted to regular geometric tank shapes such as cylindrical and rectangular whose walls are straight and upright. Furthermore, their fundamental equations are still not fully developed for large sloshing amplitudes, e.g., in the case of three dimensional problems. Further, the nature of sloshing dynamics in cylindrical tanks is better understood than in prismatic tanks, but for other tank geometries with variable depth, we can determine the natural frequencies and mode shapes either experimentally or numerically.

The majority of studies that have been done can be classified in different categories. These categories depend on multiple factors related to the type of tank (the shape, the material, etc.) or to the methods that will be used for the analysis (numerical, analytical, experimental, linear or nonlinear, etc.) or to the type of base connection with the foundation. This chapter will cover some of these methods applied to the design and analysis of specific shapes of tanks where some of these studies will be identified and discussed. As mentioned, the most common geometrical container shape in the world are cylindrical and rectangular shape and fewer of them are quadratic. Furthermore, there are different methods of analysis to this type of structure and some of them which are more common and more popular are cited in this section.

2.2. Numerical Modelling Methods

2.2.1. Finite Elements Methods

Edwards in 1969 completed the first use of a digital computer in analyzing LCTs, which was the first finite element method for evaluating the seismic behavior of flexible tanks. This method was used to predict the seismic stresses and displacements in a circular cylindrical liquid filled container whose height-to-diameter ratio was smaller than one. Unfortunately, only a few studies on the dynamic response of square containers exist in this field.

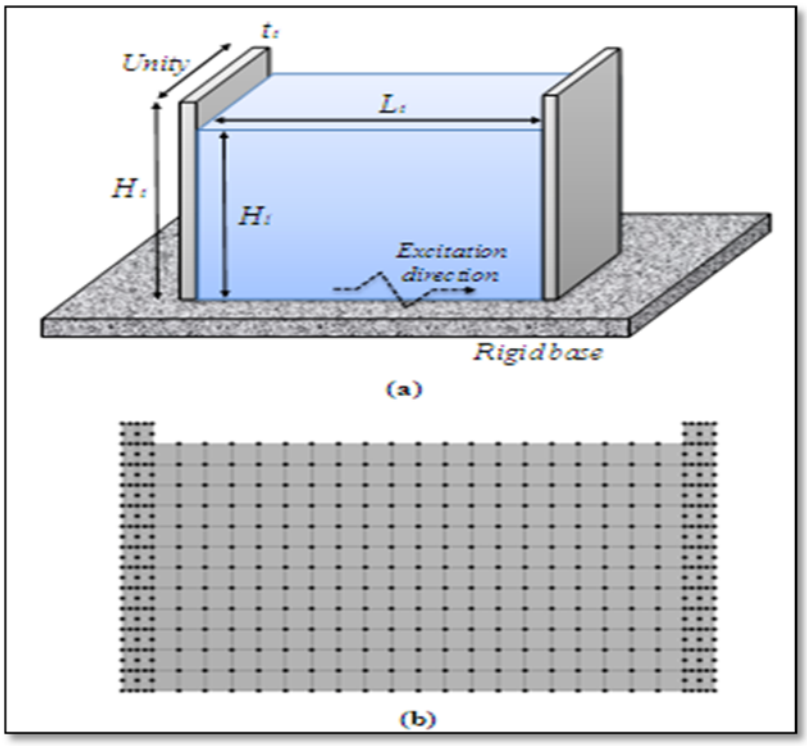

Figure 2.1: Example of two dimensional model of tank-liquid system (a) General view. (b) Finite element discretization of the coupled system (Mirzabozorg et al 2012)

Zhang and Sun (2014) studied the sloshing behavior in rectangular tanks. Some assumptions were made in this research. The fluid was assumed to be incompressible, non-rotational and inviscid water. The free surface was assumed to never become overturned or broken during the

sloshing process, when it was subjected to a translational motion along x-axis. So a 2D nonlinear motion was described in (x, z) coordinate systems, which was considered to be moving with the tank. This research was completed by analyzing the nonlinear sloshing phenomena through different methods. First, by considering the liquid as an ideal fluid, the sloshing equations were analytically and successfully derived. Second, by using a numerical process based on the potential flow theory, a finite difference method was developed after applying a σ transformation to the fluid domain. Finally, some results such as the sloshing forces and the high-frequency excitation were compared with other existing analytical and numerical solutions. Also on the same subject, Faltinsen (2010) derived a linear analytical solution for liquid sloshing in a horizontally excited 2D rectangular tank considering damping due to the additional assumption of viscous effects of the liquid.

Ikeda et al. (2012) developed Galerkin's method to derive and calculate the nonlinear modal equations of motion for sloshing in the case of a square liquid tank subjected to horizontal, narrow-band, random excitation deviated from the tank longitudinal direction by a certain angle. The method was based on the Monte Carlo simulation. The mean square responses of the predominant two sloshing modes that oscillate with different frequencies were investigated. In the theoretical analysis, the liquid was assumed to be a perfect fluid. It was also shown that the mean square responses of the modes created by direct excitation will be decreased by the one occurred by indirect excitation. This is known as auto-parametric interaction phenomena.

During an earthquake, the ground will shake in horizontal and vertical motion due to the presence of P waves and S waves. In most previous studies, the vertical component of the earthquake ground motion was neglected in the dynamic analysis of the structure.

Aslam (1981) presented a finite element analysis to predict the sloshing displacements and hydrodynamic pressures in liquid filled tanks subjected to earthquake ground motions. Finite element equations were derived using the Galerkin formulation, and the predicted results were checked against experimental data, showing a good agreement between the test and finite element results. The investigation was initiated as a result of a concern expressed by the designers of nuclear reactors regarding the sloshing response of water in pressure-suppression pools of boiling water reactors (BWR). The main objective of this study was to predict the water surface displacements and hydrodynamic pressures during an earthquake and to check the obtained analytical results with test data. This was necessary to ensure that the surface displacements were not excessive to the point of causing leakage of superheated radioactive materials. In the performed finite element analysis, the tank was assumed to be axisymmetric due to arbitrary ground motions. The flexibility of the tank was neglected, as this would have a small effect on the response because, in practice, such tanks have thick concrete walls. Also, the nonlinear sloshing problem was linearized for this analysis. The finite element equations were first derived for a completely general three dimensional problem and then were modified for an axisymmetrical tank subjected to arbitrary horizontal ground motions. The equations were derived using the Galerkin principle. This principle is a class of methods to transform a continuous problem (e.g. a differential equation) into a discrete problem. This method is commonly used in the finite element method. We start from the weak formulation of the problem. The method involves using a Galerkin mesh area of study, and considers the restriction of the function on each cell solution. A comparison was made with experimental results to verify the accuracy of the finite element results and a good agreement was found between the test and predicted results. The paper assumed that the displacements were small and the fluid was

incompressible and inviscid, the velocity potential existed at every point and satisfied to Laplace which is based on the conservation of mass. In this study case,

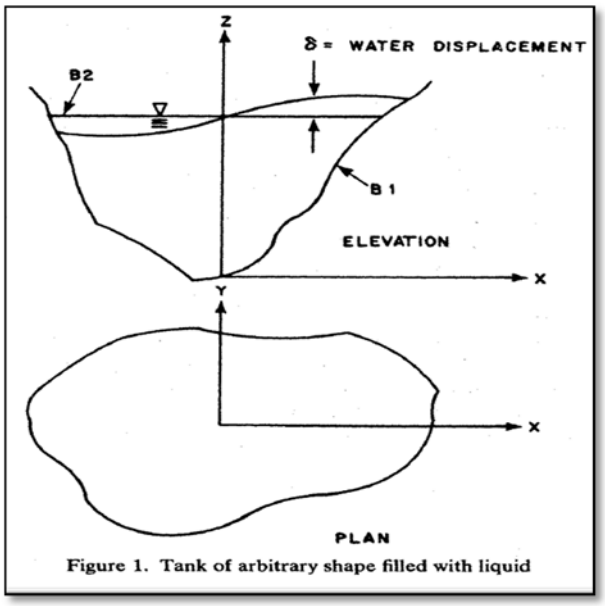

Figure 2.2: Tank of arbitrary shape filled with liquid (Aslam 1981)

a rectangular coordinate was adopted. The resulting mathematical equations represent the nonlinear free surface boundary conditions, which can be simplified and combined into one boundary condition by neglecting higher order terms. The discretization of the continuum into finite elements is completed by the implementation of finite element equations and the incorporation of the free surface. Liquid and loading element matrices result in a set of linear, coupled, second order, ordinary differential equations. Newmark's step-by-step integration method with $\beta = 1/6$, was used. A computer code was developed in which the earthquake input could either be as an accelerogram or a displacement time history digitized in the appropriate format. The program derives the velocity time history by integration or differentiation depending upon the type of ground motion input. The earthquake input must be properly adjusted for baseline correction such that at the end of earthquake, the acceleration, the ground velocity and the displacement vanish. The 'effective' equilibrium equations were solved using the linear

equation solver COMSOL, and the sloshing displacements and hydrodynamic impulse pressures at time t and t+Δt were determined. To validate the results obtained from the finite element analysis, an annular tank was chosen to conduct the experiment. To simulate the earthquake motions, a 20' x 20' 'shaking table was accelerated by time-responses histories similar to the El Centro 1940 earthquake. The study showed that there is close agreement between the test and finite element results under the same ground motion limited to the annular and cylindrical tanks. These results dealt with the sloshing response and the impulsive pressure. The technique presented in the study could successfully predict the sloshing displacements and hydrodynamic pressures in fluid-filled rigid tanks under arbitrary ground motions. The linearized small displacement theory was found to be satisfactory for predicting the sloshing response in pressure-suppression pools of BWRs due to strong earthquake motions.

Kyung-Hwan Cho et al (2007) established a general numerical algorithm for the analysis of the seismic responses of a cylindrical steel liquid storage tank in a three dimensional coordinate system, and a dynamic response analysis was performed. The liquid content was assumed to be inviscid and incompressible; and the flow of the liquid was assumed to be irrotational for simplicity. To overcome the limitations of the boundary and finite element methods and to accurately evaluate the seismic response of the cylindrical steel liquid storage tanks, the authors used a coupling method that combined the finite elements and the boundary elements (referred to as the FE-BE method). This coupled dynamic system considers fluid structure interaction effects and sloshing of the free surface. The finite elements for the structure and the boundary elements for the liquid were coupled using the equilibrium condition and the compatibility condition. To satisfy the compatibility condition, the nodal displacement vector was divided into the displacement vector of the wet nodes and the dry nodes. Two models that

have different aspect ratios were used for the analyses: a tall tank and a wide tank. Using the boundary element method (BEM), the linear partial differential equations which have been formulated as integral equations (i.e. in boundary integral form)) were solved to obtain the sloshing frequencies of the free surface and natural frequencies of the fluid structure interaction system. The governing equations of the liquid motion were represented by the Laplace equation and the boundary integral equation derived from the Lagrange-Green Identity. The natural frequencies of the free surface sloshing and the corresponding mode shapes were compared with the analytical solutions reported by Abramson (1966). However, the effect of fluid structure interaction described by the corresponding frequency was compared with the results achieved by Haroun and Housner (1982). The modal and seismic analysis results calculated using the proposed method were in reasonable agreement with published results. The structure was modelled from finite degenerated curved shell elements, which could easily model the arbitrary shape of the external structure. This was because the rigid tank concept could not be retained for the modelling of tanks because real steel tanks deform significantly under earthquake loads. Indeed, only the tank base was assumed to be fixed to a rigid foundation and, consequently, the nodes of the tank bottom were assumed to have had a specified acceleration equal to the ground acceleration (similar to the North-South component of the 1940 El Centro earthquake that had a peak acceleration of 0.348 g). The Rayleigh damping coefficient was taken as 2% damping for the flexible-impulsive interaction modes and 0.5% damping for the sloshing modes. In this study, all of the seismic responses presented by the Displacement, Moment, Shear, Sloshing and Fundamental hydrodynamic pressure distributions were investigated for both types of tanks (tall and broad) and were also compared with the previous results of Abramson 1966 and Haroun 1983. In addition, it was found that the responses of a flexible tank were much greater than those

of a rigid one, and it was also discovered that the flexibility of the tank wall had a significant effect on the dynamic response of both tall and wide tanks. It was observed that the maximum values of the sloshing height were much greater than those calculated using Haroun's method, which considered only one sloshing mode (see Figure 2.3). Therefore, it was concluded that to obtain an accurate sloshing height, a sufficient number of sloshing modes must be considered.

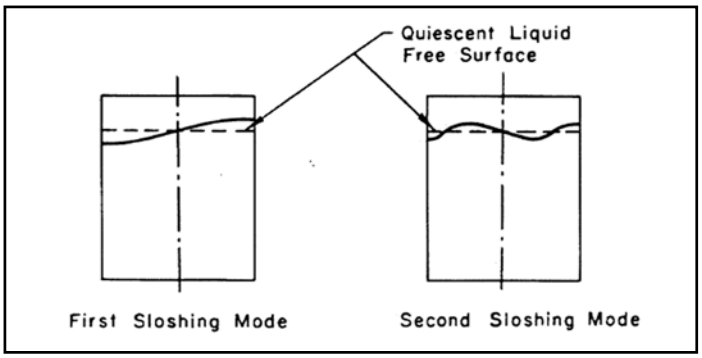

Figure 2.3: Sloshing modes in rigid tanks (Haroun 1980)

2.2.2 Boundary Element Methods (BEM)

Chen et al. (2007) performed extensive research studies about sloshing behaviors of rectangular and cylindrical tanks subjected to harmonic and seismic excitations. They presented a numerical analysis of such tanks based on Boundary Element Methods (BEM) and second order Taylor Series Expansion (TSE). They adopted this method to simulate a nonlinear sloshing problem in three dimensional space. To present the sloshing characteristics, some assumption were taken into consideration. The rectangular and cylindrical tanks were assumed to be rigid and fixed to the ground. The liquid inside the tank satisfies the assumptions of potential flow: inviscid, incompressible, and irrotational. The excitation was limited to a single horizontal motion. Two types of motion were used in this study: harmonic oscillations and two earthquake records related to Chi-Chi (Taiwan 1999) and Kobe (Japan 1995). The objective of this research was to

calculate two physical quantities: the transient wave elevation, and the base shear forces at different frequencies in the presence of the sloshing phenomenon. Those frequencies are chosen to be under-resonant, resonant, and over-resonant frequencies, and the resonant frequencies were calculated using the linear wave theory of the first natural frequency ($\omega_1 = \sqrt{\frac{\pi g}{L} tanh \frac{\pi h}{L}}$). In order to validate the numerical results, an experimental test of a small-scaled tank was carried out and a shake table was used to stimulate the excitation motion. It was concluded that the shear base force values are close to the difference of pressure forces at two sides of the lateral walls (named as the hydrostatic force) when the excited frequency is not much higher (lower or close) than the first fundamental frequency of the tank and when the amplitude of motion is small enough. However, when the excited frequency is higher or much higher than the fundamental frequency, the force from the hydrostatic pressure formula is no longer valid to predict the base shear force, and the hydrodynamic pressure can take important and significant values. In that case, the base force is dominated by the inertial force (impulsive component) due to the weak effects of the convective component. It is also observed that the wave amplitude grows with time, which is a characteristic behavior of resonance.

2.2.3. Numerical Schemes in 3D

Wu et al (2012) developed a numerical scheme to be used for a 3 D study of an excited tank sitting on the ground. This study covered a 3D motion considering six degrees of freedom. The 3D analysis is more expensive and complicated than 2D methods. For this case, it has been relatively ignored by most studies in the literature. Under an earthquake excitation, or for a tank floating on the sea, the excitation direction can combine multiple degrees of freedom, including surge, sway, heave, pitch, roll and yaw (see Figure 2.4). Therefore, the wave motion in a three

dimensional tank presents more components than a two dimensional tank. This study also showed that it was possible to determine the sloshing mode of a square base tank simply by solving the linearized natural sloshing standing wave problem when the tank is excited by a time history period related to an event earthquake. The natural modes of a 3-D tank with a square base can be obtained by solving the linearized natural sloshing standing wave problem.

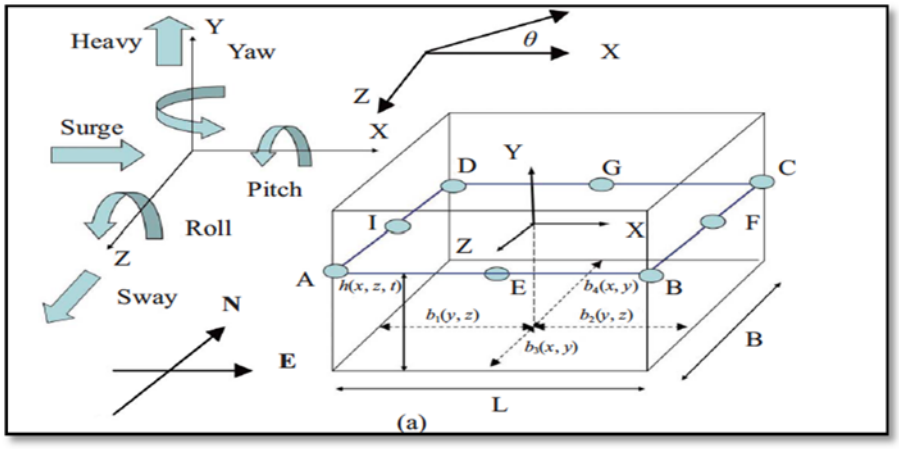

Figure 2.4: Sketch of different excitation directions (Wu et al 2012)

Instead of including six degrees of freedom, as shown in Figure 2.4 in the present study, only two of them are presented to stimulate a coupled surge-sway model. It is also concluded that, for a strong shallow-fluid sloshing and large excitation amplitude, the numerical simulations failed to satisfactorily reproduce measured data and the used simulations were beyond the current capability of the model chosen. Also it was demonstrated in this study that if the tank was excited in the longitudinal direction ((θ=0°) or by diagonal motion (θ= 45°) with respect to the horizontal ground motion, four waves can be expected: planar waves, swirling waves, irregular waves and square-like waves. The phenomenon of square-like waves corresponds to waves travelling primarily on two opposite sides of the tank.

Faltisen et al. (2003) studied and discussed square-like waves for a tank excited at near-

resonant conditions. With visual observation, they showed that square-like waves can be found when the tank is excited at non-resonant frequencies and the three dimensional waves are only observed when the tank is under near-resonant excitation.

For practical engineering applications, for example in a tank excited by a real earthquake, the ground motion will be a complex combination of surge, sway, heave, pitch, yaw and roll, and it may vary with time. Faltisen et al. (2003) identified other types of waves that can appear and characterize the free surface during its sloshing. These waves are called diagonal waves. They can be identified when they are travelling in a diagonal direction. Faltisen et al. (2003) also demonstrated that the diagonal waves can be found at different periods of excitation when (θ = 45°). However, if the tank is accelerated at other angles ($\theta \neq 45°$), the diagonal waves disappear. This is unlike the horizontal excitation. When ($\theta = 0°$), the diagonal waves can be observed only when the periods are far from the first natural frequency.

2.2.4. Numerical Analysis of Resonance Between Liquid in a Tank and the Ground Motions

Vakilaad Sarabi, A. and Miyajima, M. (2012) studied the effect of ground motions inside a sloshing tank. They used the VOF method (Volume of Fluid method) to describe the water displacement and to validate and compare the results. The main focus of this study was to obtain the effects of the period and the duration of the seismic motion on the sloshing phenomena in water tanks. The liquid was assumed to be irrotational, invicid and incompressible and to be inside a rigid container. The study emphasized the importance of considering the long duration ground motions and the long period to effectively predict the dynamic response of liquid tanks. In that study, the volume of liquid in the tank was divided into two parts. The first part was located in the lower level of the tank, which moves with the same speed as the tank. This mass of

water developed a hydrodynamic pressure proportional to the acceleration of the tank. The second part is the upper part of the volume of the liquid, which represents the free surface of liquid in motion. This part elaborates a component called convective pressure. Some important points were mentioned in this study about the sloshing subject, as described below:

- Sloshing in liquid tanks occurs depending on the dimension of tanks and the water height. Also, the severity of sloshing and its dynamic pressure load depend on the tank geometry, the depth of the liquid, the amplitude and the nature of the tank motions. Also sloshing depend on the frequency of excitation when it's close to the range of the natural frequency of the fluid.
- Sloshing is a difficult mathematical problem to solve analytically. Thus analytical methods are restricted to small motions of the sloshing fluid. It is also noted that the methods developed in the previous studies of sloshing fluid motion inside the tanks have been represented with mathematical equations such as Laplace, Euler, wave or Navier-Stokes. This equation can be solved using numerical methods such as the boundary element method (BEM), the finite difference method (FDM) or the finite element method (FEM).
- The liquid height can play an important role on the liquid behavior during sloshing. For a shallow liquid height, hydraulic jumps and travelling waves will be created when the frequencies of the motion is close to the resonance of the liquid. Therefore, the walls will be subjected to higher intensity of pressure. At the same range of frequencies and in the case of higher water depths, large standing waves are formed through the free surface.
- Since 1953, the modelling of the sloshing phenomena (initiated by Morse and Fesbach) has evolved around the world. However, it is still imprecise in some aspects and requires further research with respect to the determination of the natural period.

- Long period ground motions depend on the following parameters of earthquake: the magnitude, the epicentre location and the geological structure through which seismic waves propagate.
- The ground motion source is considered as a parameter based on the period of motion. Two types of motions were identified: the far-from-source long period ground motion and the near-fault long period ground motion. They can be identified by their duration. The duration of long period ground motion can continue for 1 min or longer, whereas the near-fault long period ground motions last only for 10 to 20 seconds.

2.3. Analytical Methods

2.3.1. Simplified Analytical Models

Housner (1963) examined the sloshing dynamics under horizontal excitation for circular and rectangular rigid tanks using an analytical approach. The idea was to present the dynamic analysis of such tanks by taking into account that the motion of the water is relative to the tank, and the motion of the tank is proportional to the ground excitation. In case a tank has a free surface, Housner observed that in certain parts of the tank structure, the sloshing of the water was the dominant factor, whereas for other parts, the sloshing had a small effect. For this study, he separated the hydrodynamic pressure into convective and impulsive components. The impulsive component is the portion of the contained liquid that moves simultaneously with tank structure and the convective component is the portion of the liquid that experiences sloshing. A single degree of freedom oscillator was proposed to model the convective component (Figure 2.5). The proprieties of this mechanically analogous system can be computed from the geometry of the tank and the characteristics of the contained liquid. This technique can provide the values of

convective and impulsive masses and their locations and presents the forces and the moments exerted by the liquid on the tank. In this model, fluid is assumed incompressible which means its volume remains constant under the action of external pressure. Housner's theory is indeed a simplified method of analysis. It has served as a guideline for most seismic designs of liquid storage tanks. However, failures of liquid storage tanks during past earthquakes suggested that Housner's theory might be conservative and needs certain modifications.

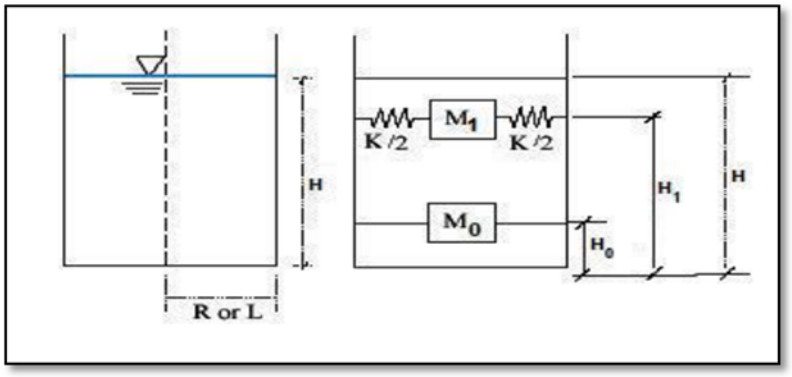

Figure 2.5: Mechanical model related to simplified method (Housner 1963)

2.3.2. More Detailed Analytical Models

Kianoush and Chen (2005) studied the response of concrete rectangular storage tanks while considering the importance of the vertical component of ground motion because of their higher records obtained at the near-field region of earthquake and the associated destruction of structures observed. In most design codes such as ASCE7-05, the responses due to the vertical motion (referred to as "V") are taken into consideration by only reducing the horizontal spectra ("H") to two thirds. Many assumptions are made in this study. First, the liquid is assumed to be incompressible, inviscid (no viscosity). At the liquid free surface, the hydrodynamic pressure is zero, the vertical velocity on the rigid base of the tank is equal to the vertical ground velocity

and, finally, at the interface of the liquid and the flexible walls, the boundary conditions must satisfy the compatibility along the height of the wall. This study was based on the combination of the added mass method and the sequential method. The wall of the tank was considered to be flexible. An analytical equation was developed in this study. The hydrodynamic pressure computed based on the first part of the equation was due to the vertical excitation based on the assumption of rigid walls. The second part was related to the horizontal hydrodynamic pressure corresponding to the transverse vibration of the flexible wall due to the vertical ground motion, which was treated separately from the first part. Similar to the horizontal ground motion, the vertical ground acceleration can lead to hydrodynamic pressures transmitted into the tank wall. Thus, the wall of the tank undergoes horizontal displacement in addition to the axial displacement due to the vertical excitation. As the transverse vibration of the flexible wall can be significant, the dynamic response of liquid storage tanks in the horizontal direction due to the vertical excitation was also investigated in this study. The FEM used in the analysis took two different models (Figure 2.6 (a): Model 1 – Figure 2.6 (b): Model 2) and assumed a two dimensional condition for the tank wall. The wall was considered to be fixed at the base and free at the top. The walls parallel to the direction of the horizontal ground motion were assumed to be rigid and also to have no significant effect on the flexibility of the other two walls on which hydrodynamic pressures are applied. It should be noted that at the wall edges, the effect may be different, but under 2D analysis, it is not possible to study this effect. So a 3D analysis was used to study the edge effects for different tanks dimensions.

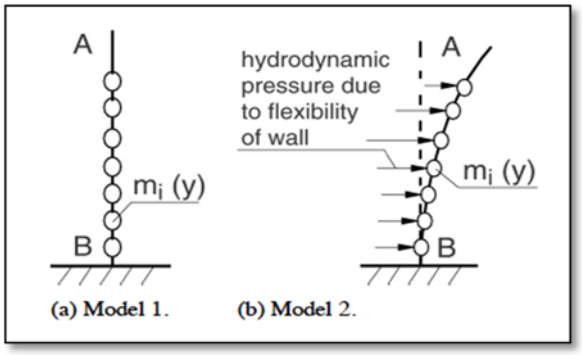

Figure 2.6: Models used in the analysis for vertical ground motion Kianoush and Chen (2005).

A tall tank and a shallow tank of rectangular shape were analysed. In model 1, the effect of tank flexibility was ignored in the calculation of hydrodynamic pressures, while, in model 2, this effect was included. Two realistic time history responses were used in this analysis corresponding to the vertical components of the 1940 El Centro Earthquake (Imperial Valley) and the 1994 Northridge Earthquake (Sylmar Hospital). The sequential method was applied in the dynamic analysis of the second model. In this technique, the two fields of liquid and structure were coupled applying the results from the previous steps as loads or boundary conditions for the current step. The sequential method is a technique in which the two fields of fluid and structure are coupled by applying results from the first analysis as loads or boundary conditions for the second analysis. Basically, the dynamic response of the liquid storage tank must be solved by a "strong" coupled method, by which the data must be transferred or shared between at each step of the solution to maintain accuracy of dynamic response analysis. The sequential method is carried out by the following procedure. First, the dynamic response of the flexible tank wall subjected to an earthquake is analysed at time step "t". Then, the hydrodynamic pressure is determined, which also includes the effect of flexibility of the tank wall. Finally the hydrodynamic pressure is applied on the tank wall at the next time step $t+\Delta t$. The procedure is then repeated at each time step until the analysis is complete.

Since the maximum response due to vertical and horizontal ground motions may not occur simultaneously, it is common practice to use the Square Root of the Sum of the Squares (SRSS) method to include both effects. This procedure is used in ACI 350.3 in the design of concrete liquid containing structures. As both the horizontal and vertical accelerations can induce transverse vibration, the total dynamic response of the tank is calculated by the summation of the two responses corresponding to each time step. In this study, only model 2, which is the combination of the added mass and the sequential method, was used. This study presented the displacement-time history at the top of the tank wall due to the combination of horizontal and vertical ground motions, so the combined response resulting from both horizontal and vertical ground accelerations was calculated separately based on time history analysis. The results in this study showed that in most cases, the hydrodynamic pressure due to the horizontal ground acceleration is more significant than that of vertical ground acceleration. However, this does not indicate that the effect of vertical acceleration could be neglected in the dynamic analysis of liquid storage tanks. If a near-field earthquake record is used in the analysis, this effect may be even more significant when compared with the response due to horizontal ground motion. In this paper, the dynamic response of concrete liquid rectangular tanks subjected to the vertical ground motion is discussed. The hydrodynamic pressures induced by vertical ground motions on the tank walls were determined using two different methods. In the first method, the conventional added mass approach was used, while in the second method the combination of added mass and the sequential method was used. In the latter case, the effect of the flexibility of the tank wall can be considered in the calculation of hydrodynamic pressure. It was found that the time history response of a rectangular tank including the effect of tank flexibility can be different to its counterpart, which is obtained assuming rigid wall boundary conditions. The effect of tank

flexibility can either increase or decrease the response as compared with that of rigid wall boundary conditions. The total response of the tank wall due to horizontal and vertical ground acceleration was also investigated. The direct sum of the responses obtained from the horizontal and vertical ground motions were compared with the responses obtained by that using the SRSS method. The responses obtained from the two methods were very similar. Results of analysis showed that in some cases, the maximum response due to vertical acceleration can be as high as 45% than due to the horizontal component, so the effect of the vertical component of ground motion should be considered.

In another study, Praveen et al. (2000) dealt only with the elastic analysis of fully anchored, rigidly supported tanks, without taking into consideration the effects of the foundation flexibility and base uplifting on the tank response. The procedure took into account impulsive and convective (sloshing) actions of the liquid in flexible steel or concrete tanks fixed to rigid foundations. The seismic responses such as the base shear; the overturning moment, and the sloshing wave height were determined by using the site response spectra. This procedure is based on the work of Veletsos (1984) with certain modifications to make it simpler and more generally applicable and yet accurate. This modification can be summarized in four main components: first the tank-liquid system is represented only by the first impulsive and first convective modes. Second, the higher impulsive modal mass is combined with the first impulsive mode and the higher convective modal mass is combined with the first convective mode. Third, the impulsive and convective heights are adjusted to account for the overturning effect of the higher modes. And finally, the impulsive period formula is generalized in order to be applicable for steel tanks as well as for concrete tanks of various wall thicknesses (Figure 2.7).

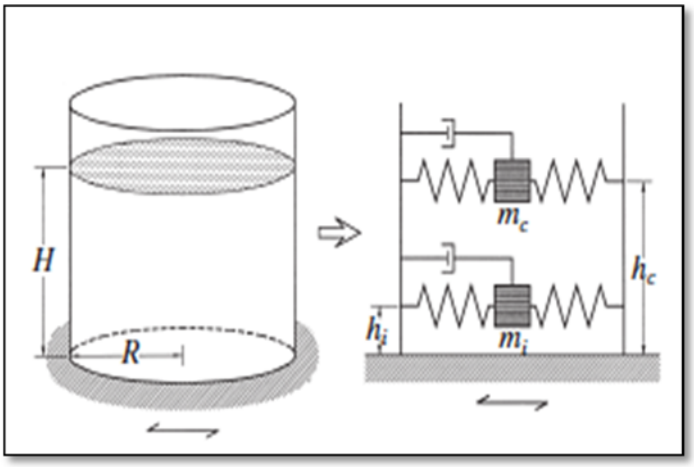

Figure 2.7: Tank model analyses using a single degree of freedom system (Praveen et al. 2000)

The same procedure was used in Eurocode 8 and was integrated in its limit state design concept. However, according to Eurocode 8, the analysis has to assume linear elastic behavior, allowing only for localized nonlinear phenomena without affecting the global response, and to include the hydrodynamic response of the fluid. Particularly, it should account for the convective and impulsive components of fluid motion as well as the tank shell deformation due to hydrodynamic pressure and interaction effects with the impulsive component. The procedure takes into account impulsive and convective (sloshing) actions of the liquid in flexible steel or concrete tanks fixed to rigid foundations. The dynamic analysis of a liquid filled tank may be carried out using the concept of generalized single degree of freedom (SDOF) systems representing the impulsive and convective modes of vibration of the tank-liquid system. For practical applications, only the first few modes of vibration need to be considered in the analysis. The mass, height and natural period of each SDOF system are obtained by the methods described by Velestos (1984). For a given earthquake ground motion, the response of various SDOF systems may be calculated independently and then combined to give the net base shear and the overturning moment. It was shown in previous study (Velostos 1984) that the flexibility of the tank wall might cause the impulsive liquid to experience accelerations that are several times greater than the peak ground

acceleration. Thus, the base shear and overturning moment calculated by assuming the tank to be rigid can be non-conservative. Tanks supported on flexible foundations through rigid base mats experience base translation and rocking, resulting in longer impulsive periods and generally greater effective damping. The convective (or sloshing) response is practically insensitive to both the tank wall and the foundation flexibility due to its long period of oscillation. Tanks analysed in many studies were assumed to be completely anchored at their base. In practice, complete base anchorage is not always feasible or economical. As a result, many tanks are either unanchored or only partially anchored at their base. The effects of base uplifting on the seismic response of partially anchored and unanchored tanks supported on rigid foundations were therefore studied by (Malhotra 2000 and Veletsos 1984) and it was shown that base uplifting reduces the hydrodynamic forces in the tank, but significantly increases the axial compressive stresses in the tank wall. Unlike ductile building systems, tanks lack a mechanism to dissipate large amounts of seismic energy in a ductile manner. Methods of improving the seismic performance of tanks by increasing their ability to dissipate seismic energy need to be examined. The tank could either be anchored to its foundation with energy dissipating devices or seismically isolated by special bearings.

2.4. Experimental Methods

Extensive experimental studies have been conducted using shake tables to analyse the resistance of various systems during earthquake oscillations. A shaking table is a platform excited and driven by one or more actuators. It is used to simulate different types of periodic and random motions such as artificial or recorded earthquakes. In the same way, it can improve the understanding of the behavior of various structures under the effects of seismic forces and allow professionals or researchers to calibrate different digital tools for dynamic analysis.

The test results obtained by the shaking table can be oriented to study different types of structures such as buildings, mechanical components and LCTs, etc. A single axis shake table is the simplest form of earthquake simulator. It is useful to investigate excitations in only one axis. Due to its simplicity; the interpretation of the test results collected by this system is more convenient.

An experimental study was conducted by Jaiswal et al. (2008) to investigate the dynamic response by obtaining experimental data related to the sloshing frequency of LCTs with different shapes. Various shapes were used including circular, square, rectangular, circular conical, and truncated pyramids of square shape. The experiment was done by using an electro-magnetic shake table along with a digital amplifier (Figure 2.8). Small-scale model tanks made of transparent glass were used in this experiment. These tanks were partially filled with different heights of dyed water and were excited harmonically under specific frequency. At each test the frequency and the amplitude of excitation were kept constant (harmonic motion). The same test procedure was repeated by changing only the frequency of the excitation for each tank shape or liquid volume. During the tests, the sloshing motion of the water was observed and the excitation frequency at which the liquid sloshed with large amplitude was taken as the sloshing frequency of the liquid. In addition, the excitation frequency value was driven and controlled with the help of a computer. Then, it was possible to collect data related to the frequency of the sloshing liquid at each test and with each shape.

Figure 2.8: Set up for experimental work (Jaiswal et al. 2008)

The first sloshing frequency of liquid was obtained experimentally and was compared with analytical or/and numerical results. The experimental results for the first set of tank shapes (circular, square, rectangular) were compared with analytical values given by the closed form expression formulas (Housner 1963) and with the numerical data using the finite element software ANSYS. For the second set of shapes (circular conical and truncated pyramid of square shape), the ANSYS software was still useful to determine the numerical values, but no analytical expressions were available for the sloshing frequency. Thus an approximate approach was used to compare the experimental results. In this approach, the circular conical tank was replaced by an equivalent circular tank of a diameter equal to the diameter at the liquid surface and by keeping the same volume of water. The same approach was followed for truncated pyramid of rectangular tanks. The experimental measurements were basically based on camera recordings. It was found that the experimental and the numerical results using the ANSYS software were in good agreement with the analytical solutions for circular, square and rectangular tanks. Further, the approximate method used to investigate more complicated shapes such as conical and truncated pyramid type also led to reasonable results compared with the experimental and numerical solutions. However, for the tank having a rectangular plan with increasing dimensions at the top, the results were higher than those obtained by the experimental method. Also it was

observed that the sloshing stiffness of the water decreased when an obstruction was placed inside a square tank. Therefore, the sloshing height decreases proportionally as the size of this obstruction increases.

Giannini et al. (2008) explored some experiments to test a steel liquid storage tank with a diameter of 4m, which represented a 1:14 scale model of a real (larger) liquid storage tank used for petrochemical plants. This experiment was elaborated using two different configurations. In the first configuration, the tank was fixed base, with and without a floating roof. In the second configuration, the tank was equipped with two types of isolators called elastomeric and sliding bearing with elasto-plastic dampers (Figure 2.9).

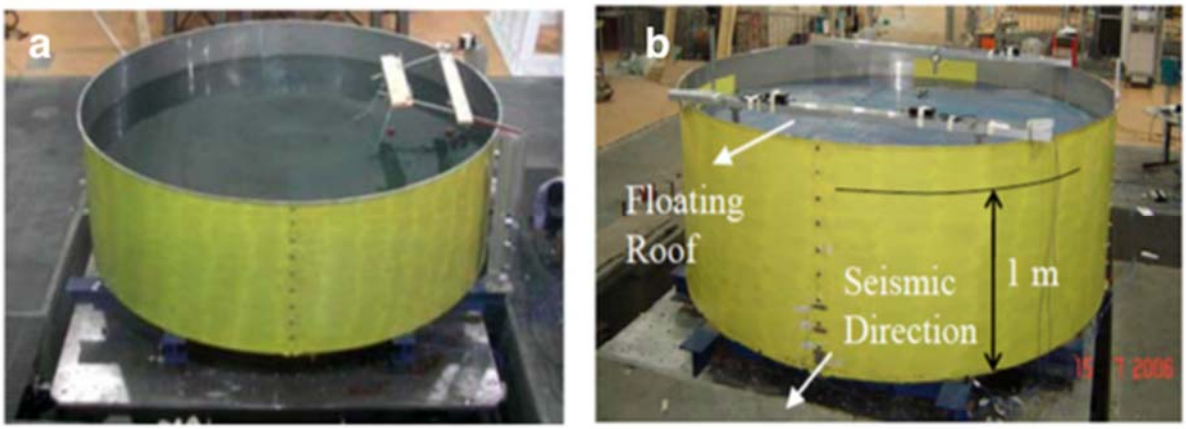

Figure 2.9: (a) The tank without floating roof (b) The tank with Floating roof (Giannini et al. (2008).

In each configuration, a series of dynamic tests were conducted using a shaking table. The base of the tank was fixed to the platform of the shaking table, which was programmable to excite the tank by six degrees of freedom. This table was monitored by several accelerometers. Six different base motion histories were used in each configuration, four of them were natural, from PEER (Pacific Earthquake Engineering Research) Center database and two were synthetic. The tank was also tested using white noise and harmonic signals with variable frequency. The response signals were measured using pressure transducers strain-gauges and laser transducers

placed on the tank wall (Figure 2.10).

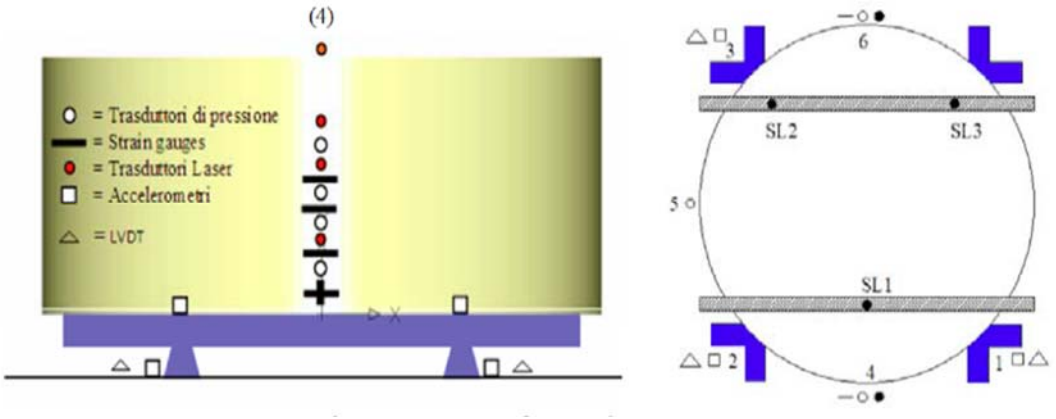

Figure 2.10: Experimental set up of cylindrical tank (Giannini et al. (2008)

Laser transducers were used to stimulate the sloshing motion of the liquid or the floating roof. The goal of these experiments was to evaluate the seismic effects on the tank by investigating the pressure on the tank wall and the effect of the sloshing behavior against the floating roof. The wall tank was considered to behave as a flexible body. The results confirmed the effectiveness of the two isolation systems for reducing the pressure on the tank wall and its influence of the floating roof. On the other hand, for the case of the isolated base, a small increase of the vertical oscillations of the floating roof was recorded, with a reduction in the number of free oscillations in the post-earthquake phase due to the existence of an advanced damping system. It was also expected that the base isolation technique could cause high displacement between the tank and the ground, which may induce dangerous damage to the pipe-tank connections.

Molin et al (2013) experimentally investigated Tuned Liquid Dampers (TLDs), which consist of a rectangular tank (Figure 2.11) with four vertical perforated screens (Figure 2.12), and is filled with water to an appropriate level, serving the purpose of reducing the dynamic

response of tall buildings and other structures (offshore structures, long span bridges etc.) under wind or earthquake vibrations. The most important motion of vibration explored by the previous

Figure 2.11: The tank mounted on Mistral Hexapod

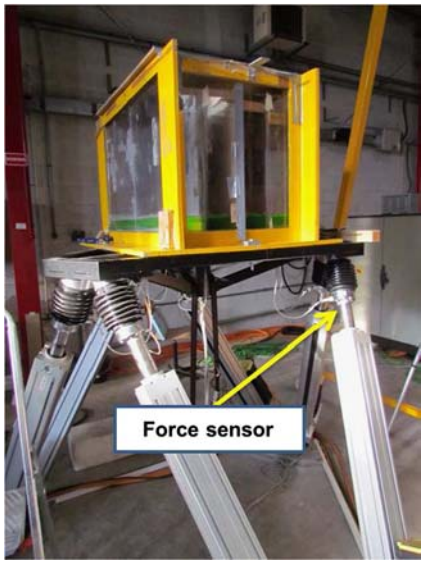

Figure 2.12: Perforated screens.

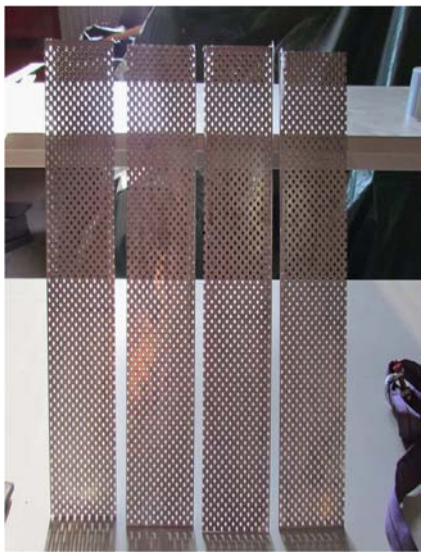

Molin et al (2013)

literature concerning this system is in the horizontal direction because the excitation response of this kind of system and where the TLDs mostly takes place is in the horizontal direction. The purpose of these tests was to complement the results of Faltinsen (2011) et al. to determine hydrodynamic loads in a rectangular tank of identical depth-over-length ratio. The experimental values of the free surface elevation at the end wall and the hydrodynamic coefficients (added mass, damping coefficients, wave elevations, hydrodynamic loads, hydrodynamic moment with respect to the mid-bottom point) were measured and compared to the value found by the numerical method when the tank was successively subjected to forced motions in sway and roll at different frequency values. Good concordance was found between experimental and numerical results up to motion amplitude of 10 mm.

Chapter 3. Experimental Study

3.1. Introduction

The experiment is a very powerful source to validate theoretical and numerical solutions about the behavior of liquid in storage tanks when it is subjected to external loading such as earthquakes. For this case, an experiment was implemented in this study to obtain information about some fundamental problems such as liquid sloshing, maximum sloshing height and naturel period (or fundamental period). Such information can be the key factors for many engineering applications. For example, liquid sloshing corresponding to the oscillation of the liquid surface due to the exterior excitation can have significant effects on the tank response. This phenomenon is of great importance. It was studied in the past numerically, theoretically and experimentally by linear and nonlinear analysis (Figure 3.1).

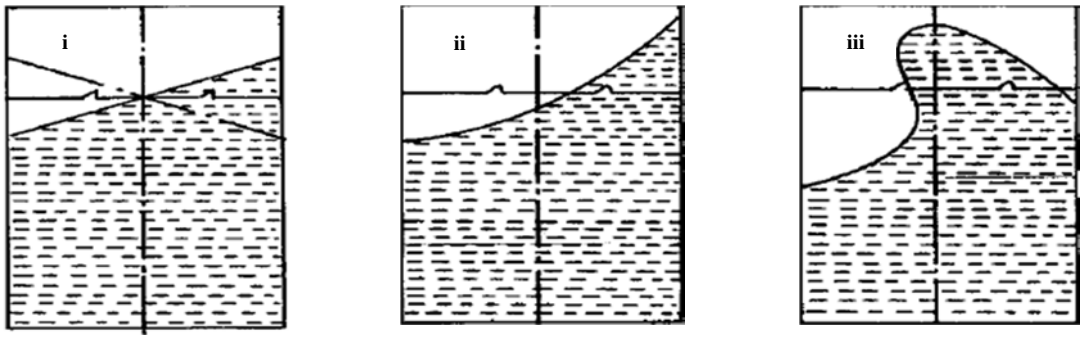

i-Linear ii -Weakly nonlinear iii- Nonlinear

Figure 3.1: Different Types of the 2D sloshing behavior of the free-liquid surface inside a rigid container excited by horizontal harmonic motion (Book Liquid Sloshing Dynamics Theory and Applications, Ibrahim 2005).

In case (i), the free surface remains flat during the small oscillations. This is known as a linear sloshing, but when the liquid undergoes oscillations with more intensity (case (ii)), its surface

will no longer be flat. Then it becomes more complicated to analyse with simple analytic equation. For case (iii), the liquid sloshing is a highly nonlinear motion. This is mainly due to the rapid changes of speeds associated with the impact of the hydrodynamic pressure in the vicinity of the free surface of the liquid. This kind of behavior needs very elaborate methods of calculation. In the most published papers of previous literature, the analytical expressions of sloshing are based on the linear wave or shallow water liquid theory.

However, when the exciting period is close to the fundamental period of the liquid tank, the linear wave theory fails to exist because it is not enough to solve the response of the liquid sloshing in such boundary conditions. For the case of nonlinear waves, it is very difficult to derive the sloshing phenomenon by using the analytical method. Thus, it is inevitable for this kind of problem to use numerical simulation to investigate the three parameters (sloshing, maximum height, and periods of resonance), which are correlated to each other. Furthermore, to validate the numerical results, several experimental tests are presented in this study. A small-scale tank was used to verify some numerical results. These experiments were chosen to be limited to a harmonic motion in this study, due to the scope of the present research project. The fresh water used inside the tank is also assumed to be ideal fluid (homogeneous, incompressible and inviscid). If the collected results show a concordance between the numerical, experimental and analytical values, the research can be extended by using the same numerical methods, but with other types of motion, such as recorded time history data of earthquake events.

3.2. Experimental Setup

In this research the experimental work was conducted using a shake table set up as shown in Figure 3.2. This set up comprises a small shake table installed in the Structural Laboratory at the University of Ottawa. The top platform of the table had the following approximate size:

1.10mx1.20m, and was made from aluminum material to reduce its weight. It could move horizontally on bearing rails. The motion of this table was driven by a Mechanical Testing and Simulation system (MTS) connected to a hydraulic actuator model 244 with 25 kN force capacity and a 250 mm (10 in) stroke length. This actuator was able to move the shake table back and forth at different levels of frequencies, through a hydraulic pump (Figure 3.2).

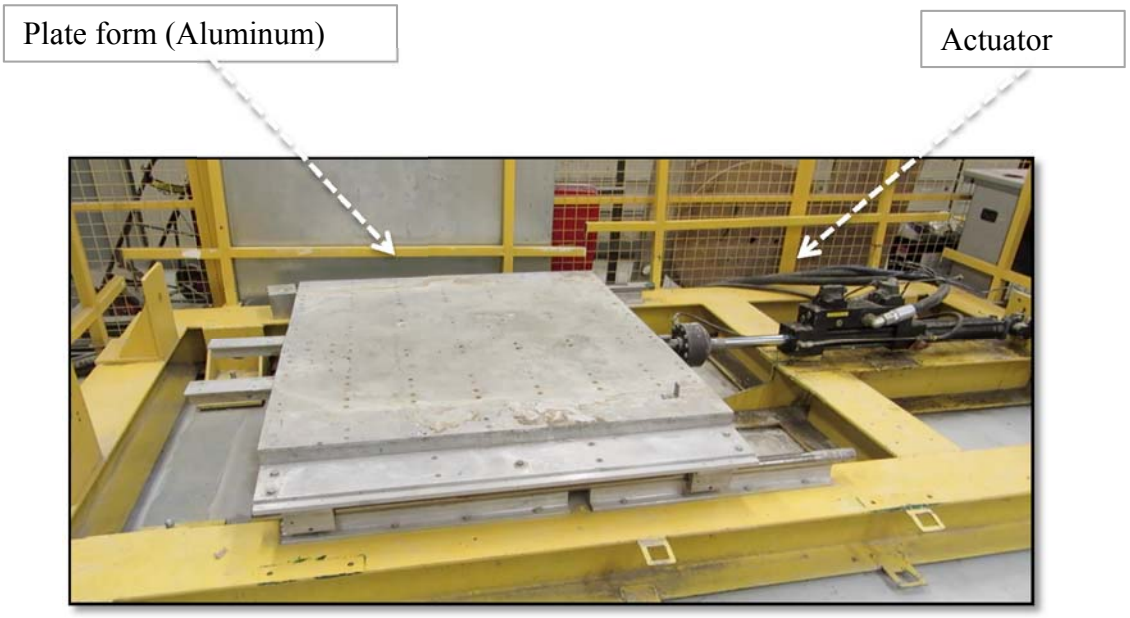

Figure 3.2: Shake table at University of Ottawa Laboratory.

In this experiment a ground water tank fixed at the bottom and excited by a shaking table was tested as mentioned before. MTS controller and computer software were used to control hydraulic pressure, to apply the required forces on the shaking table and to obtain the desired period and displacement. Also, the same computer was used to control the frequency, the amplitude and the duration of excitation (Figure 3.3).

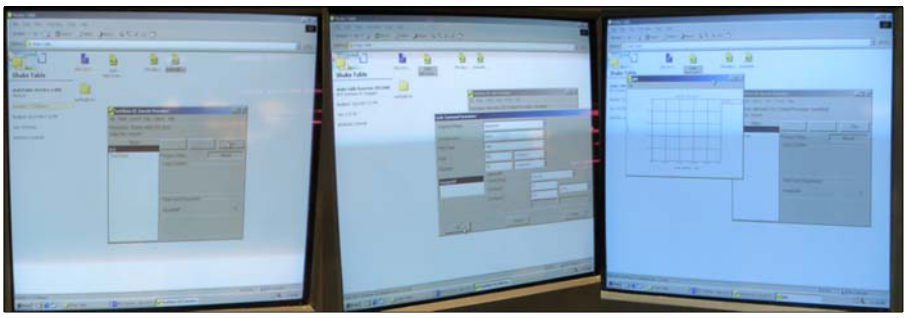

Figure 3.3: MTS Controller and computer software

A small-scale tank with square base of size 442x442mm and 470mm height was chosen to accomplish this experiment (Figure 3.4). This tank is made of transparent glass, which allows for observing the behavior of the fluid inside during the excitation. The only acceptable motion in this experiment was pure translation in the horizontal direction. For this case, the tank was suitably fixed with silicon at edge and with a strong attachment tape at the base to avoid any rotation around the z-axis or any sliding along the shaking table platform.

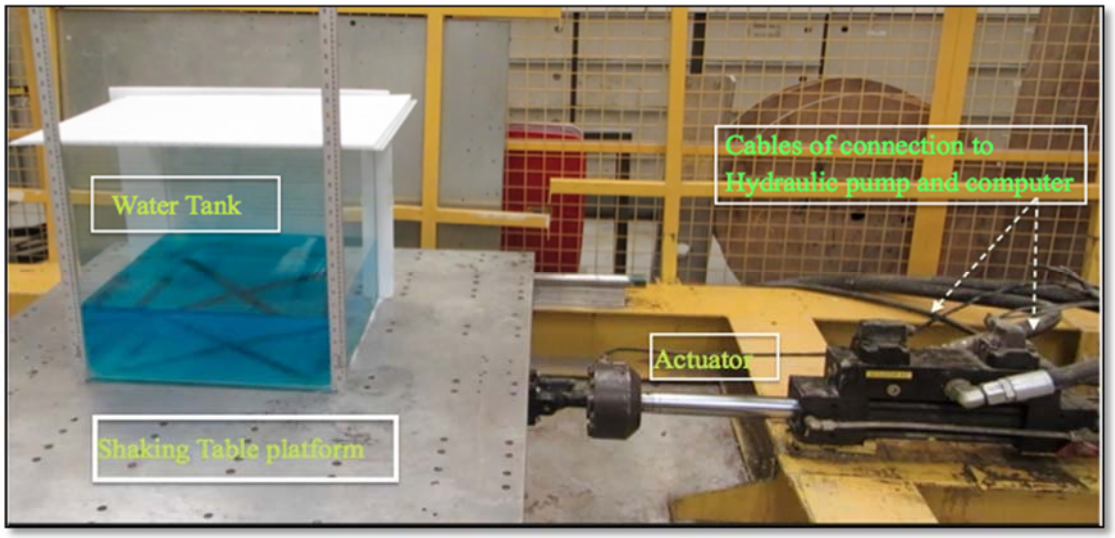

Figure 3.4: Experimental set up

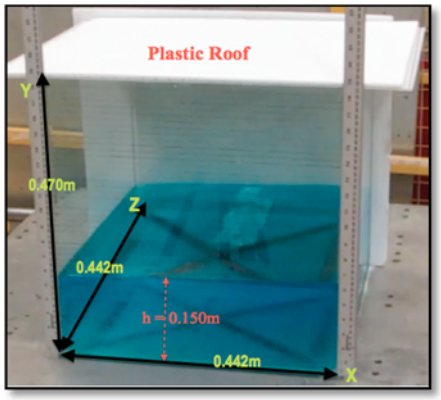

Figure 3.5: Details of tank dimensions

Therefore, this system can be identified as a fixed base tank (Figure 3.5). The water used to fill the tank at different levels was mixed with a dye (colorant). The table was excited harmonically with a particular period using a harmonic motion. During this experiment, different values of periods were tested. The set of experiments covered a harmonic motion with six different periods and single amplitude (displacement) as described in the Table 3.1.

Table 3.1: Experimental Cases of Time – Displacement Motions

Table 0.1 Experiment Cases of Time - Displacement motions

Case1	Depth of liquid (mm)	Period T(s)	Frequency f (Hz)	Displacement D (cm)
1	150	2	3.14	5
2	150	1.6	3.93	5
3	150	1.0	6.28	5
4	150	0.81	7.76	5
5	150	0.7	8.98	5
6	150	0.5	12.57	5

The depth of the water was kept the same (0.15m) during the entire test duration. This depth was chosen equal to 0.15 m, which represents approximately one third of the height of the tank wall (47 cm). The reason was to be able to see the sloshing of the water liquid profile with large

displacements during the excitation of the tank. So it was more reasonable for this study to choose a filled tank with an unrestricted free surface, as it exists in practical cases. Consequently the free surface can undergo large deformations, which is known as a non-linear effect. However, at higher water depths, to respect the wall height, the behavior of the fluid tends to be more linear, which represents a conservative method of analysis.

In order to obtain experimental data, the fluid interface motion was recorded using two video cameras. The first camera was installed perpendicular to the direction of the motion of the container in order to record the entire interfacial region and the colored water surface motion during the sloshing period. The second camera was fixed perpendicular to the Z direction of the tank to investigate the behavior of the water in this axis. However, basically a 2D visualization of flow inside the moving tank was recorded. The main objective of this experiment was to obtain data for water surface movement to be compared with the results of models based on computational fluid dynamics simulation (using OpenFoam).

3.3. Experimental Work Tests Results

In this experiment two parameters related to the sloshing behavior of water contained in a square tank were of interest. These parameters are the sloshing period (T) and the maximum height of water elevation during the sloshing (D_{max}). The square tank was fixed on the platform of the shaking table, which was driven by a harmonic motion at different particular periods. The periods selected in this experiment correspond to three different conditions of the water behavior. The first condition corresponds to the resonant period of the tank filled water. This period was determined first theoretically by using Housner's formula; to be presented in Eq (3.2) below. The second and third conditions correspond respectively to under-resonant and over-resonant periods. As mentioned before, the glass square tank used in this experiment corresponds to small

size models. The dimensions of the base are 442mmx442mm and 470 mm height. In engineering projects, this model can be used to design a real ground-supported tank with a fixed base connection.

The equation of harmonic motion can be described as shown in Figure 3.6 and by equation 3.1.

$$Y = A\sin(wt) \qquad (3.1)$$

With:

- A= Maximum amplitude of the shaking table displacement (0.05 m).
- w= Circular frequency of the shaking table.
- T = Oscillation period of the table.

The resonance period is determined using Housner's formula developed based on the linear wave theory.

$$T = 2\pi \sqrt{\frac{L}{3.16\ g * \tanh(3.16\frac{h}{L})}} \qquad (3.2)$$

$h = Height\ level\ of\ the\ water, L = Lenght\ of\ the\ square\ tank.$

Using the equations 3.2 and 3.3, one obtains the following values for the period of motion for the present experiments:

$$f = \frac{1}{T} \Rightarrow \omega = 2\pi f \qquad (3.3)$$

Table 3.2: Parameter values of the shaking table motion at T=0.81s

$\boldsymbol{T(s) =}$	**0.81**
$\boldsymbol{f(Hz) =}$	1.24
$\boldsymbol{w(rd/s) =}$	7.76

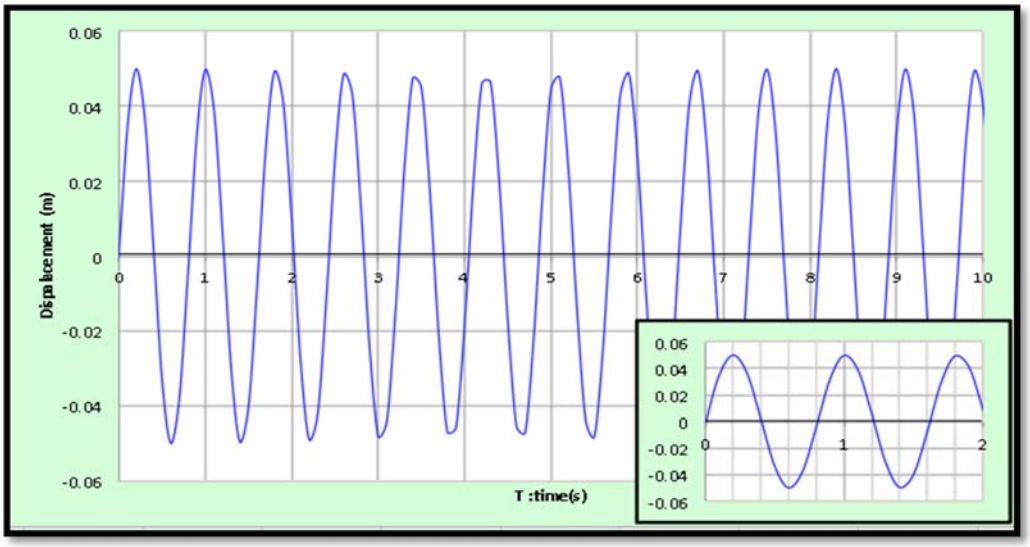

Figure 3.6: Excitation curve

3.3.1. Sloshing Profiles

During this experiment, the sloshing of the water was recorded by two cameras. Then a set of images (Figure 3.7) of maximum water elevation was selected from the video of each run. As mentioned before, six different periods were chosen in this experiment as: T=2s, T=1.6s, T=1s, T=0.81s, T=0.7s, T=0.5s. The highest elevation reached by the water during each period of excitation was chosen as the maximum height of sloshing D_{max}. Also, based on these images, the profiles of the free surface of the water at this maximum level of elevation were investigated using the "GraphClick" application to draw a scaled graphic (Appendix B). The frame of these pictures represents the tank wall parallel to the horizontal direction of excitation. The width of the tank represents the axis X [From 0 to 0.442m] of the graph and the height of the tank represents the axis Y [From 0 to 0.470m].

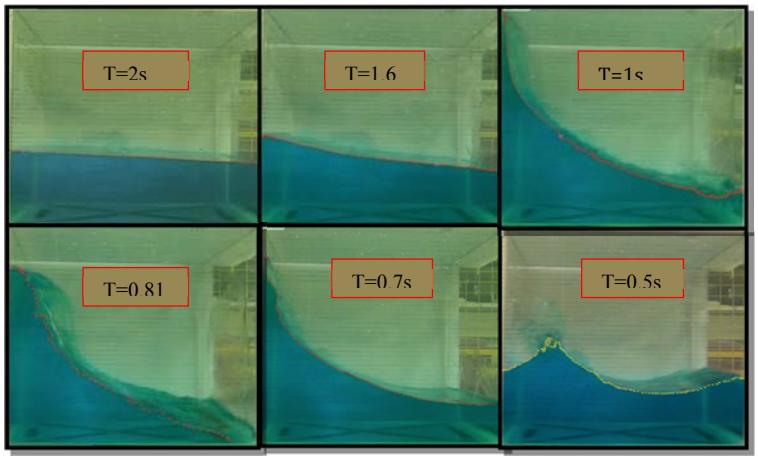

Figure 3.7: The snapshots of the 2D results of maximum elevation during the water sloshing at different period values.

With the "GraphClick" application, the profile of the free surface of these images was detected and a set of data was collected. These data represented the coordinate (X, Y) of the graphical curve of this profile in 2 D. This data was exported to Excel to produce an Excel curve similar to the original so these curves could be presented all in the same graph (Figure 3.9).

The shaking periods, which the sloshing wave moves in a continuous circular motion, are considered as the sloshing periods (also called natural period or fundamental period) of the liquid (water) inside the tank.

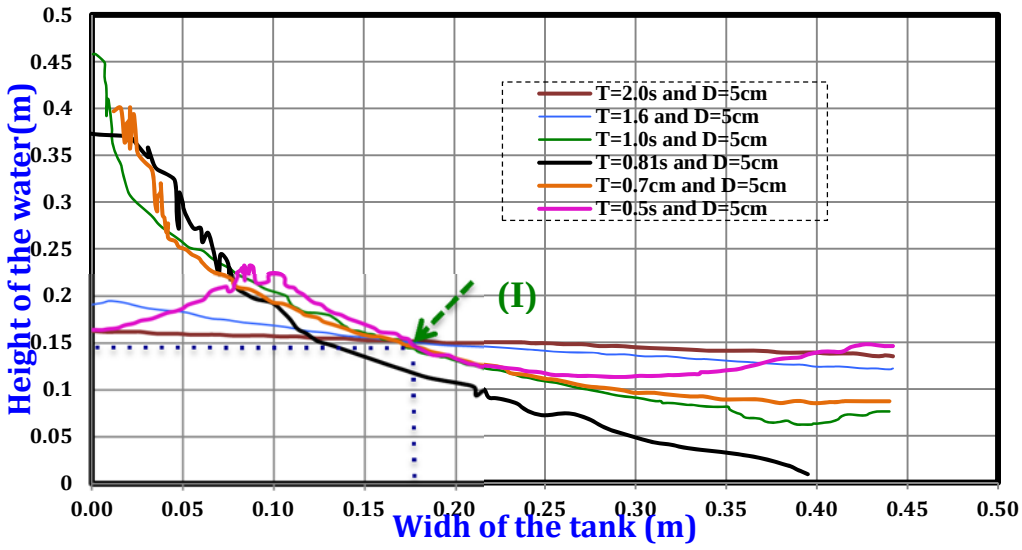

Figure 3.8: Maximum water surface elevation (m) for different experimental excitation periods and at fixed displacement D=5cm.

3.3.2 Maximum Elevation of the Water during Sloshing

Based on the Housner formulation, the sloshing height is given by the equation 3.3 when the rectangular tank is excited in harmonic horizontal motion. The values collected during this experiment can be compared to theoretical value found by the Housner formula.

Table 3.3: Experimental values of maximum elevation D_{max} at different periods of excitation

T (s)	D_{max} (m)
0.5	0.232
0.7	0.4
0.81	0.373
1	0.458
1.6	0.195
2	0.163

The graph obtained using Excel can be used to approximately determine the maximum experimental value of water elevation. For this purpose, the application "GraphClick" was utilized to obtain the coordinates of each point on the graph in accordance with the initial scale of the axes (Figure 3.9 and Figure 3.10).

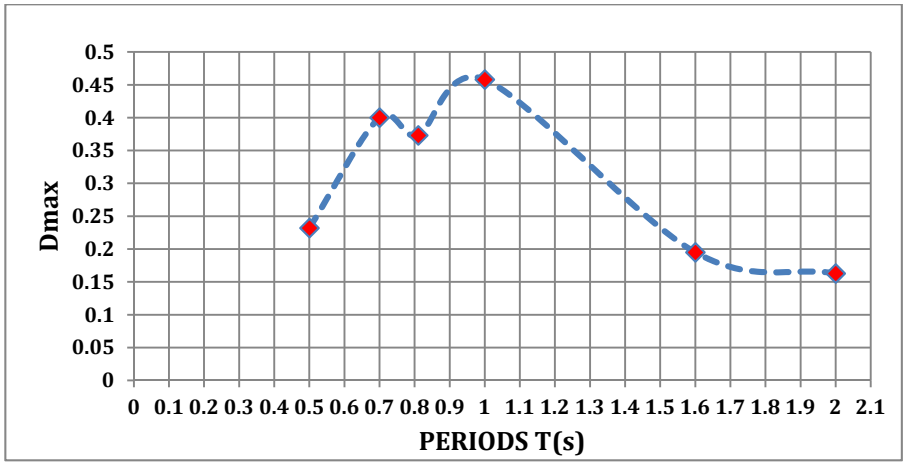

Figure 3.9: Experimental maximum surface elevation (D_{max}) for different values of excitation periods.

Referring to this graph, it is clear that the maximum elevation calculated from the bottom of the tank that was reached experimentally is about 0.466 m from the bottom of the tank, then:

$$D_{\max(Experimental)} = 0.466 \text{ m}$$

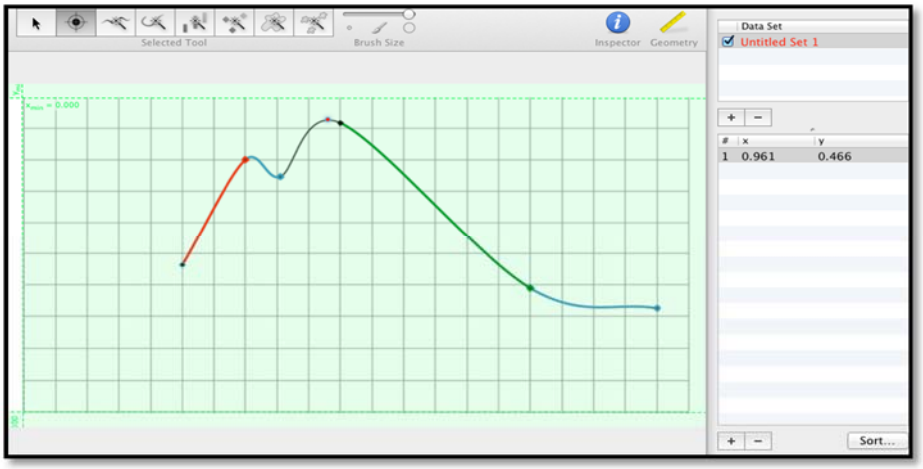

Figure 3.10: Determination of experimental maximum elevation of water using "GraphClick" application.

- D_{max} Theoretical:

Based on Housner's formula described by the equation (3.3), which has been adopted by many codes in the world, such as ACI 350.3 (2001), NZSEE 1986 code, and Eurocode8 (1998), we can determine the maximum elevation of the water during its sloshing for the different sets of periods applied to the shaking table. This formula estimates this elevation for rectangular tanks in general, and it can be used for particular cases when the tank is square shaped. Maximum sloshing was measured from the liquid surface at rest. We have to add the height of the water (0.15 m) to find D_{max} theoretical. It should also be mentioned that this parameter was investigated in this study based on two-dimensional geometry.

$$D_{max} = (\boldsymbol{L/_2})(\boldsymbol{ZSI} \times \boldsymbol{C_c}) + H_{water} \quad (3.3)$$

$$For\ T_c = 0.81s < 2.4s \implies C_c = 1.5 \times \frac{1.25}{T_c^{2/3}} \leq \frac{2.75}{S} \quad (3.4)$$

$$\Longrightarrow C_c = 1.5 \times \frac{1.25}{T_c^{2/3}} = \frac{1.875}{T_c^{2/3}} \leq \frac{2.75}{S} \Longrightarrow C_c = 2.16$$

$S = 1$ Because we can assume the table is similar to the rock foundation $L = 0{,}442m$ and C_c is the spectral amplification factor.

In our case, we deal with an unrestrained sloshing height. Taking in consideration that the tank will be in critical seismic map zone (characterized by the number 3 or 4) the seismic zone factor will be Z_{max}=0.4 and designed for importance factor greater than 1 (I=1.5)

$$D_{\max(Analytical)} = \left(^{0.442}/_{2}\right)(0.4 \times 1 \times 1.5 \times 2.16) + 0.15 = 0.436\, m$$

$\Delta_{R(A/E)}$: The relative error between the experimental and the analytical results concerning D_{max} values is:

$$\Delta_{R(A/E)} = \frac{D_{\max(Analytical)} - D_{\max(Experimental)}}{D_{\max(Analytical)}} \times 100\% = 6.4\ \%$$

which shows a very good agreement between experimental and theoretical results.

3.4. Discussion

The graphs in Figure 3.8 represent the maximum elevation profile of water at different periods in the Y direction. From these graphs, we can observe that the fives curves have a common intersection point (I), which has the coordinates X = 0.175m, Y =0.15m. The value of depth at Y=0.15 m corresponds to the height of water at initial condition, so this point remains at the same position when the excitation motion changes its periods (or frequency) value. However, if the excitation period meets the natural frequency of the tank, this point does not match the previous characteristics and changes its position to a lower height. This is an important

observation that can be taken into consideration for future work and can be explained by using governing fluid flow equations to describe the profile of water surface elevation. It was also observed that the sloshing elevation of the water was more critical and higher when the excitation period was closer to the naturel period. At this interval the liquid sloshed with large amplitudes, the elevation of the water became higher and the behavior of the water could be more disastrous. Figure 3.10 also indicates this fact, so a part of the green and the black interval of the curve represent the maximum value of the elevation data. In this experiment and during the excitation period that coincides with the natural period, the sloshing is higher than the other period of excitation and also the body of water that rises in the tank is wider (Figure 3.11). That makes the water behavior more critical because the amount of moving water is more important in terms of weight and travelling speed. This causes more damage to the tank structure on roofs, on walls or on the bottom.

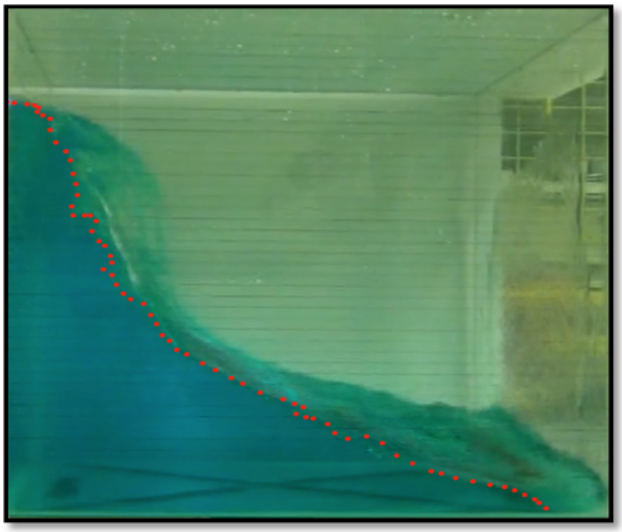

Figure 3.11: The snapshots of the 2D maximum elevation during the water sloshing at T=0.81s (Resonance period).

Figure 3.12 (From 1 to 12) shows the motion of the water at various times, when the tank was excited under the period T=0.81s, which represented the resonance period of the convective part

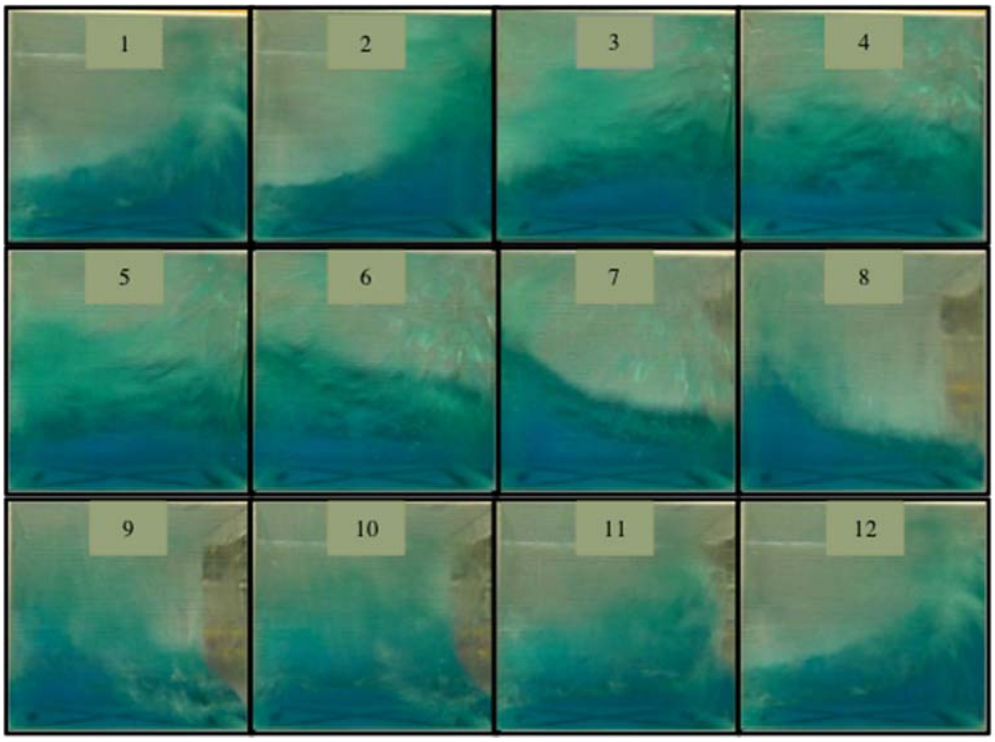

Figure 3.12: 2D Snapshots in X direction describing the behavior of the water in circular motion around the walls and the corners of the tanks at T=0.81s (Resonance period).

of the water motion. At this range of period, the water surface was in swirling motion known as rotary sloshing. This type of motion usually occurs near the liquid natural periods or slightly below this value (Ibrahim 2005). Furthermore, this behavior can happen regardless of the shape of the container. Thus, the geometry of the tank does not play any role in the occurrence of this motion (Ibrahim 2005). This can be compared to the vortex phenomena produced during the drainage of the tank. The direction of the motion was observed to be clockwise. Similarly, Kana (1989) demonstrated in his study with a set of experimental tests that the rotary motion is in a clockwise direction when the naturel period (or the naturel frequency) was approached from below.

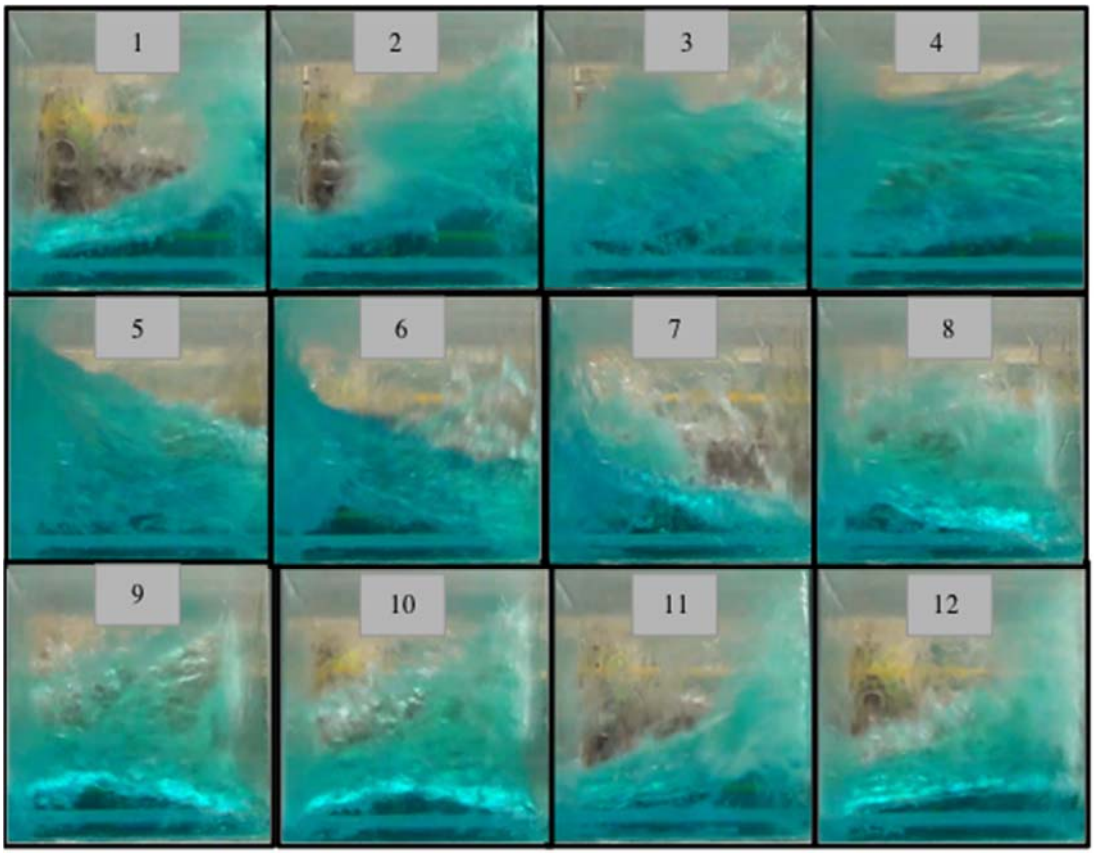

Figure 3.9: 2D Snapshots in Y direction describing the behavior of the water in circular motion around the walls and the corners of the tanks at T=0.81s (Resonance period).

Abramson (1961) identified the rotary sloshing by the following description: ‘‘at the onset of this motion, the first mode of sloshing began to transform itself from translational into rotational motion, increasing in angular velocity in one direction until it reached a maximum. Then, the angular velocity decreased to approximately zero, reversed its direction, and increased in angular velocity in the new direction.’’

During the rotary motion, the quantity of water travelling around the tank in circular motion hit the corners of the tank during each rotation. This allowed us to see clearly a hydraulic jump. This jump travelled periodically from corner to corner successively and between the walls, in a clockwise direction.

Verhagen and Wijngarden (1965) studied this hydraulic jump in a rectangular tank subjected to lateral excitation. They characterized such hydraulic jump as a nonlinear phenomenon.

3.5. Conclusion

The experiments performed in this chapter dealt with the main results of the sloshing phenomena and with its related parameters such as the maximum height of the sloshing (D_{max}) and its fundamental period.

First, based on the analytical equation, the fundamental period was calculated (T=0.81s). Therefore, a set of period values close to the excitation period were chosen below and above the fundamental period value. The tank was filled up to a constant depth of h=0.15m of fresh water and was forced to oscillate in X direction using the shaking table at a constant amplitude of excitation (A=0.05m). The sloshing motion of the water was observed and recorded by a camera during each period of excitation. It was observed that if the period of excitation was higher or lower than the calculated natural period of the tank, the amplitude of sloshing was lower. However in the case where the excitation period was close to the fundamental period, the motion of the water changed and water exhibited nonlinear behavior with very large amplitudes. Therefore, sloshing visualization showed that the natural period calculated by the analytical formula (T=0.81s) is closer to the experimental result. When the value of the excitation periods was changed above and below the natural period, the amplitude of sloshing becomes less important. As mentioned, during this period the water moves in a circular direction and with higher speed. Furthermore, the quantity of mass travelling around the reservoir hits the corners periodically. This collision between the mass of moving water and the corners of the tanks shows the severity of this condition, which is known as resonance. Base on the observation, the sloshing period was experimentally detected. Therefore, at this stage of experiment we could confirm a

very good agreement between analytical and experimental results concerning the value of the resonance period (or fundamental period).

On the other hand, the maximum elevation that water can reach during the excitation is an important parameter. To investigate this value, the maximum level at each period was measured and presented in the same graph (Figure 3.10). Also, the experimental value of D_{max} was determined (D_{max}= 0.466m). The relative error between the experimental and the analytical value of the D_{max} was around 6.4%, which is reasonable considering the many factors involved. The two dimensional geometry was a factor affecting the accuracy. It should be mentioned that during the 1983 Nihonkai-Chubu earthquake, the sloshing height under nonlinear conditions was determined to be about 10~25% larger than the value determined under linear condition (Shimada et al. 1988). Taking this effect into account, the difference between analytical (linear) and experimental values can be considered to be acceptable.

In general, the experiments successfully stimulated the sloshing height. Therefore, the experimental approach can be considered as a good method for comparing and obtaining the fundamental period as well as the maximum height of sloshing.

Chapter 4. Numerical Simulation

4.1. Introduction

In this thesis, the behavior of water tanks under harmonic motion is studied. Some data were collected in Chapter 3 using analytical and experimental methods. The data focused primarily on two important parameters, the resonance period and the maximum sloshing height of water. It was found that the results concerning the two parameters obtained by these two methods are very close. A third method is employed in this chapter to compare and validate these results, that is a numerical modelling approach which has become a precious tool to conduct research, to solve problems or to design systems related to different industries. This numerical approach is based on the computational fluid dynamics (CFD) software, known as OpenFoam simulation (Version2.4). The CFD simulations now play an essential role in conducting research and can provide highly accurate solutions in three dimensions for fluid dynamics problems, while the theoretical methods are mainly based on two dimensional cases. Furthermore, numerical methods can consider complex cases that are either difficult or expensive to obtain analytically or by experimental tests. Figure 4.1 illustrates the position it takes among the conventional methods (analytical and experimental) and the relationship between them. The CFD approach presents a key field of science with an importance similar to the experimental or the theoretical fields. One can describe this field by presenting the role that it plays beyond the scope of other research fields (experimental and theoretical).

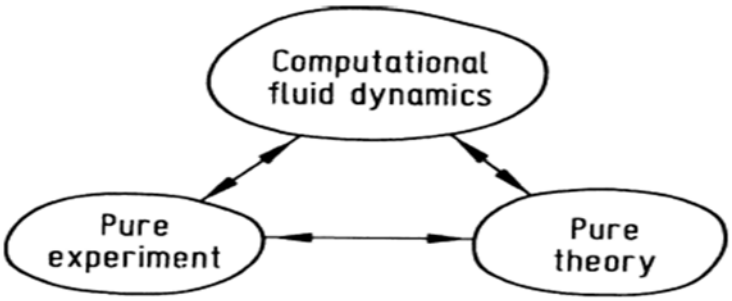

Figure 4.1: Position and relationship of CFD methods with respect to the classical methods (experimental and theoretical)
(Isaac Newton's Principia 1687Wendt, F 2009)

First, the fluid flow simulation can be generated by using the three fundamental principles (Appendix E)

- The conservation of mass
- The conservation of momentum
- The conservation of energy

One can mathematically express these physical laws by using equations and, in most cases, with partial differential equations, which are often impossible to solve analytically, so the CFD methods can be used to solve these governing partial differential equations of fluid flow by numerical values while taking into account the variation of space and time in order to predict the behavior of the fluid flow. In general, the solution presented by a CFD software package is established in the following order:

- Creation of the geometries of the system (dimensions, shapes etc…..).
- The grid generation process (choice of the type of grid: structured, block structured, unstructured, hybrid).
- Choice of the models (two- or three dimensional, inviscid or viscous flow, turbulent or laminar etc….).

- Application of the boundary conditions (inlet, outlet and wall etc.…).
- Computation of the flow field (with solvers, generally already available for users of the package).
- Post-processing (flow analysis).

There are various such CFD packages that are focused basically on fluids dynamic simulation. Among them, one can cite Abaqus/CFD, ANSYS FLUENT, or SOLIDWORKS...

A list of such models is available at this reference:

http://www.directindustry.com/industrial-manufacturer/cfd-software-74890.html

In this thesis, the OpenFoam (Open Field Operation and Manipulation) model was chosen as a CFD method to support and complement both the experimental and the analytical solutions.

4.2 OpenFoam

OpenFoam is an open source code used mainly for CFD, but it can perform simulations for other fields such as stress analysis and financial mathematics. It is a C++ library of tools for physical simulations, but primarily for fluid mechanics. OpenFoam was created in 1989 by David Gosman and Radd Issa at the Imperial College of London and with the principal developers Henry Weller and Hrvoje Jasak. In 1996, the first version of OpenFoam was presented. This software solves partial differential equations using the finite volume method FVM (Appendix E).

OpenFoan was chosen in this project for various reasons related to the advantages that it can offer. It is a useful tool with more than 200 programs, equivalent to commercial software, and gives even more accurate results in some aspects. The prices of commercial software licences are typically significant while OpenFoam is an open source model without license limitation and is able to create individualized solutions unlike commercial software. It is possible for the users to access the source (i.e., it is not a black box) and it is a modular program.

OpenFoam can solve most types of fluid mechanic problems, including steady or unsteady, compressible or incompressible, single phase or multi-phase, using FVM. This flexibility is offered by choosing the adequate solver for the problem or by modifying an existing solver or sometimes creating a new solver to better describe various cases.

4.2.1. Solvers

Table 4.1: List of some standards OpenFoam solvers

Solver name	Type of problem to solve
potentielFoam	Initialize a simple potential flow before starting the resolution.
icoFoam	Transient solver for incompressible, laminar flow of Newtonian fluids.
pisoFoam	Transient solver for incompressible flow.
apalcianFoam	Resolution of the Laplace equation (e.g., thermal diffusion).
SimpleFoam	Turbulent flows stationary.
SonicFoam	Laminar or turbulent flows for compressible gas.
bubbleFoam	System of two incompressible fluids with a dispersed phase.
reactingFoam	Flow burning reagents.
buoyantBoussinesqSimpleFoam	Solver suitable for thermal calculations. for steady flows, turbulent and compressible.

OpenFoam presents many solvers in different fields of application. The solvers are designed to simulate a given problem. Table 4.1 names and describes some of more useful solvers in the fluid mechanics problems. Figure 4.2 describes how OpenFoam solver (e.g. simpleFoam) first converts a physical problem case to fundamental equations and then numerically solves these equations. Generally, in order to simulate sloshing problems, the user can use the pre-built solvers offered by this software. Also, it is possible to design a specific solver when necessary.

In this numerical simulation, a solver called interDyMFOAM in the openFoam package was used. This solver is able to stimulate two incompressible fluids (air and water) using a VOF. During the sloshing and at the two present interphases, the water can be in mixture with the surrounding air and can contain breaking waves. InterDyMFOAM can handle this complex phenomenon. This solver also provides the opportunity to use a dynamic mesh, which means that the mesh moves depending on the movement of the tank, so it can re-mesh between each time step depending on the movement of the fluid. In the tutorials for sloshing tanks in openFoam cases, the same solver was used. This simplified the set up when coupling occurs between two liquids.

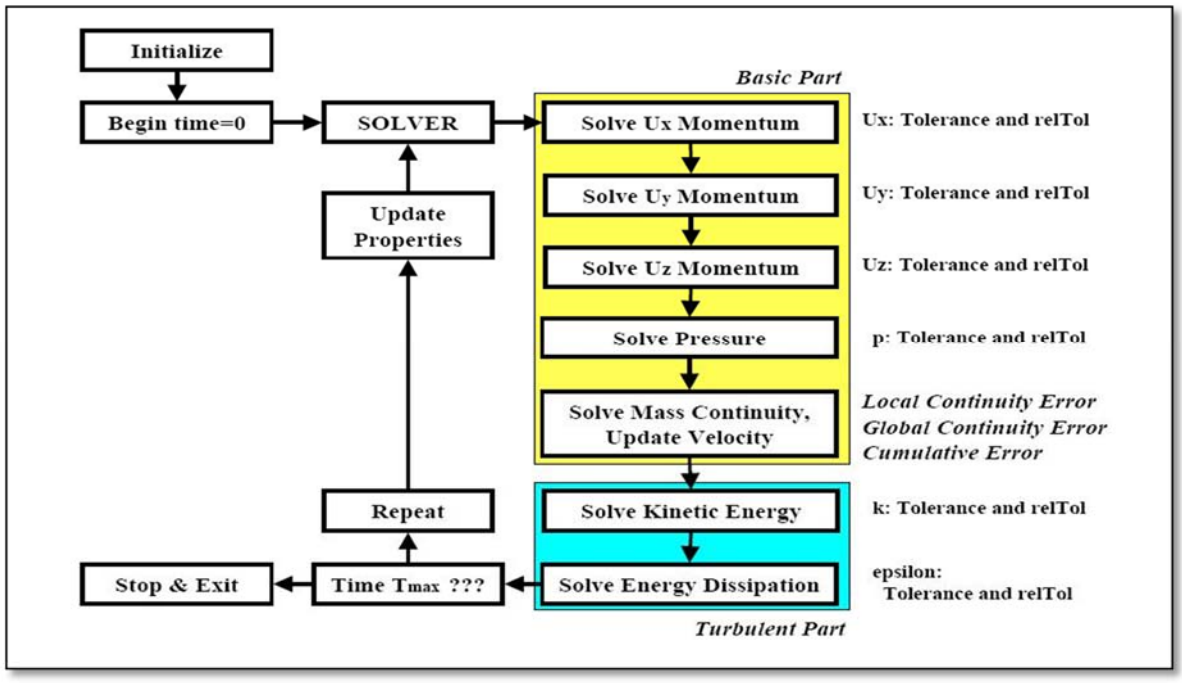

Figure 4.2: Algorithm of simpleFoam solver overview (http://www.openfoam.org/docs/cpp/)

OpenFoam also contains standard utilities that are designed for data manipulation. One of the utilities is designed for mesh generation (blockMesh) and can be used for simple geometries such

For example boxes, cylinder, spheres planes, etc. For more complex geometries there is "snappyHexMesh," That meshes to surfaces from CAD (Computer-aided design), but also allows users to define simple geometries too. Another utility is "extrudeMesh," which is meant to generate mesh by extruding cells from a patch of an existing mesh. Other utilities are also available in OpenFoam that have the role of converting the mesh such as "AnsysToFoam," or"fluent3DMeshToFoam,". Some utilities are also available to manipulate or check the mesh like "attachMesh," which can attach topologically detached meshes using prescribed mesh modifiers and

"checkMesh," which checks the validity of a mesh. Other tools for meshing and post-processing, such as post-processing graphics and post-processing data converters, are available as well in the utilities library.

OpenFoam also provides post-processing and visualization tools for the results. The most widely used tool is ParaFoam. It's a very useful tool that makes it possible to show quantities of interest to the user and their following evolution, and can extract the desired data.

4.2.2. Creating Solvers

While OpenFoam can be used as a standard simulation package, it is flexible in defining new models and solvers in an efficient way. Users can create their own solvers and models. An example is presented below related to the momentum equation, which shows that the solver is written in a programming language similar to mathematical language, which is familiar for users and can be easily understood or handled:

$$\frac{\partial \rho U}{\partial t} + \nabla . \phi U - \nabla . \mu \nabla U = -\nabla p \qquad 4.1$$

Equation (4.1) represents a partial differential equation. This equation can be presented in OpenFoam by its natural language using the following code:

```
Solve
(
    fvm::ddt: ddt(rho, U)
  + fvm::div(phi, U)
  - fvm::laplacian(mu, U)
    ==
  - fvc::grad(p)
);
```

This open source possibility and specific programming environment makes OpenFoam an excellent choice for customisation compared to other software.

4.2.3. General Structure of OpenFoam Case

The algorithm of the general structure of an OpenFoam case is shown in Figure (4.3). The code presented in this figure describes a logical hierarchy to follow in order to solve the different problematic cases.

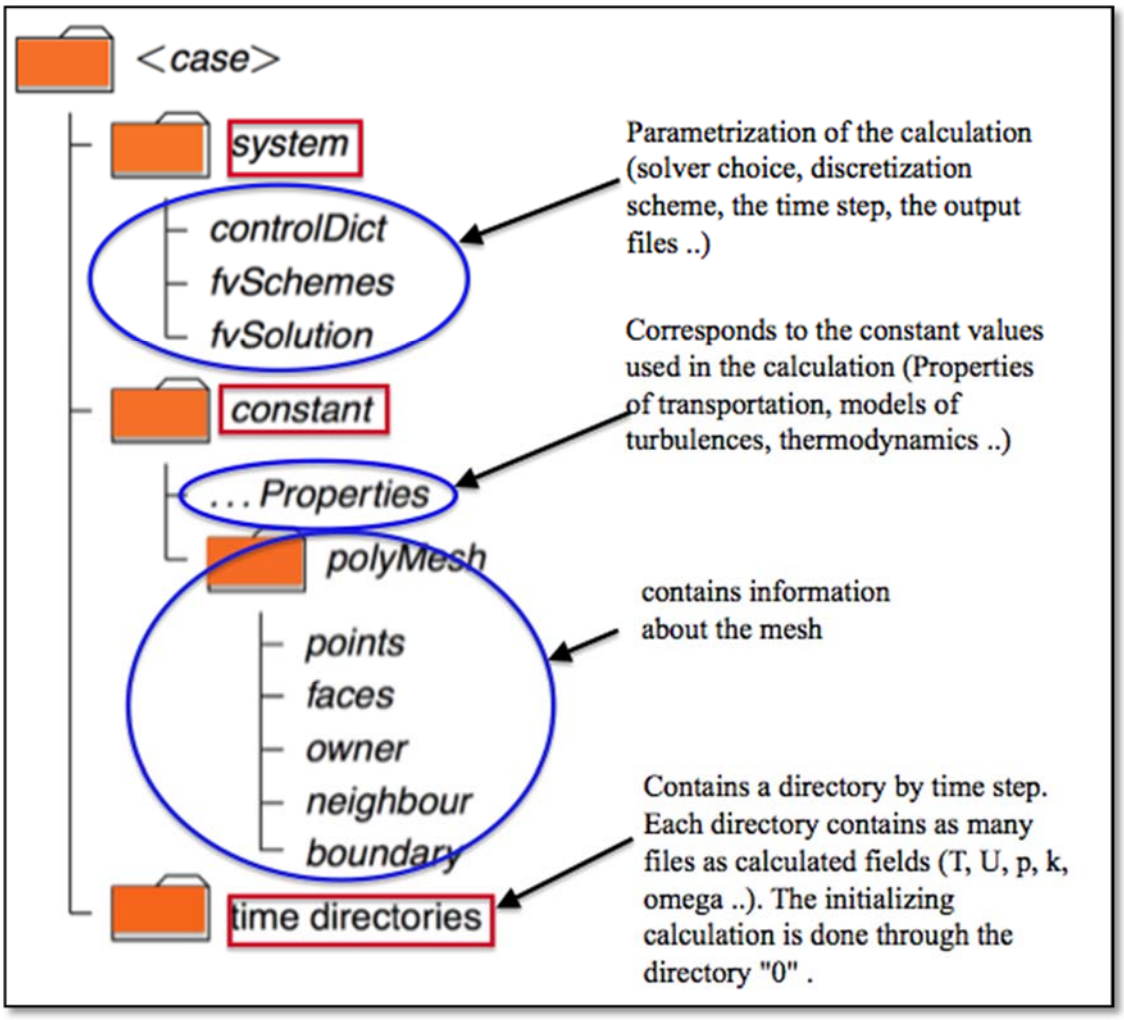

Figure 4.3: Diagram of General Structure of OpenFoam case (User Manuel OpenFoam).

4.2.4. Folders Description

4.2.4.1 "0" Folder.1

This folder contains the initial values and boundary conditions of different sizes. The boundary conditions in OpenFoam are the most delicate point. It is a list of patches, each of which encloses a set of faces and labels with the associated boundary condition. These patches clearly must contain only boundary faces and no internal faces. Also they are required to be closed. Therefore, the sum of all boundary face area vectors will be equal to zero machine tolerance. The role of the

boundary in the modelling is not just in the geometry, but is an integral part of the solution. Each variable to solve (U, p, k...) by the solver must be initialized in all areas of the event and within the domain. It should be noted that any border is generally divided into a set of so-called "patches". The boundaries of the mesh are given in a list named “border.” It was divided into patches, so the boundary was applied on the patch not on the surface. Each patch can contain one or more closed areas of the border in question which may not be physically connected. There are three attributes that can be associated to a "patch".

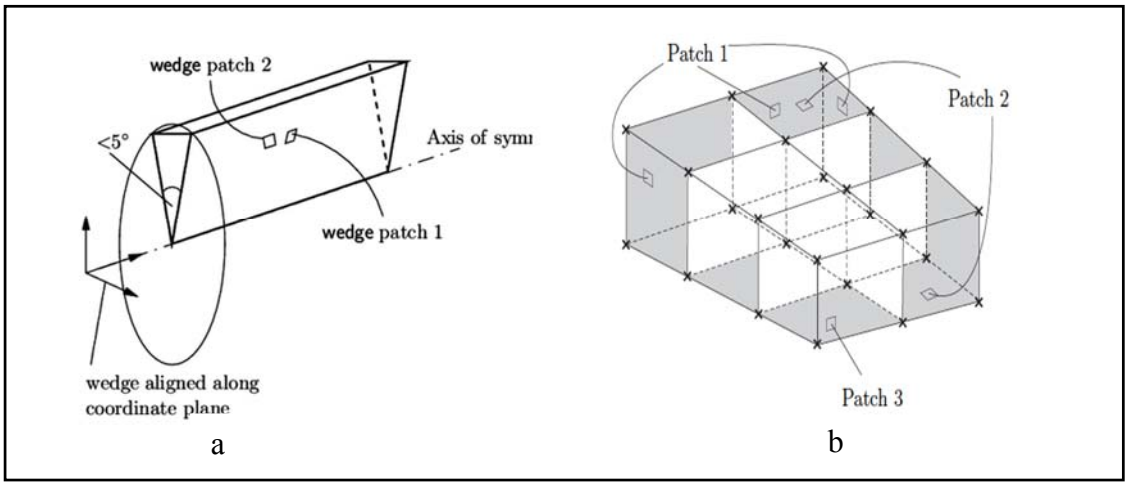

Figure 4.4: (a) Axisymmetric geometry (b) Each patch is constructed from a slide and word (http://www.openfoam.org/docs/cpp/)

- Base Type:

This attribute is purely described as geometrical or in terms of data (Figure 4.4). It is defined in the boundary file located in the constant subfolder “Polymesh.” This information is useful for the construction of mesh geometry. It should be noted that for this attribute, all patches are of the "patch" type, except those with geometric constraints: empty, symmetryPlane, wall, wedge, cyclic and processor. More specifically, 1 and 2 dimensional problems use the empty patch type and axi-symmetric problems use the wedge type (Figure 4.4). The meaning of each type of patch is briefly given below.

- Patch: Concerns a border that contains no geometric or topological information (e.g. an input

or output) (Figure 4.5).

- Empty: As OpenFoam generates 3D meshes; when the users want to solve a 2D problem, they have to specify an empty special condition on the borders that requires no solution.
- Cyclic: Can treat two patches to be physically connected. This is useful for repeated geometries (a bundle of tubes for example).
- Processor: This option allows dividing the grid so that each part is processed by a processor if the code is running in parallel, which is convenient for complicated geometries with a heavy mesh.
- Primitive and Derived Type: Both attributes are specified in the folder 0 for each size. Obviously these types are different depending on the size. Speed and pressure will not have the same condition in the same border.

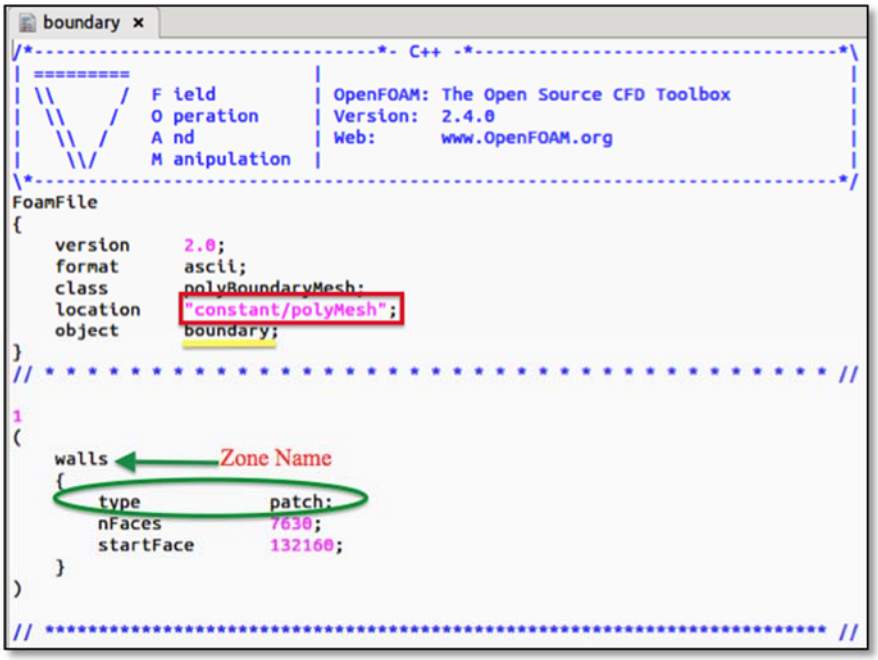

Figure 4.5: Boundary file related to the case study of this project

- The type of boundary of computational domain used in this system is rigid wall, as described in this OpenFoam file: constant/polyMesh/walls (Figure 4.5).

4.2.4.2. Constant Folder

This folder contains the necessary parameters for the mesh and constants of the problem (fluid properties...). The mesh generation is done in the subfolder "Polymesh," and the definition of the problem is constant in files properties, so the double functionality of this folder is described in the two points mentioned below:

1) Mesh generation

Above all it must be noted that OpenFoam only takes 3D meshes (if the problem is 2D, we must create a thick mesh). As has already been mentioned, OpenFoam offers two mesh tools: blockMesh and snappyHexMesh. The first is intended to create a structured mesh from one or more geometric blocks juxtaposed against each other. This type of grid is made from a blockMeshdict file. BlockMesh reads this file, then generates the mesh and writes the data of the mesh: the files points cells and boundary constant into the same directory: *constant / Polymesh /*. The principle of this tool is to break the geometry of the field by one or more three dimensional hexahedral blocks. The edges of the blocks may be lines or arcs. Each block of the geometry is defined by eight vertices, one at each side of the hexahedron. It is also possible to generate blocks of less than eight vertices (by folding one or more pairs of vertices) (Figure 4.6). This set of vertices provides a list of peaks. The first number is along X, the second is along Y and the third is along Z.

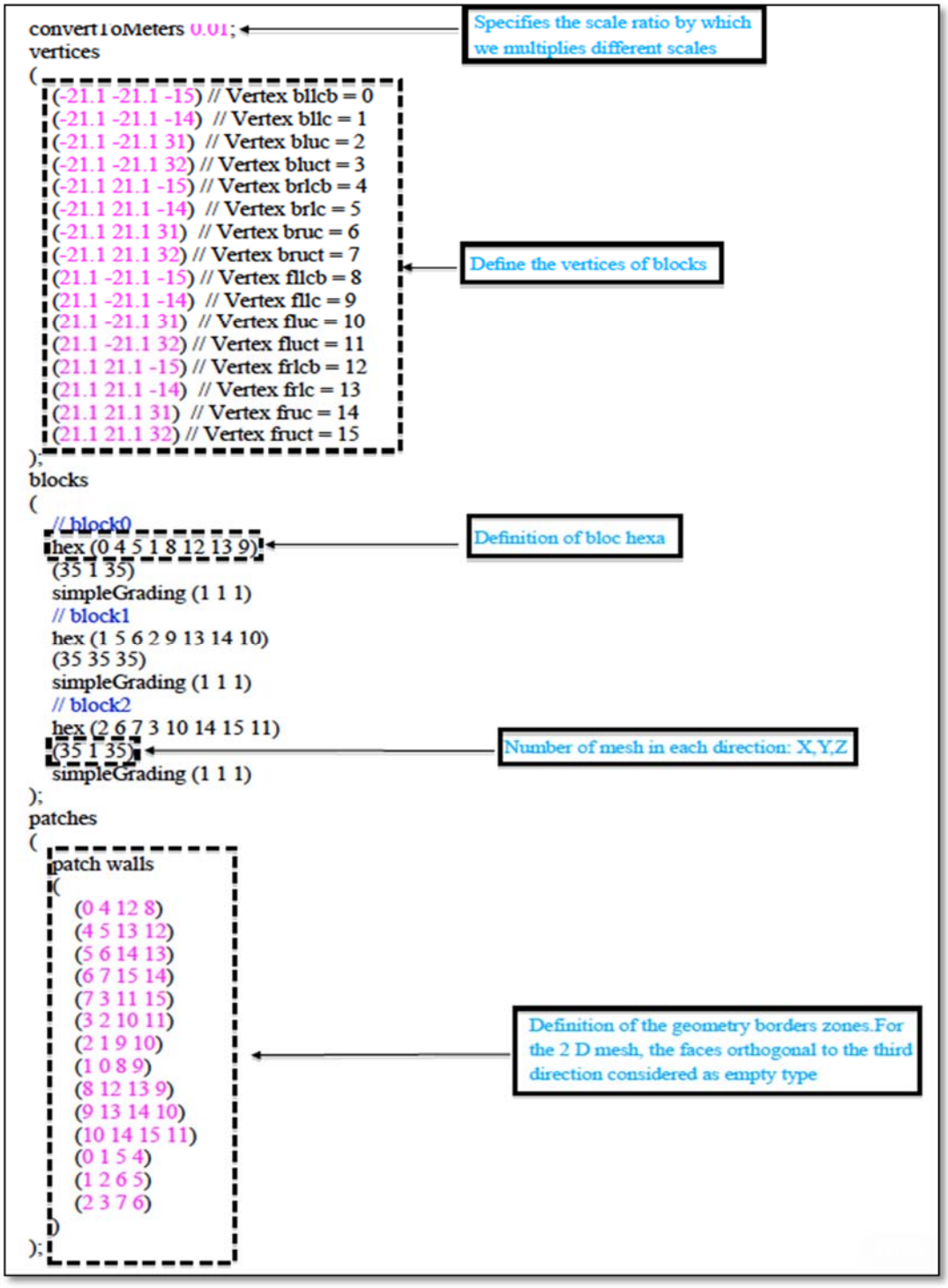

Figure 4.6: BlockMesh file related to the case study of this project

2) Properties Files

These files are used to inform the solver about the flow properties. They can be placed into two categories:

a) The files containing physical, thermal and energetic properties of the system, for example: Transportproperties, mixtureproperties, Thermophysicalmodel etc. In this study, Transportproperties was the file that was used to describe the flow proprieties. In OpenFoam, each measurement should be given with its unit. For this, an exponent is given to each international unity in the bracket. For example, as described in Figure 4.7, the kinematic viscosity (nu) and the density (rho) for each phase of the water are described respectively by the following brackets:

nu [0 2 -1 0 0 0 0] $1e^{-06}$ and rho [1 -3 0 0 0 0 0] 998.2

The unit must be given in the order described in Table 4.2:

Table 4.2: Description and order of the unit presented in the transports Proprieties file.

Order	**1**	**2**	**3**	**4**	**5**	**6**	**7**
Propriety	Mass	Length	Time	Temperature	Quantity of Materiel	Flux intensity	Light Intensity
Unit (SI)	Kg	m (meter)	s	K (kelvin)	mol	A (Ampere)	Cd (candela)

So the unit of (nu) and (rho) can be read respectively by the OpenFoam solver as:

$m^2.s^{-1} = m^2/s$ and $Kg^1m^{-3} = Kg/m^3$

Figure 4.7: transports Proprieties files related to the case study of this project.

b) The files that contain information on turbulence modelling (Figure 4.8). The file

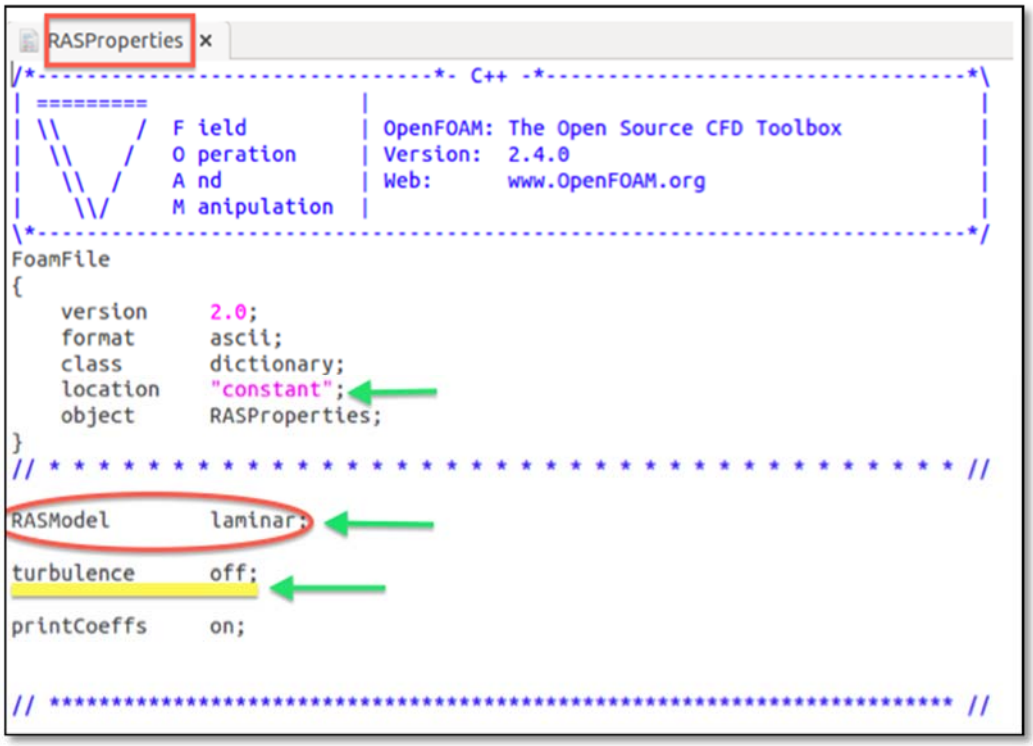

Figure 4.8: RASProprieties file related to the case study of this project.

turbulenceproperties defines two modelling approach RANS (Reynolds-Averaged Navier-Stokes equations) and LES (Large Eddy Simulation). Both of them should be specified in the file RASproperties.

4.2.4.3. System Folder

This folder contains three essential files to run a simulation with OpenFoam.

1) The file Controldict:

   This file is used to set the time step and the creation of the database. The file syntax is presented in Figure 4.9. All of the content of this file is detailed in the following Table 4.3.

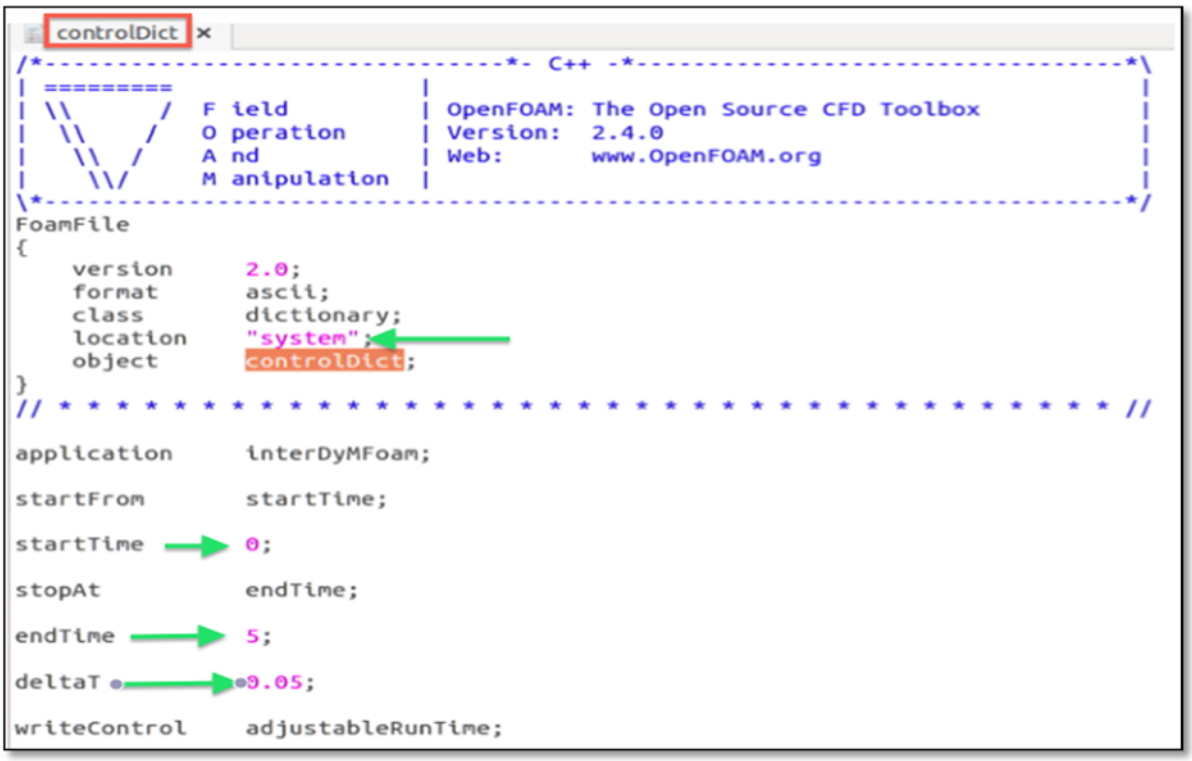

Figure 4.9: controlDict file related to the case study of this project

Table 4.3: Description list of the Controldict file content (http://www.openfoam.org/docs/cpp/)

Keyword	Description
Application	Defines the solver used (e.g.interDyMFoam).
Startfrom	The type on which the solver will hang.
Starttime	The time for which the solver will hang on to start the iterations.
StopAt	Determines the type which the solver will build to stop iterations.
endTime	The time at which the solver will stop.
deltaT	Defines the time step of the simulation.
writecontrol	Determines the type to generate a temporal folder, for example generate a report every n time "time step" or simulated n seconds "runtime".
writeinterval	Determines the number of time steps or simulated seconds between two time records.
purgeWrite	Specifies the number of time to keep files on the hard disc as the iterations.
writePrecision	Parameterizes the accuracy of the output data (Another advantage over fluent example).
writeCompression	Chooses whether the user wants to generate output files compressed or not (save memory).
timeFormat	Chooses the format of the names of the time records.
runTimeModifiable	This interesting option to make instant and ongoing iterations and changes to this file "controdict".

2) The file fvschemes:

This file (Figure 4.10) allows the choice of discrete numerical schemes for solving partial differential equations. In this file, the user determines the method of solving mathematical operators (divergence, laplacian, gradient) and the type of interpolation values. OpenFoam offers a wide choice both for the type of interpolation (default linear example), and for the type of discretization. The different schemes and the particularity of each can be found with more detail and information in the following link:

http://www.OpenFoam.org/docs/user/fvSchemes.php#x20-1070004.4

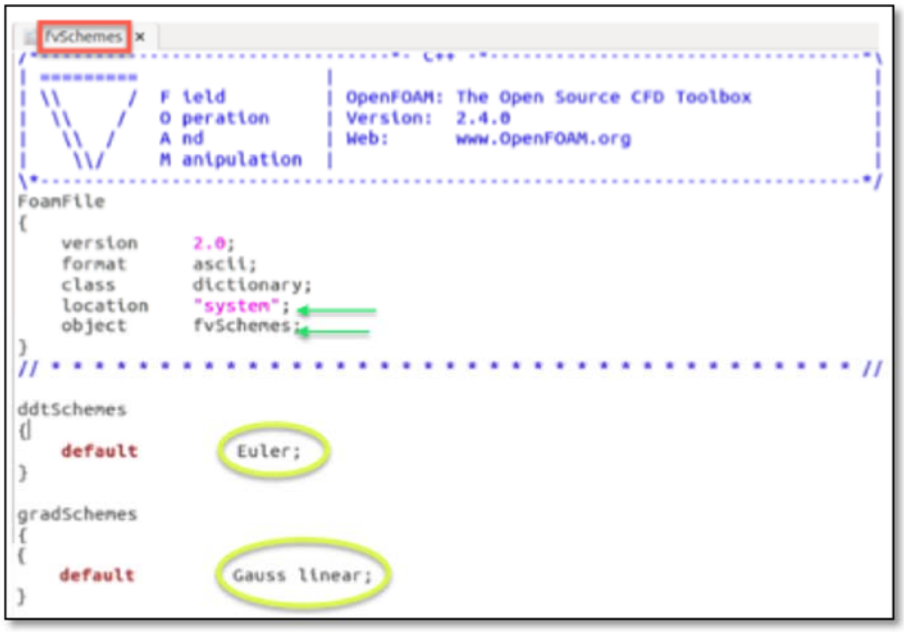

Figure 4.10: fvShemes file related to the case study of this project

3) The file fvSolution:

The fvSolution file specifies the convergence criteria for different sizes (Figure 4.11). In fact, in this file the user can set the solver for discretization of a given magnitude, the tolerance and the algorithms of control. Tolerance represents the value of the residue from which the iterations cease. The reltol represents the ratio of final residue to the initial residual below, which the iterations stop. Usually this parameter is zero, which means that the residue falls below tolerance. Before we solve an equation for a given size, the initial residue is based on the existing values of this magnitude. After each iteration, the residue is re-evaluated. It should also be noted that the iterations stop if one of the following conditions is true:

- The residue is less than the value of the tolerance of the solver.
- The ratio of the current residue on the original residue falls below the reltol.
- The number of iterations exceeds a maximum number maxilter.

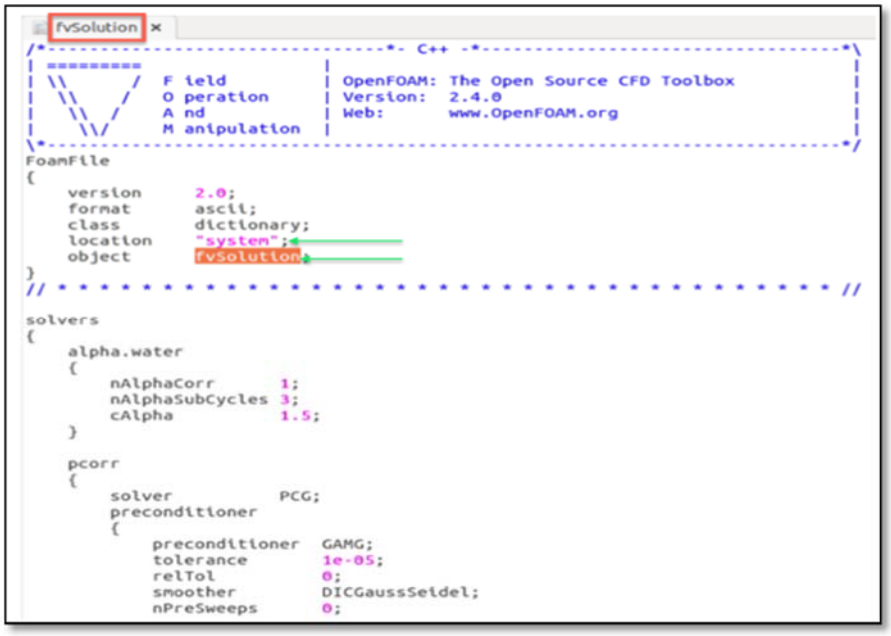

Figure 4.11: fvShemes file related to the case study of this project

4.2.4.4. Visualization and post-processing tool

The main post-processing tool provided by OpenFoam is paraFoam (Figure 4.12). This open source tool is actually a script that launches the reader module supplied with OpenFoam. It is implemented as one of the OpenFoam utilities only by typing paraFoam in the case file in question. This tool is very powerful; it can display the fields, vectors, contours, streamlines, and it makes it easy to create animations and track the evolution of a given size along any line in the field of study. It is also easy to extract data in column format and export it to treat from another tool (matlab for example). OpenFoam also provides access to the tailings during the iterations for each variable to solve. For this, following command just needs to be typed into the study case file:

PyFoamPlotRunner.pyinterDyMFoam, for example, and the name of the solver interDyMFoam.

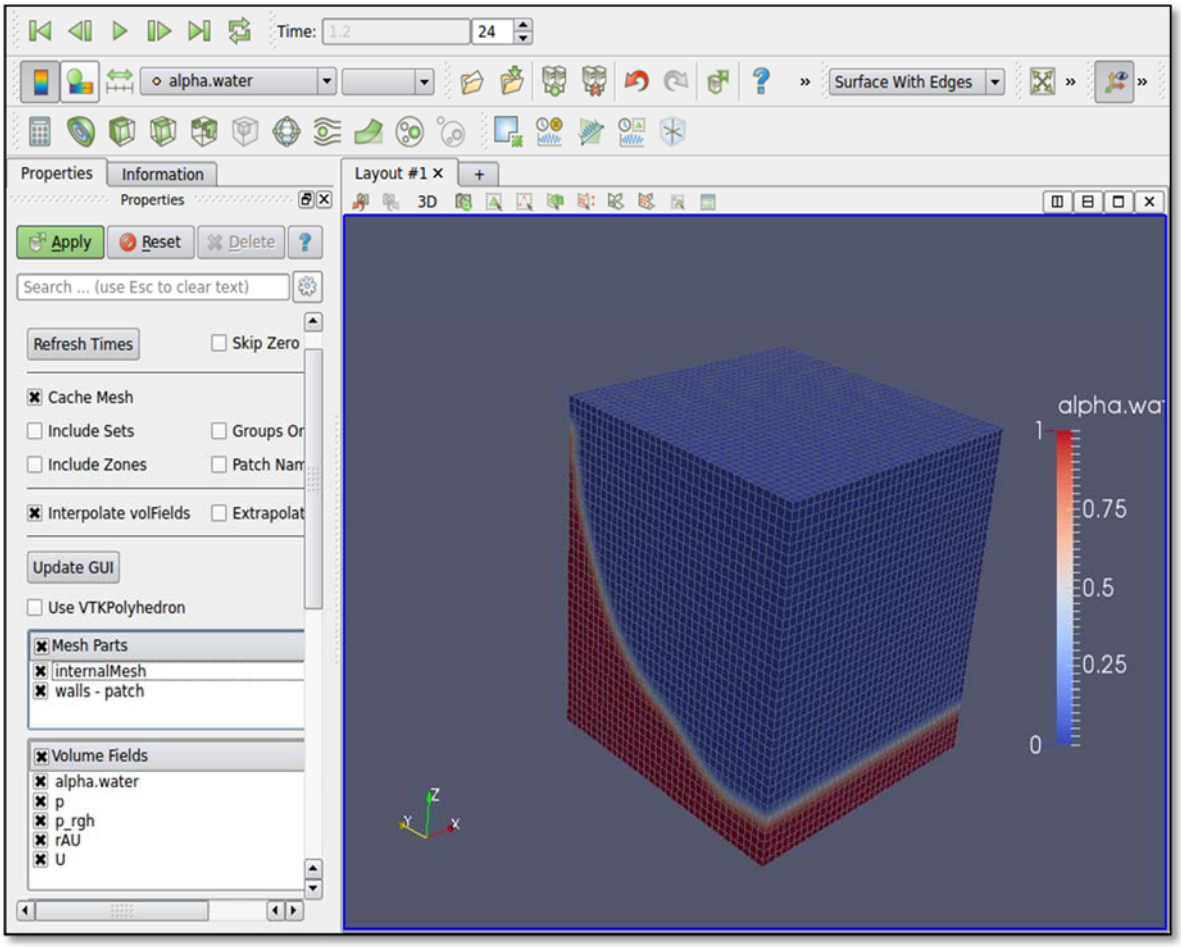

Figure 4.12: ParaFoam window

4.2.5. Numerical Results

As mentioned, our interest is in two parameters related to the sloshing behavior of water contained in a square tank. These parameters have to be investigated using OpenFoam via a numerical simulation method in this study. The corresponding parameters are the sloshing period (T) and the maximum height (D_{max}) of water elevation during the sloshing. Using the OpenFoam software, we end up with the results described in table 4.4.

Table 4.4: Numerical values of maximum elevation D_{max} at different periods of excitation

T (s)	D_{max} (m)
0.5	0.298
0.7	0.457
0.81	0.395
1	0.470
1.6	0.233
2	0.195

4.3. Comparison Between Numerical and Experimental Results

The objective of this section is to examine the CFD (OpenFoam) capacity to predict the behavior of the free surface related to the fluid in the tank when it is subjected to sinusoidal motion. The results of the OpenFoam software and the visualization of experimental flow visualization can be used to investigate a 2D flow field of the water-air interface in a moving square container. The method to track interface of the maximum sloshing motion at different times of oscillation given by the OpenFoam simulation is described in Appendix C. Using the reconstructed image presented in Figure 4.13, one can notice that the experimental profiles at the maximum sloshing are very close to the CFD results. Then a reasonable agreement is observed between the CFD and the experimental results summarized in Figure 4.13. In addition, the maximum experimental height of the sloshing water surface is close to the stimulated results by OpenFoam. This comparison will be discussed in more detail in the discussion part of this chapter. Finally, the behavior of the water when it oscillates by the resonance value of period (T=0.81s) is summarized in Figures 4.15 and 4.18.

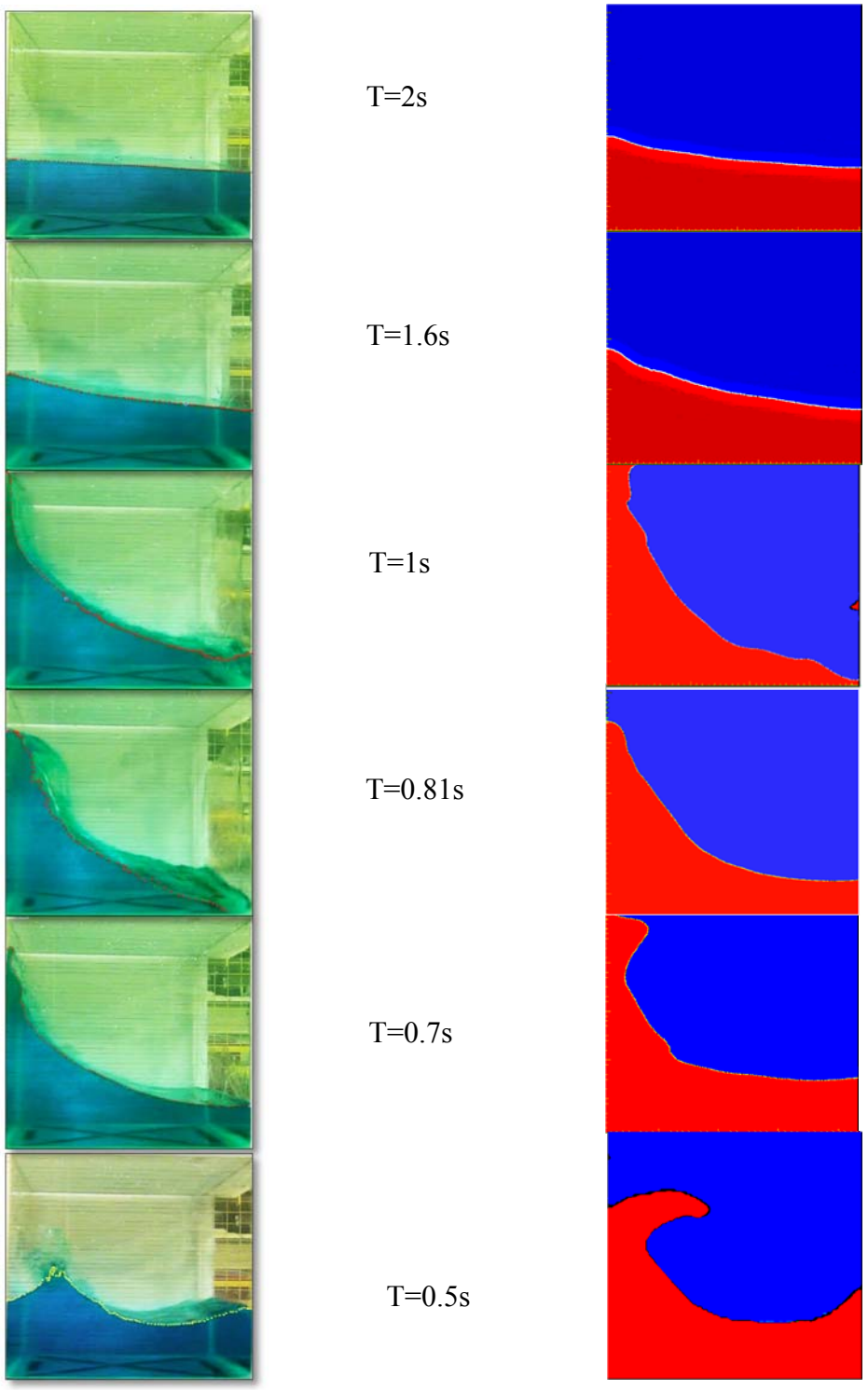

Figure 4.13: Comparison between the experimental and the CFD results as regards the maximum elevation of the sloshing water and the geometry profile.

By the same procedure of analysis, from the snapshots of the OpenFoam simulation, the profiles of the water at the maximum level of sloshing were recorded and plotted in the same graph (see Figure 4.14). While this graph does not have a common point, as was observed in the experimental results, it does represent a noticeable similarity to the previous graph (see Figure 3.8) related to the experimental section. The source of errors can be due to many factors and will be cited in the discussion section.

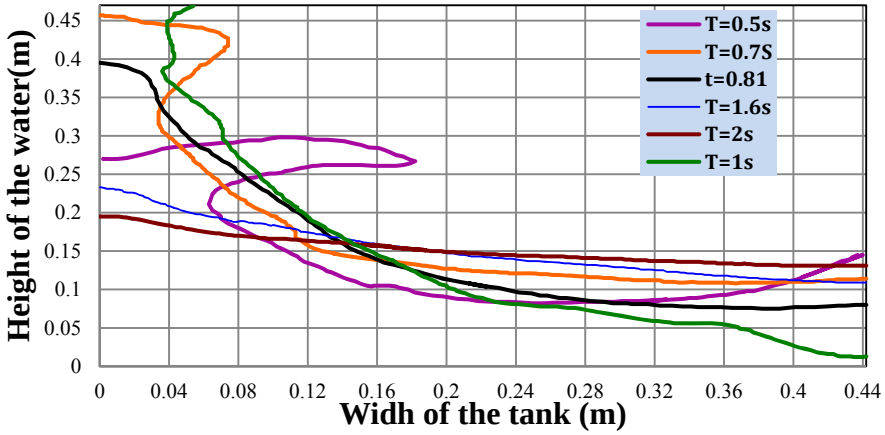

Figure 4.14: Maximum water surface elevation (m) for CFD simulation at different Excitation periods and at fixed Displacement D=5cm.

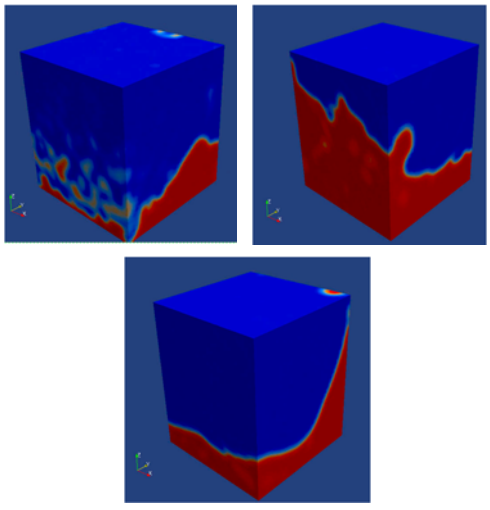

Figure 4.15: The behavior of the tank at the fundamental period oscillation of the tank in 3 D simulation (From ParaFoam)

4.4. Discussion

The results of the two methods (experimental and numerical) are presented in Table 4.5.

Table 4.5: Experimental and numerical results of Dmax

Period N	T (s)	D_{max} Experimental (m)	D_{max} Numerical (m)
1	0.5	0.232	0.298
2	0.7	0.400	0.457
3	0.81	0.383	0.395
4	1	0.458	0.470
5	1.6	0.195	0.233
6	2	0.163	0.195

This table shows that the numerical results were closer to experimental data than the results of the analytical solution at (Figure 4.16 and 4.17) because these two methods are based on three dimensional space and nonlinear analysis while the analytical solutions are based on two dimensional space and linear analysis (Figure 4.18).

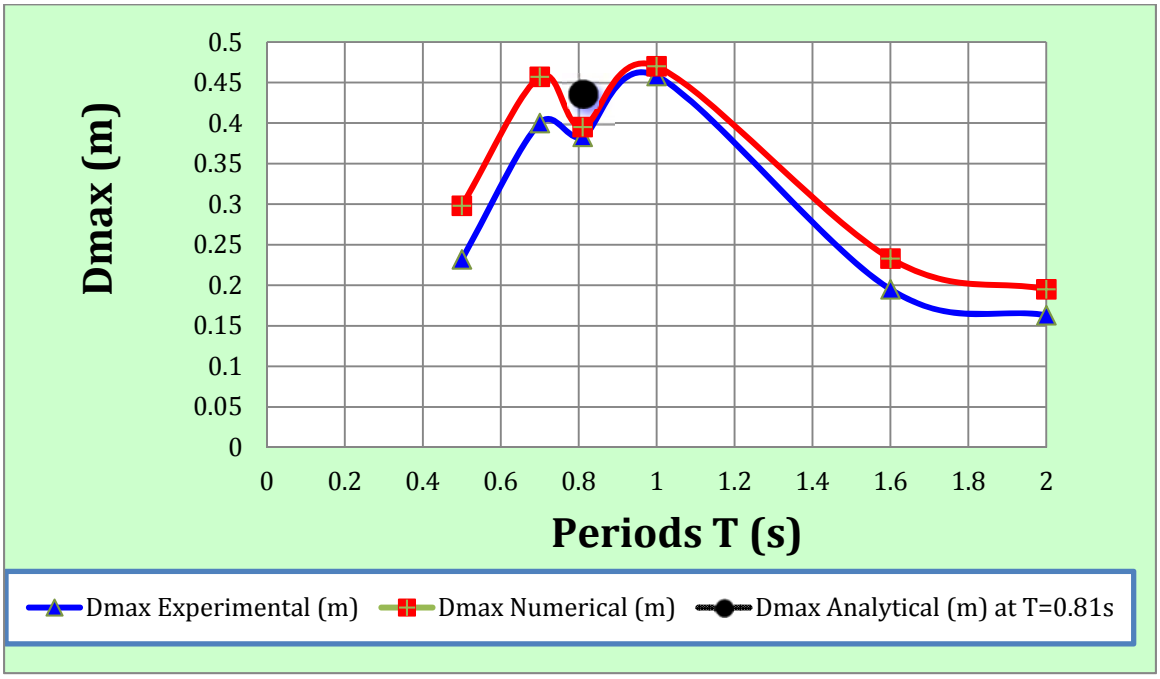

Figure 4.16: The maximum height of sloshing (Dmax) found by the numerical and the experimental methods t different periods T.

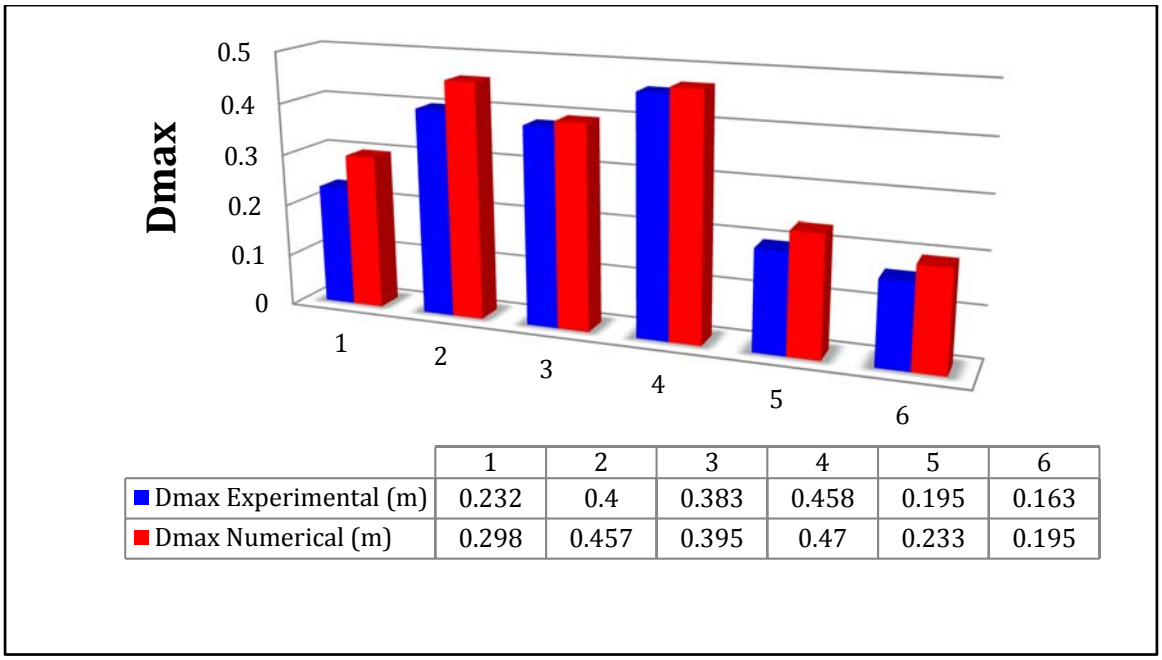

	1	2	3	4	5	6
Dmax Experimental (m)	0.232	0.4	0.383	0.458	0.195	0.163
Dmax Numerical (m)	0.298	0.457	0.395	0.47	0.233	0.195

Figure 4.17: D_{max} Experimental vs D_{max} Numerical

Figures 4.16 and 4.17 present the solution to D_{max} found by the experimental and numerical methods and, as can be observed, there is a reasonable agreement between the two methods.

It should be noted that the camera used for the experimental investigation did not show the entrapment of the water due to limitations on its speed. For this case, it is observed that the numerical values are higher than the experimental results at different periods of oscillation. These results were compared using the relative errors between the experimental and numerical values of the D_{max} at each period of oscillation. These errors are calculated using the equation (4.16) and are summarized in Table 4.5.

$\Delta_{R\ (N/E)}$: The relative error between the numerical and the experimental results concerning D_{max} values is:

$$\Delta_{R\ (N/E)} = \frac{D_{\max(Numerical)} - D_{\max(Experimental)}}{D_{\max(Numerical)}} \times 100\% \quad (4.16)$$

Table 4.6: **Relative errors between Experimental and Numerical results**

Period N	T (s)	$\Delta_{R\,(N/E)}$(%)
1	0.5	22.1
2	0.7	12.5
3	0.81	3.0
4	1	2.6
5	1.6	16.3
6	2	16.4

The Table 4.5 shows that the relative error between the experimental and the numerical results ranges from 2.6% to 22.1%. As mentioned, these values are reasonable considering the source of the errors (linearity and space of study). Therefore, this CFD approach leads to a successful solution for D_{max}. On the other hand, the comparison between the analytical solution and the CFD results related to the D_{max} at the resonance period (T=0.81s) is also determined by using the relative error $\Delta_{R\,(N/A)}$ calculated by the equation (4.18).

$$\Delta_{R\,(N/A)} = \frac{D_{\max(Analytical)} - D_{\max(Numerical)}}{D_{\max(Analytical)}} \times 100\% \quad (4.18)$$

Therefore

$$\Delta_{R\,(N/A)} = \frac{0.470 - 0.436}{0.470} \times 100\% = 7.2\%$$

This value ($\Delta_{R\,(N/A)}$) is higher than the value of $\Delta_{R\,(N/E)}$(Relative error between numerical and experimental results). As mentioned, the reason is that the analytical solution is based on linear analysis and on two dimensional space, while the numerical solution is based on nonlinear conditions. Recalling from chapter three that the value of sloshing height under the nonlinear condition can be 10~25% larger than the determined under linear condition (Shimada et al. 1988), one can confirm the reasonable accuracy of the numerical method. The three results of D_{max} at the fundamental period of oscillation are shown in Figure 4.17, which shows the

accuracy of the CFD result compared to the analytical and experimental solution at the fundamental period of oscillation.

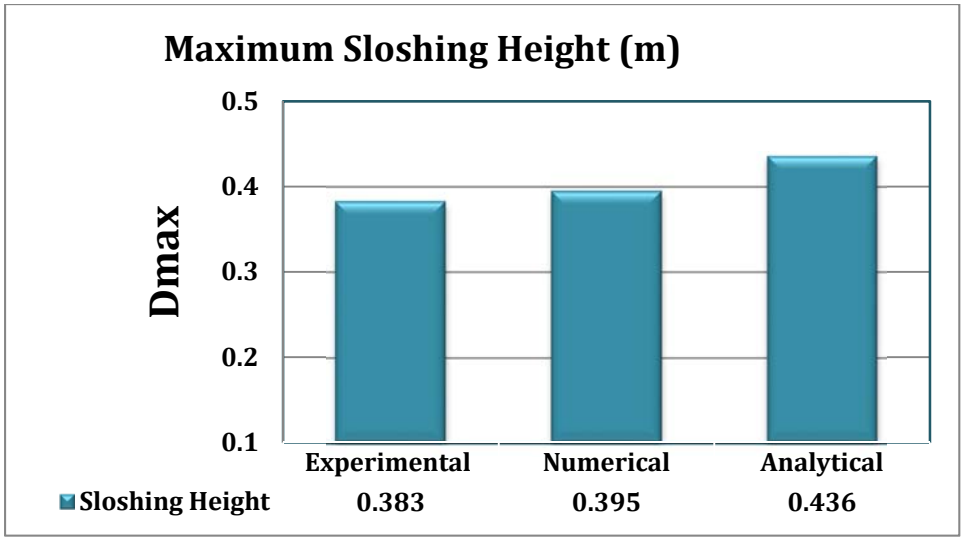

Figure 4.18: D_{max} value related to experimental, numerical and analytical solution at T=0.81s 11(Fundamental period)

4.5. Conclusion

In this chapter, we used the CFD software OpenFoam as a numerical tool to stimulate the behavior of the sloshing water tank under harmonic oscillations. Two dynamic parameters (T: fundamental period and D_{max}: maximum sloshing height) were investigated in Chapter 3, but by using analytical and experimental methods. The comparison between different results related to different methods was made in the previous section. Some important points can be mentioned here based on the CFD computations, experimental visualizations and analytical calculations. First, it was observed that the CFD results show a reasonable degree of accuracy with those from experimental investigations. Second the geometry of the surface profile at the maximum height of sloshing presented in Figure 4.13 was found to have a higher similitude. In addition, the maximum height of sloshing D_{max} at different periods is in good agreement and the relative errors ranged between 2.6% and 21.2%. The average value of these errors was 12.2%. However,

for the comparison between the analytical and the experimental solution at the fundamental period of oscillation, the error was higher due to the assumptions of the linearity and the two dimensional space. Despite that, the error was limited to 7.2%, representing a logical and reasonable value. In conclusion, one can reasonably confirm the accuracy of the numerical method based on OpenFoam simulations to justify the values of the natural period and the maximum sloshing height found analytically.

Chapter 5. Summary, Conclusion and Recommendation for Future Works

5.1. Summary

Various studies have been reported in the literature to investigate the dynamic behavior of liquid containing structures for different shapes and using different methods of analysis. According to the previous research studies, most cases used the cylindrical and rectangular shapes. These previous research projects have been mainly conducted under some different assumptions and different design cases. However, it should be noted that still unsolved design problems with additional factors remain to be investigated including square shaped tanks, type of excitation (random, horizontal, inclined…), three dimensional geometry analysis, rigidity or flexibility of the walls, linear and nonlinear sloshing theory and the type of base fixity, etc. The present study was performed to investigate two important parameters that have a direct effect on the stability and performance of excited liquid containing structures, which are the natural period and the sloshing height of the liquid inside the tank.

It should be mentioned that some limitations and assumptions were taken into consideration during this study. They are described in detail in Chapters three and four. For example, the excitation was limited to harmonic and horizontal motion. The tank was assumed to be square and fixed on the ground. The height of the water and the amplitude of the tank excitation at different periods were kept constant during the experimental tests.

The major concern of this work was to investigate the two dynamic parameters using analytical, experimental and numerical methods with a comparison of the obtained results. The analytical

method is based on analytical solutions obtained by Housner (1963). These equations concern the natural period and the maximum sloshing height. While this method was adopted by different codes and guidelines, it still remains limited for linear conditions of sloshing and for two dimensional space cases. For this reason, an experimental investigation was planned to predict these parameters under realistic behavior of sloshing, which represent nonlinear conditions and three dimensional space. In addition to these two investigations, a numerical method (CFD method) was used, first to compare the results found by the analytical and experimental method, and second to check the validity and accuracy of this numerical method based on OpenFoam software.

5.2. Conclusions

Based on the three methods of analysis and their results reported in this thesis, the following conclusions can be drawn:

1. In design, it is very important to know the liquid free surface natural periods of the LCT subjected to different types of excitations. The principal goal is to keep the natural period of the liquid away from any resonance conditions.

2. It was observed in the experimental tests that the height of sloshing was less important than that created by the natural period if we move below or above the resonance period value.
3. However, in the case where the excitation period is close to the fundamental period, the motion of the water changes and water exhibits nonlinear behavior with very large amplitudes.

4. The natural period value of the liquid inside the tank proposed by the analytical method shows a good agreement with the experimental investigation related to the resonance period value.

5. At the fundamental period of excitation, the water moves on a circular direction and with higher speed. Furthermore, the quantity of mass travelling around the reservoir hits the corners periodically. These collisions between the mass of moving water and the corners of tanks show the severity of this condition known as resonance.
6. On the other hand, the maximum elevation of the sloshing water (D_{max}) during the natural periods of excitation was calculated analytically and compared with the experimental results. The relative error between the two solutions was around 6.4%, which is reasonable considering the source of errors and many factors involved. For example, the two dimensional geometry and the linearity of the analysis were factors affecting the accuracy and the concordance between these methods.

7. It should be mentioned that during the 1983 Nihonkai-Chubu earthquake, the sloshing height under nonlinear conditions was determined to be about 10~25% larger than the value determined under linear condition (Shimada et al. 1988). Taking this effect into account, the 6.4% value of the relative error between analytical (linear) and experimental (nonlinear) values can be considered negligible and the difference can be considered acceptable.
8. In general, the experiment successfully stimulated the sloshing height. Therefore, the experimental approach can be considered as a good way to compare and to obtain the fundamental period as well as the maximum height of sloshing.

9. The CFD simulation demonstrated that OpenFoam can be a valuable tool for the identification of the resonance period and the maximum height of the liquid sloshing inside an excited tank with harmonic motion. The comparison was made first between the analytical and the numerical solution concerning the value of the natural period. Using the OpenFoam simulation and the experimental investigation, it was shown that the behavior of the water was similar in numerical and laboratory models and the water inside the tank moved in a rotary motion. Second the relative error concerning the sloshing height at the natural period of oscillation was equal to 6.4% between the analytical and the experimental results (Figure 4.18), 7.2% between the analytical and the numerical results and 0.3% between the experimental and the numerical results. In the same context, the relative error between the experimental and the numerical results was 3% at D_{max}. This shows the better consistency of the experimental and numerical results compared to analytical results. This consistency is explained by the fact that the experimental and numerical analyses were conducted under the same conditions of study regarding the dimensional space (3D) and the type of analysis (nonlinear).
10. This comparison was expanded to other values of excitation periods. These values, as mentioned, were chosen above and below the natural period value. The relative errors between the experimental and numerical results ranged between 2.6% and 22.1%, with an average equal to 12.2%. Therefore, it has been shown that OpenFoam can be successfully used to stimulate the natural period and the maximum sloshing height of the water during harmonic excitation.
11. In addition, from the experimental videos, snapshots of the profile of the water at the maximum level of sloshing were recorded and plotted in the same graph. It was observed that

these graphs intersect at one point: I (X=0.175m, Y=0.150 m). The value of depth at Y= 0.150 m corresponds to the height of the water at the initial condition, so this point remains at the same position when the excitation motion changes its period value. Furthermore, if the excitation period meets the natural period of the tank, this point moves to a lower position.

12. By the same procedure of analysis, using the OpenFoam animation, the profile of the water at the maximum level of sloshing during the different periods of oscillation was drawn in the same graph. This graph does not show a common point as we had observed in the experimental result, but it does confirm an important convergence to compare to the experimental results.

13. This study shows reasonable agreement between the analytical, numerical and experimental results for both non-resonant and resonant periods of excitation concerning the natural period and the sloshing height. Therefore, we can confirm that the objectives of this study were met. Consequently, the numerical method using OpenFoam software represent a successful tool to validate and to justify either the analytical or the experimental results.

14. We can find the natural period first analytically and can confirm its value by using OpenFoam simulation to justify the results since this numerical method show an accurate solution when compared to an experimental result.

5.3. Recommendations for Future Works

Based on the computed results, the following recommendations on seismic design of square liquid containers are proposed:

1. A limited number of parameters in this work were investigated (resonance period and maximum sloshing water height). Future work can be undertaken to investigate the effects of other parameters related to the liquid properties (pressure distribution on the wall, roof and base, dynamic forces and moments…) or to the tank characteristics (flexible walls, floating roof, different types of base isolators…).
2. Real time history response recorded from previous earthquakes or random excitation can be chosen for the shaking table, instead of the horizontal harmonic oscillation.
3. The results presented in this study are only limited to tanks with rigid floors resting on rigid foundations. As a suggestion for future studies, such an analysis can be extended to semi rigid base condition by taking the soil structure interaction effect into consideration. It should be noted that the analytical equation of the natural period depends on the characteristics of the soil profile.
4. Additional studies can be focused on simulating the resulting pressure on tank roofs and walls due to the impact of the free surface sloshing.
5. It also recommended to use different levels of water to find a corresponding relationship between the height of the water and its period of resonance.
6. At the point I (X=0.175m, Y=0.150m) already mentioned, we can install a perforated screen inside the tank perpendicular to the direction of the excitation to see if we can decrease the sloshing height of the water as well as the pressure on the roof and on the walls. This is useful because it is a common point for the water profile at different periods of excitation, from which the water moves beyond its equilibrium position.

Bibliography

ACI 318. (1995) “Building Code Requirements for Reinforced Concrete (ACI 318-95).” and commentary (ACI 318R-95).

ACI 350. (2006) “Code requirements for environmental engineering concrete structures (ACI 350-06) and “Commentary (ACI 350R-06).” American Concrete Institute.

ACI 350. (2006) “Seismic design of liquid containing concrete structures (ACI 350.3-06) and “commentary (ACI 350.3R-06)” American Concrete Institute.

ACI 371R-08 Guide for the Analysis, Design, and Construction of Elevated Concrete and composite Steel-Concrete Water Storage Tanks.

API 650:2012 Welded Steel Tanks for Oil Storage, “American Petroleum Institute”.

API 653:2003 Tank Inspection, Repair Alteration, and reconstruction, “American Petroleum Institute”.

ASCE/SEI 7-10 ”American Society of Civil Engineers, Structural Engineering Institute, Minimum Design Loads for Buildings and Other Structures” Reston, (VA): 2006.

Aslam, M. (1981). “Finite Element Analysis of in Axisymmetric Tanks Earthquake-Induced sloshing” international journal for numerical methods in engineering, vol. 17,159-170 San Francisco, U.S.A.

AWWA Standard D100, American Water Works Association, Welded carbon steel tanks for water storage.

Brar, G. S., and Singh, S. (2014). “An Experimental and CFD Analysis of Sloshing in a tanker,” 2nd International Conference on Innovations in Automation and Mechatronics engineering (ICIAME), Procedia Technology, 14: 490 – 496.

Calugaru, V., Mahin, S.A. (2009). “Experimental and Analytical Studies of fixed base and

Seismically Isolated Liquid Tanks, "Journal of Pressure Vessel Technology 173 (3).

Chen, Y.H., Hwang, W.S., and Ko, C.H. (2007)."Sloshing Behaviors of Rectangular and Cylindrical Liquid Tanks Subjected to Harmonic and Seismic Excitations." Earthquake Engineering & Structural Dynamics, October 10th, 36: 1701–1717.

Chen, Y.H., Hwang, W. S., Ko, C. H. (2000). " Numerical Simulation of the Three Dimensional Sloshing Problem by Boundary Element Method," Journal of the Chinese Institute of Engineers, 23 (3): 321-330.

Cho, K.H., and Cho, S.Y. (2007). "Seismic Response of Cylindrical Steel Tanks Considering Fluid Structure Interaction" Korean Society of Steel Structures 7 (2007), 147-152.

De Angelis, M., Giannini, R., and Paolacci, F. (2010). " Experimental Investigation on the Seismic Response of a Steel Liquid Storage Tank Equipped with Floating Roof by Shaking Table Tests, " Earthquake Engineering and Structure Dynamics," 39(4): 377-396.

Design Recommendation for Storage Tanks and their Supports with Emphasis on Seismic Design (2010 edition), Architectural Institute of Japan.

Djermane, M., et al. (2014). "Dynamic Buckling of Steel Tanks Under Seismic Excitation: Numerical Evaluation of Code Provisions," Engineering Structures 70: 181–196.

Doğangün, A., and Livaoğlu, R. (2008). "A Comparative Study of the Seismic Analysis of Rectangular Tanks According to Different Codes," The 14th World Conference on Earthquake Engineering October 12-17, Beijing, China.

Dotoli, R., et al. (2006)."Sloshing Response of a LNG Storage Tank Subjected to Seismic Loading," 6th European LS-DYNA Users' Conference.

Figure 1.1: Refinery Tanks in Ichira Chiba Earthquake and Tsunami (Japan 2011- 9.0 magnitude quake). (http://www.dailymail.co.uk/news/article-1366395/Japan-tsunami earthquake-Rescuers-pick-way-apocalypse-wasteland.html).

Fluid Structure Interaction Effects on and Dynamic Response of Pressure Vessels and Tanks Subjected to Dynamic Loading," Part 1, (2007). The Steel Construction Institute.

Giannini,R., Paolacci, F., De Angelis, M., and Ciucci, M. (2008). "Shaking Table Tests Upon a Base Isolated Steel Liquid Storage", 14th World Conference on Earthquake Engineering, October. 12-17th, Beijing, China.

Gupta, R.K., and Hutchinson, G. (1988). " Free Vibration Analysis of Liquid Storage Tanks," Journal of Sound and Vibration 122(3): 491-506.

Hamda, F.H. (2000). "Seismic Behaviour of Cylindrical Steel Liquid Storage Tanks," Journal of Constructional Steel Research, 53: 307–333, London SW7 2BU, UK.

Haroun, M.A. (1983). "Vibration Studies and Tests of Liquid Storage Tanks." Earthquake Engineering and Structural Dynamics, 11,190-206.

Housner, G. W. (1963). "The Dynamic Behavior of Water Tanks." Bulletin of the Seismological Society of America, 53(2), 381-387.

Housner, G.W. (1957). "Dynamic Pressure on Accelerated Fluid Containers", Bulletin of the Seismological Society of America, 47:1,15-37.

Ibrahim, R.A. 2005. "Liquid Sloshing Dynamics: Theory and Applications." Cambridge University Press: New York, 2005.

Ibrahim. R.A., Pilipchuck. V.N., and Ikeda. T. (2001). "Recent Advances In Liquid Sloshing Dynamics" Applied Mechanics Reviews, Vol. 54, No. 2, pp. 133-199.

Ifrim, M., and Bratu, C. (1969). " The effect of Seismic Action on the Dynamic Behaviour of Elevated Water Tanks," Proceedings of the Fourth World Conference on Earthquake Engineering, B-4: 127–142, Santiago.

Ikeda, T., Harata1, Y., and Ibrahim, R. A. (2012). "Nonlinear Responses of Sloshing in Square Tanks Subjected to Horizontal Random Ground Excitation," MATEC Web of Conferences,1, 03006.

Isaacson, M. (2010). "Earthquake-induced Hydrodynamic Forces on Reservoir Roofs," Canadian Journal of Civil Engineering, 37(8): 1107-1115.

Jaiswal, O.R., Rai, D.C., and Jain, S.K. (2007). "Review of Code Provisions on Seismic Analysis of Liquid Storage Tanks." Earthquake Spectra, 23:1, 239–260, February Earthquake engineering Research Institute.

Jaiswal1, O.R., Kulkarni, S., and Pathak, P. (2008). "A Study on Sloshing Frequencies of Fluid-Tank System," 14th World Conference on Earthquake Engineering, October 12-17, Beijing, China.

Jin, B.M., et al. (2004). "Earthquake Response Analysis of LNG (Liquid Naturel Gas) Storage Tank by Axisymmetric Finite Element Model and Comparison to the Results of the Simple Model," 13th World Conference on Earthquake Engineering, Paper No. 394, August 1-6, Vancouver, B.C., Canada.

Khezzar, L ., Goharzadeh, A., and Seibi, A. (2007). "Liquid Sloshing in a Moving Rectangular Container Subjected to Sudden Impact," Costantine, Algeria.

Khezzar. L., Seibi. A., and Goharzadeh, A. (2009). "Water Sloshing in Rectangular Tanks – An Experimental Investigation & Numerical Simulation", International Journal of Engineering (IJE), Volume (3): Issue (2), 174-184

Kianoush, M.R., and Chen, J.Z. (2006).“Effect of Vertical Acceleration on Response of Concrete Rectangular Liquid Storage Tanks” Engineering Structures 28, 704–715.

Maekawa, A. (2012). “Recent Advances in Seismic Response Analysis of Cylindrical Liquid Storage Tanks,” INTECH Open Access Publisher, Institute of Nuclear Safety System, inc. Japan.

Malhotra, P.K., Wenk, T. and Wieland, M. (2000). “Simple Procedure for Seismic Analysis of Liquid Storage Tanks.” Structural Engineering International March, 197-201.

Molin, B., and Remy, F. (2013).“Experimental and Numerical Study of the Sloshing Motion in a Rectangular Tank with a Perforated Screen. ” Journal of Fluids and Structures. 43, 463-480.

Moslemi, M. and Kianoush, M.R. (2012). “Parametric Study on Dynamic Behavior of Cylindrical Ground-Supported Tanks. “Engineering Structures, September 42, 214-230, Toronto, Ontario, Canada

Moslemi, M., Kianoush, M.R., and Pogorzelski, W. (2011). “Seismic Response of Liquid-Filled Elevated Tanks” Engineering Structures, 33 (6): 2074-2084, Toronto, Ontario, Canada

NBC 2010 “National building Code Of Canada 2010”.

Praveen K. Malhotra. (2005). “ Sloshing Loads in Liquid-Storage Tanks with Insufficient Freeboard,” Earthquake Spectra, 21 (4): 1185-1192.

Royon-lebeaud, A., Hopfinger, A.E., and Cartellier, A. (2006). “Liquid Sloshing and Wave Breaking in Circular and Square-Base Cylindrical Containers,” J. Fluid Mech, 577: 467–494, February, Grenoble, France.

Shao, J.R., Li, et al. (2012). “An Improved Smoothed Particle Hydrodynamics (SPH) Method for Modeling Liquid Sloshing Dynamics,” Computers and Structures, 100-101:18–26.

Shimada, S., Noda, S., and Yoshida., T. (1988). “Nonlinear Sloshing Analysis of Liquid Storage Tanks Subjected to Relatively Long-period Motions ” Ninth Word Conference on Earthquake Engineering, August,2-9th, Tokyo, Japan.

Takashi Ikeda., et al. (2012). “Nonlinear Liquid Sloshing in a Square Tank Subjected to Obliquely Horizontal Excitation” J. Fluid Mech, 700: 304-328, Cambridge University Press.

The Open Source CFD, User Guide Version 2.3.0, 5th February 2014.

Virella, J.C., Godoy, L.A., and Suárez, L.E. (2006). “Fundamental Modes of Tank-Liquid Systems Under Horizontal Motions,” Engineering Structures, March 29, 28:1450–1461.

Wu, C.H., and Chen, B.F. (2012). “Transient Response of Sloshing Fluid in a Three Dimensional Tank,” Journal of Marine Science and Technology, 20 (1): 26-37.

http://www.learnengineering.org/2013/05/computational-fluid-dynamics-rans-fvm.html

APPENDICES

Appendix A

General Description of Finite Volume Method (FVM)

As mentioned, the problem related to fluid motion in an existing tank consists of solving the fundamental equations of fluid flows (Appendix A). In fluid dynamics all of these equations represent conservation laws which means that the variation of a conserved flow quantity with a given volume is due to the net effect of some internal sources and the amount of that quantity crossing the boundary surface. These flow equations can be expressed in different forms (PDE or Integral form). In the case of the PDE form, the flux required to be differentiable does not always satisfy. In addition, when discontinuities occur, the solution of the partial differential equations is to be interpreted in a solution of an integral form of the equations. At this purpose the finite volume method (FVM) was inspired to respond to this need.

The finite volume method (FVM) is used in fluid mechanics, but is not limited to flow problems. It is based on balance principles. These important principles basically express the conservation of mass, momentum and energy in a volume closed by a surface using the integral form.

The working principles can be summarized in the following points:

- It is a very general and flexible method. The mesh can be unstructured or structured unlike the case of the finite difference method (FDM), which is limited only to a structured gird. Consequently, unstructured meshes have the ability to match the boundary shape of CFD solution domains of arbitrary and complex geometries.
- The most natural characteristic of this method is to discretize the integral form of the equations and not the differential form. This is the basis of an FVM.

  This method subdivides the domain to be studied into small subdomains called finite

volumes. These subdomains can be triangles, rectangles or arbitrary quadrics that cover the whole domain (Figure1). The discretization of the domain is based on infinitesimal control volumes. Consequently, it uses a set of small non-overlapping cells (finite volumes) rather than a set of points like the differential finite element method (DFE).

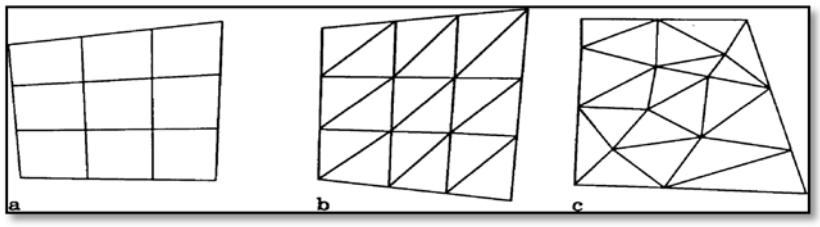

Figure A1: Typical choice of grids in the FVM; (a): structured quadrilateral grid; (b): structured triangular grid; (c): unstructured triangular grid (E. Dick, Introduction to Finite Volume Methods in Computational Fluid Dynamics).

- The finite volume method (FVM) is based on the approximate solution of the integral form of the conservation equations (Equation 1). Furthermore, these conservation equations are applied to each finite volume. They are also evaluated in terms of the function values of what we call computational nodes. In fact, the surface and volume integrals will be approximated using appropriate quadrature formula in terms of the function values at computational nodes. This allows the conversion of the integration form of conservation laws into discrete algebraic equations.
- At this stage, we need to collect the algebraic equations corresponding to the whole finite volumes to obtain a system of algebraic equations in terms of unknown values of the variable at computational nodes.

  In addition, depending on the nature of the system, linear or nonlinear solvers can be used to solve the resulting system of algebraic equations in order to obtain values of the variable at each computational node.
- There are two different approaches to finite volume discretization of computational nodes.

The first approach is called the cell-centered approach. In this approach, the control volumes (CV) are defined by an appropriate grid and computational nodes are assigned at the CV center. The second approach is the face-centered approach. In this approach, the nodal locations are defined first, and the CVs are then constructed around them in the way that leaves the faces lying midway between the nodes. It can be used only with structure grids.

The general integral form, as described in equation 6, can be obtained from the conservation equation in deferential form (Equation 1). Thus, we can find it by following these steps:

$$\frac{\partial(\rho\emptyset)}{\partial t} + \nabla.(\rho V\emptyset) = \nabla.(\Gamma\nabla\emptyset) + q_{\emptyset} \qquad \text{Equation 1}$$

Integrate this equation over an arbitrary cv:

$$\int_{cv} \frac{\partial(\rho\emptyset)}{\partial t} d\Omega + \int_{cv} \nabla.(\rho V\emptyset) d\Omega = \int_{cv} \nabla.(\Gamma\nabla\emptyset) d\Omega + \int_{cv} q_{\emptyset}\, d\Omega \qquad \text{Equation 2}$$

For a fixed CV, $\frac{\partial}{\partial t}$ and $\int_{cv}() d\Omega$ commute, so:

$$\int_{cv} \frac{\partial(\rho\emptyset)}{\partial t} d\Omega = \frac{\partial}{\partial t} \int_{cv} \rho\emptyset d\Omega \qquad \text{Equation 3}$$

By using Gauss Divergence theorem:

$$\int_{cv} \nabla.(\rho V\emptyset) d\Omega = \int_{cv} \rho\emptyset \overrightarrow{V}.d\vec{A} \qquad \text{Equation 4}$$

$$\int_{cv} \nabla.(\Gamma\nabla\emptyset) d\Omega = \int_{cv} \Gamma\nabla\emptyset d\vec{A} \qquad \text{Equation 5}$$

Substitute Equation3, 4 and 5 in equation 2

$$\frac{\partial}{\partial t} \int_{cv} \rho\emptyset d\Omega + \underbrace{\int_{cv} \rho\emptyset \overrightarrow{V}.d\vec{A}}_{CONVECTION} = \underbrace{\int_{cv} \Gamma\nabla\emptyset d\vec{A}}_{DIFFUSION} + \underbrace{\int_{cv} q_{\emptyset}\, d\Omega}_{SOURCE} \qquad \text{Equation 6}$$

This is the integral form required for finite volume method. This quantity can be used either for mass or for momentum component.

Appendix B

GraphClick

We have a picture of a graph, but not the corresponding data. GraphClick is graph digitizer software that allows users to automatically retrieve the original (x, y) data from the image of a scanned graph or from a QuickTime movie. In the beginning, we started by inserting the image of the related graph. This was done by dropping the image file into the GraphClick document window (Figure 1).

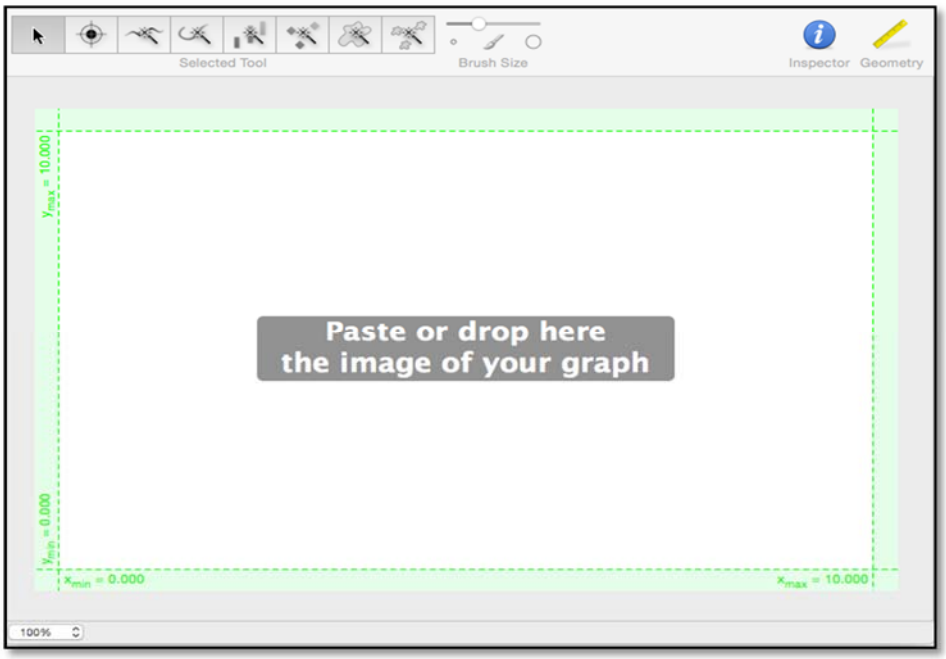

Figure 1: GraphClick document window

After inserting the image, we adjusted the coordinate based on two-dimensional space (x, y) by choosing the preferred method. There are different ways to adjust the coordinates (Figure 2).

In my case, I choose the coordinate based on three points. The first point is the origin of the graph (0;0), the second point is (0.442; 0), which represent the width of the square tank, and the third point represent the height of the tank defined by

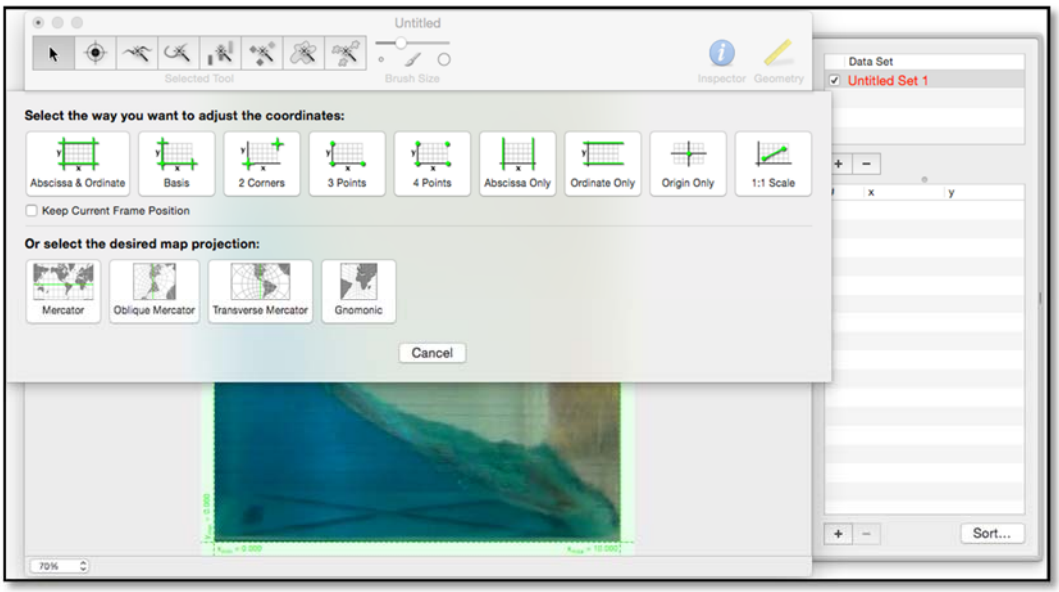

(Figure 2) The adjustment of the coordinate

the coordinate (0; 0.470). This task was useful to calibrate the image in the given coordinate offered by the GraphClick software (Figure 3).

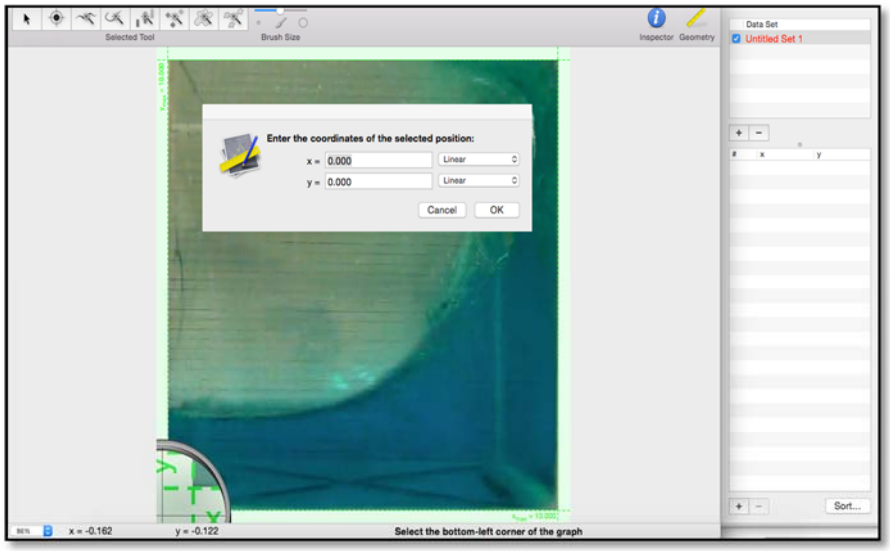

Figure 3: Calibration of the image in x and y coordinate

Then, users simply click on the indicated positions each time and enter the corresponding coordinates (Figure 4).

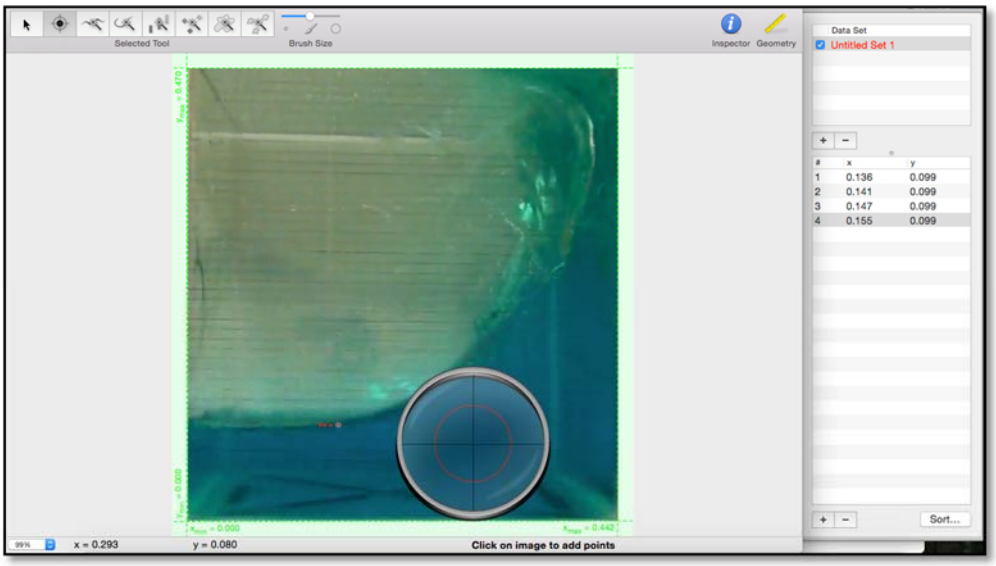

Figure 4: Selection of the graph position point by point

Users just have to click on the image and the obtained coordinates of the points can be directly exported into a table located on the right-hand side of the window (Figure 4). It should also be mentioned that the coordinate values of x and y can be obtained with precision when chosen in advance by opening the window for geometry information.

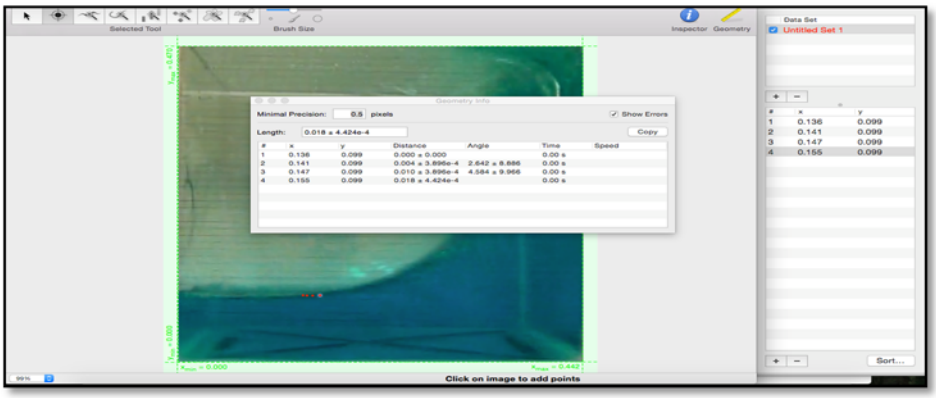

Figure 5 (a): Minimal precision related to the errors of the coordinate data

Then the collected data will be defined with errors related to the selected minimal precision (Figure 5 (a) and (b)).

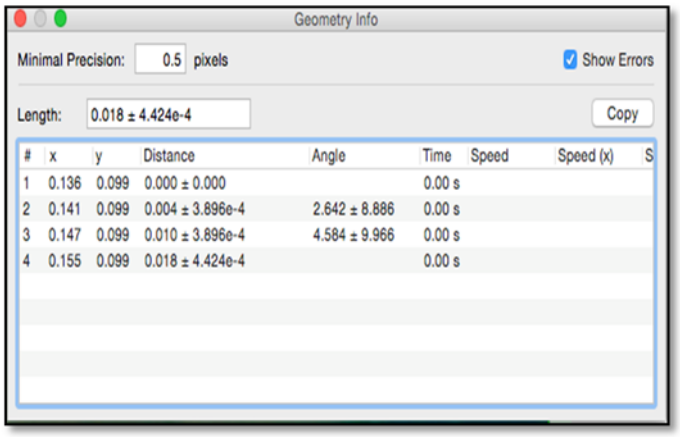

Figure 5 (b): Table describing the error value of each point

This software allow users to chose other options from the window toolbar, such as logarithmic scales, fully deformable coordinate system, error bars, etc. (Figure 6)

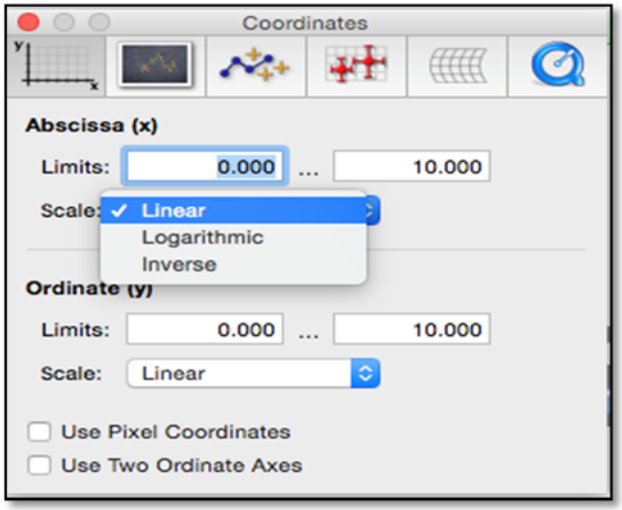

Figure 6: Coordinate options interface

Appendix C

The coordinate (X, Y) of the water free surface at the maximum sloshing at different periods
(Data related Experimental Results recorded using Graph Click application)

Point /N°	T= 2s		T=1.6		T=1s		T=0.81s		T=0.7s		T=0.5s	
	X	Y	X	Y	X	Y	X	Y	X	Y	X	Y
1	1.60E-04	0.163	-7.53E-05	0.191	5.78E-04	0.458	-9.11E-04	0.373	0.012	0.397	9.93E-05	0.164
2	0.007	0.162	0.006	0.193	0.002	0.458	0.004	0.372	0.016	0.4	0.003	0.164
3	0.013	0.162	0.01	0.195	0.004	0.455	0.014	0.371	0.018	0.364	0.006	0.164
4	0.015	0.162	0.018	0.193	0.007	0.449	0.019	0.37	0.019	0.369	0.009	0.165
5	0.019	0.162	0.024	0.19	0.007	0.442	0.021	0.364	0.019	0.376	0.014	0.166
6	0.023	0.162	0.031	0.187	0.007	0.438	0.022	0.368	0.019	0.383	0.018	0.169
7	0.027	0.162	0.04	0.185	0.007	0.432	0.025	0.361	0.021	0.389	0.023	0.171
8	0.036	0.16	0.051	0.183	0.008	0.421	0.031	0.348	0.021	0.4	0.027	0.174
9	0.047	0.16	0.059	0.179	0.008	0.392	0.031	0.358	0.021	0.357	0.033	0.176
10	0.054	0.159	0.066	0.176	0.009	0.41	0.035	0.337	0.023	0.394	0.041	0.182
11	0.063	0.159	0.073	0.175	0.011	0.379	0.042	0.329	0.025	0.354	0.046	0.184
12	0.07	0.159	0.083	0.172	0.011	0.367	0.046	0.321	0.027	0.347	0.05	0.187
13	0.077	0.158	0.094	0.17	0.013	0.352	0.047	0.28	0.03	0.341	0.053	0.191
14	0.087	0.158	0.107	0.167	0.016	0.34	0.048	0.272	0.033	0.335	0.061	0.196
15	0.095	0.158	0.118	0.163	0.017	0.331	0.048	0.309	0.034	0.325	0.063	0.2
16	0.103	0.157	0.129	0.161	0.019	0.317	0.05	0.3	0.035	0.297	0.066	0.206
17	0.113	0.157	0.138	0.158	0.021	0.307	0.051	0.29	0.036	0.29	0.073	0.21
18	0.118	0.156	0.151	0.156	0.026	0.297	0.056	0.272	0.036	0.304	0.074	0.21
19	0.124	0.155	0.169	0.152	0.033	0.285	0.06	0.272	0.038	0.311	0.075	0.205
20	0.13	0.155	0.181	0.15	0.038	0.274	0.061	0.257	0.038	0.319	0.077	0.206

Point /N°	T= 2s		T=1.6		T=1s		T=0.81s		T=0.7s		T=0.5s	
	X	Y	X	Y	X	Y	X	Y	X	Y	X	Y
21	0.138	0.155	0.191	0.148	0.048	0.26	0.064	0.267	0.039	0.286	0.078	0.209
22	0.144	0.154	0.201	0.147	0.054	0.251	0.067	0.248	0.04	0.283	0.078	0.212
23	0.151	0.153	0.214	0.146	0.061	0.248	0.07	0.223	0.041	0.268	0.079	0.216
24	0.158	0.153	0.222	0.145	0.066	0.24	0.071	0.244	0.042	0.277	0.08	0.221
25	0.165	0.153	0.229	0.144	0.071	0.234	0.075	0.235	0.042	0.262	0.08	0.224
26	0.171	0.152	0.234	0.143	0.076	0.229	0.076	0.218	0.046	0.258	0.082	0.227
27	0.177	0.152	0.243	0.142	0.08	0.223	0.076	0.229	0.048	0.252	0.083	0.229
28	0.183	0.152	0.256	0.14	0.088	0.216	0.079	0.21	0.052	0.249	0.084	0.217
29	0.189	0.151	0.268	0.139	0.095	0.208	0.085	0.202	0.055	0.244	0.084	0.22
30	0.194	0.15	0.277	0.139	0.103	0.203	0.09	0.197	0.059	0.24	0.084	0.232
31	0.201	0.15	0.284	0.137	0.107	0.2	0.099	0.193	0.061	0.235	0.086	0.224
32	0.207	0.15	0.295	0.137	0.108	0.196	0.105	0.183	0.066	0.226	0.087	0.227
33	0.214	0.15	0.304	0.135	0.11	0.19	0.109	0.175	0.071	0.223	0.087	0.232
34	0.221	0.15	0.314	0.135	0.113	0.187	0.113	0.165	0.074	0.221	0.089	0.23
35	0.227	0.15	0.324	0.134	0.117	0.183	0.118	0.16	0.077	0.218	0.09	0.215
36	0.232	0.15	0.332	0.132	0.124	0.182	0.124	0.152	0.078	0.212	0.094	0.214
37	0.237	0.15	0.339	0.132	0.13	0.18	0.131	0.148	0.081	0.209	0.097	0.216
38	0.243	0.149	0.352	0.13	0.132	0.178	0.143	0.14	0.087	0.207	0.097	0.218
39	0.247	0.149	0.361	0.129	0.135	0.174	0.152	0.134	0.093	0.201	0.097	0.222
40	0.253	0.149	0.368	0.128	0.138	0.169	0.164	0.126	0.097	0.196	0.099	0.224
41	0.259	0.148	0.376	0.127	0.14	0.167	0.172	0.121	0.1	0.193	0.104	0.223
42	0.263	0.148	0.386	0.126	0.142	0.164	0.185	0.113	0.105	0.192	0.106	0.219
43	0.267	0.148	0.392	0.126	0.146	0.163	0.202	0.107	0.109	0.189	0.106	0.213
44	0.271	0.148	0.399	0.124	0.148	0.162	0.21	0.103	0.113	0.185	0.108	0.21
45	0.275	0.147	0.408	0.124	0.151	0.16	0.211	0.094	0.115	0.183	0.111	0.209

Point /N°	T= 2s		T=1.6		T=1s		T=0.81s		T=0.7s		T=0.5s	
	X	Y	X	Y	X	Y	X	Y	X	Y	X	Y
46	0.28	0.146	0.413	0.124	0.155	0.159	0.216	0.1	0.117	0.18	0.113	0.205
47	0.285	0.146	0.42	0.123	0.16	0.154	0.219	0.091	0.124	0.177	0.116	0.202
48	0.291	0.146	0.425	0.122	0.164	0.154	0.224	0.09	0.127	0.173	0.119	0.197
49	0.298	0.145	0.43	0.122	0.168	0.154	0.234	0.085	0.132	0.17	0.122	0.193
50	0.304	0.144	0.433	0.122	0.17	0.149	0.24	0.077	0.14	0.165	0.126	0.191
51	0.309	0.144	0.44	0.121	0.17	0.151	0.249	0.072	0.145	0.161	0.129	0.186
52	0.317	0.143	0.442	0.122	0.171	0.147	0.263	0.074	0.151	0.158	0.133	0.182
53	0.322	0.143	Max Y	0.195	0.173	0.145	0.274	0.068	0.155	0.157	0.137	0.18
54	0.329	0.142			0.177	0.144	0.285	0.057	0.158	0.157	0.141	0.176
55	0.333	0.142			0.179	0.141	0.297	0.05	0.164	0.154	0.147	0.172
56	0.339	0.141			0.182	0.139	0.31	0.043	0.168	0.152	0.151	0.169
57	0.345	0.141			0.187	0.137	0.318	0.041	0.172	0.148	0.155	0.166
58	0.35	0.141			0.19	0.136	0.328	0.037	0.177	0.146	0.158	0.162
59	0.356	0.141			0.192	0.135	0.341	0.034	0.182	0.144	0.162	0.161
60	0.362	0.141			0.194	0.135	0.354	0.031	0.186	0.141	0.167	0.16
61	0.368	0.141			0.197	0.133	0.364	0.028	0.195	0.137	0.17	0.156
62	0.375	0.14			0.202	0.13	0.372	0.025	0.201	0.133	0.174	0.154
63	0.38	0.139			0.206	0.127	0.379	0.021	0.207	0.13	0.175	0.15
64	0.388	0.139			0.21	0.126	0.386	0.017	0.212	0.127	0.178	0.146
65	0.394	0.139			0.215	0.123	0.389	0.014	0.221	0.125	0.181	0.143
66	0.399	0.139			0.22	0.121	0.395	0.009	0.228	0.122	0.185	0.139
67	0.405	0.138			0.225	0.12	Max Y	0.373	0.231	0.117	0.188	0.137
68	0.413	0.138			0.229	0.118			0.24	0.115	0.192	0.137
69	0.417	0.138			0.234	0.115			0.25	0.111	0.196	0.137
70	0.419	0.138			0.237	0.113			0.256	0.11	0.199	0.134

Point /N°	T= 2s		T=1.6		T=1s		T=0.81s		T=0.7s		T=0.5s	
	X	Y	X	Y	X	Y	X	Y	X	Y	X	Y
71	0.422	0.138			0.241	0.112			0.265	0.106	0.203	0.131
72	0.425	0.137			0.245	0.11			0.273	0.103	0.207	0.128
73	0.429	0.136			0.251	0.108			0.284	0.101	0.211	0.127
74	0.434	0.135			0.255	0.107			0.292	0.099	0.213	0.125
75	0.438	0.136			0.258	0.106			0.299	0.096	0.217	0.125
76	0.442	0.135			0.264	0.103			0.305	0.096	0.222	0.124
77	Max Y	0.163			0.269	0.101			0.31	0.096	0.226	0.123
78					0.275	0.099			0.314	0.095	0.232	0.122
79					0.283	0.096			0.324	0.093	0.236	0.121
80					0.29	0.093			0.331	0.092	0.24	0.119
81					0.295	0.092			0.338	0.092	0.247	0.118
82					0.299	0.091			0.347	0.089	0.255	0.115
83					0.303	0.09			0.357	0.089	0.261	0.115
84					0.308	0.088			0.367	0.089	0.268	0.114
85					0.311	0.087			0.374	0.087	0.274	0.114
86					0.314	0.087			0.38	0.085	0.279	0.114
87					0.315	0.085			0.387	0.087	0.284	0.113
88					0.321	0.085			0.392	0.087	0.291	0.113
89					0.325	0.084			0.397	0.085	0.296	0.113
90					0.328	0.083			0.402	0.085	0.301	0.114
91					0.332	0.083			0.407	0.086	0.306	0.114
92					0.336	0.082			0.411	0.086	0.311	0.114
93					0.34	0.081			0.415	0.087	0.319	0.115
94					0.343	0.081			0.423	0.087	0.325	0.115
95					0.347	0.081			0.429	0.087	0.33	0.116

Point /N°	T= 2s		T=1.6		T=1s		T=0.81s		T=0.7s		T=0.5s	
	X	Y	X	Y	X	Y	X	Y	X	Y	X	Y
96					0.351	0.081			0.436	0.087	0.335	0.116
97					0.352	0.078			0.44	0.087	0.336	0.118
98					0.355	0.075			Max Y	0.4	0.34	0.118
99					0.358	0.073					0.346	0.119
100					0.36	0.07					0.35	0.12
101					0.362	0.069					0.356	0.121
102					0.365	0.069					0.362	0.124
103					0.369	0.068					0.369	0.127
104					0.372	0.065					0.376	0.131
105					0.376	0.064					0.384	0.133
106					0.38	0.065					0.391	0.134
107					0.382	0.066					0.395	0.137
108					0.384	0.066					0.403	0.14
109					0.386	0.064					0.408	0.14
110					0.389	0.062					0.414	0.14
111					0.392	0.062					0.419	0.145
112					0.397	0.062					0.424	0.147
113					0.398	0.063					0.428	0.148
114					0.4	0.063					0.433	0.147
115					0.404	0.064					0.436	0.146
116					0.408	0.065					0.438	0.146
117					0.411	0.067					0.442	0.146
118					0.412	0.068					Max Y	0.232
119					0.413	0.07						

Point /N°	T= 2s		T=1.6		T=1s		T=0.81s		T=0.7s		T=0.5s	
	X	Y	X	Y	X	Y	X	Y	X	Y	X	Y
121					0.419	0.073						
122					0.422	0.072						
123					0.427	0.072						
124					0.429	0.074						
125					0.431	0.075						
126					0.433	0.076						
127					0.436	0.076						
128					0.44	0.076						
129					Max Y	0.458						

Appendix D

The coordinate (X, Y) of the water free surface at the maximum sloshing at different periods
(Data related to OpenFoam Simulation recorded using Graph Click application)

Point/ N°	T=0.5s		T=0.7s		T=0.81s		T=1s		T=1.6s		T=2s	
	X	Y	X	Y	X	Y	X	Y	X	Y	X	Y
1	0.437	0.145	0.442	0.114	0.442	0.08	0.442	0.013	0.442	0.109	0.442	0.131
2	0.434	0.142	0.439	0.114	0.436	0.08	0.44	0.012	0.44	0.109	0.439	0.131
3	0.433	0.14	0.437	0.113	0.43	0.079	0.439	0.012	0.438	0.109	0.436	0.131
4	0.431	0.138	0.434	0.113	0.426	0.079	0.435	0.012	0.436	0.109	0.432	0.131
5	0.428	0.137	0.43	0.113	0.419	0.078	0.433	0.013	0.433	0.109	0.43	0.131
6	0.426	0.135	0.428	0.113	0.412	0.077	0.429	0.013	0.432	0.109	0.428	0.131
7	0.424	0.133	0.425	0.113	0.406	0.077	0.427	0.013	0.429	0.109	0.425	0.131
8	0.422	0.131	0.423	0.112	0.401	0.077	0.425	0.014	0.427	0.109	0.422	0.131
9	0.419	0.128	0.42	0.112	0.392	0.075	0.423	0.016	0.425	0.109	0.419	0.131
10	0.416	0.125	0.417	0.111	0.386	0.075	0.42	0.016	0.422	0.11	0.417	0.131
11	0.413	0.122	0.414	0.111	0.382	0.075	0.417	0.017	0.419	0.11	0.413	0.131
12	0.409	0.119	0.411	0.11	0.376	0.076	0.414	0.018	0.417	0.11	0.409	0.131
13	0.405	0.116	0.408	0.11	0.371	0.076	0.41	0.021	0.415	0.111	0.406	0.131
14	0.44	0.145	0.404	0.11	0.365	0.076	0.407	0.023	0.413	0.111	0.403	0.131
15	0.402	0.113	0.401	0.11	0.358	0.077	0.404	0.024	0.41	0.111	0.401	0.131
16	0.398	0.111	0.399	0.11	0.352	0.077	0.401	0.026	0.407	0.111	0.398	0.131
17	0.396	0.109	0.396	0.11	0.345	0.077	0.399	0.028	0.406	0.111	0.395	0.131
18	0.394	0.108	0.393	0.11	0.341	0.078	0.395	0.031	0.404	0.112	0.393	0.131
19	0.392	0.107	0.391	0.109	0.336	0.078	0.393	0.032	0.401	0.112	0.391	0.132
20	0.39	0.106	0.389	0.109	0.33	0.079	0.389	0.035	0.398	0.112	0.388	0.132
21	0.387	0.104	0.386	0.109	0.323	0.079	0.387	0.037	0.396	0.113	0.386	0.132
22	0.384	0.102	0.384	0.109	0.316	0.081	0.384	0.039	0.393	0.113	0.383	0.132
23	0.382	0.101	0.38	0.109	0.311	0.081	0.38	0.042	0.392	0.113	0.381	0.132

Point/ N°	T=0.5s		T=0.7s		T=0.81s		T=1s		T=1.6s		T=2s	
	X	Y	X	Y	X	Y	X	Y	X	Y	X	Y
24	0.379	0.099	0.379	0.109	0.307	0.081	0.377	0.044	0.39	0.113	0.378	0.132
25	0.377	0.098	0.375	0.109	0.304	0.082	0.375	0.047	0.388	0.113	0.375	0.133
26	0.373	0.098	0.373	0.109	0.301	0.082	0.373	0.048	0.384	0.114	0.373	0.133
27	0.372	0.097	0.37	0.109	0.296	0.082	0.369	0.049	0.381	0.114	0.372	0.134
28	0.368	0.096	0.367	0.108	0.291	0.084	0.368	0.051	0.379	0.115	0.37	0.133
29	0.366	0.095	0.362	0.109	0.283	0.085	0.364	0.053	0.377	0.115	0.368	0.133
30	0.361	0.093	0.359	0.109	0.276	0.087	0.361	0.054	0.374	0.115	0.366	0.133
31	0.358	0.093	0.356	0.109	0.273	0.088	0.359	0.055	0.372	0.116	0.365	0.134
32	0.355	0.092	0.355	0.109	0.269	0.089	0.355	0.056	0.369	0.116	0.363	0.134
33	0.35	0.091	0.352	0.109	0.265	0.089	0.353	0.056	0.367	0.117	0.36	0.134
34	0.348	0.09	0.348	0.109	0.258	0.092	0.348	0.056	0.365	0.117	0.359	0.134
35	0.344	0.089	0.345	0.109	0.254	0.092	0.344	0.056	0.364	0.117	0.356	0.134
36	0.34	0.089	0.342	0.11	0.249	0.095	0.342	0.056	0.362	0.118	0.355	0.135
37	0.337	0.088	0.337	0.109	0.242	0.096	0.34	0.056	0.359	0.118	0.352	0.135
38	0.331	0.087	0.334	0.109	0.236	0.099	0.336	0.056	0.356	0.118	0.349	0.135
39	0.324	0.086	0.331	0.11	0.23	0.102	0.334	0.056	0.354	0.118	0.346	0.136
40	0.316	0.085	0.328	0.11	0.219	0.105	0.331	0.056	0.352	0.119	0.344	0.136
41	0.311	0.085	0.325	0.11	0.213	0.108	0.329	0.057	0.349	0.119	0.341	0.136
42	0.327	0.087	0.323	0.112	0.223	0.104	0.325	0.058	0.347	0.12	0.339	0.136
43	0.32	0.085	0.32	0.112	0.21	0.109	0.322	0.059	0.344	0.12	0.337	0.136
44	0.306	0.085	0.316	0.112	0.203	0.112	0.319	0.059	0.342	0.121	0.336	0.136
45	0.301	0.085	0.311	0.112	0.198	0.114	0.316	0.06	0.339	0.121	0.333	0.136
46	0.297	0.084	0.308	0.112	0.192	0.118	0.312	0.061	0.337	0.122	0.331	0.137
47	0.291	0.084	0.305	0.113	0.188	0.12	0.31	0.062	0.335	0.122	0.329	0.137
48	0.286	0.084	0.3	0.113	0.184	0.123	0.307	0.063	0.333	0.123	0.325	0.137
49	0.279	0.084	0.298	0.114	0.18	0.125	0.303	0.065	0.331	0.123	0.322	0.137

Point/ N°	T=0.5s		T=0.7s		T=0.81s		T=1s		T=1.6s		T=2s	
	X	Y	X	Y	X	Y	X	Y	X	Y	X	Y
51	0.263	0.083	0.291	0.115	0.17	0.132	0.297	0.067	0.325	0.125	0.317	0.137
52	0.256	0.082	0.287	0.116	0.164	0.135	0.295	0.068	0.323	0.125	0.315	0.138
53	0.25	0.082	0.282	0.116	0.161	0.138	0.292	0.069	0.321	0.125	0.313	0.138
54	0.244	0.083	0.28	0.117	0.158	0.141	0.289	0.07	0.318	0.126	0.311	0.138
55	0.236	0.084	0.277	0.117	0.155	0.144	0.286	0.071	0.315	0.126	0.308	0.138
56	0.227	0.084	0.272	0.118	0.152	0.146	0.284	0.072	0.312	0.126	0.306	0.139
57	0.218	0.085	0.269	0.118	0.148	0.15	0.281	0.073	0.311	0.127	0.303	0.139
58	0.213	0.087	0.265	0.119	0.144	0.154	0.277	0.075	0.308	0.128	0.301	0.14
59	0.206	0.088	0.261	0.119	0.141	0.159	0.274	0.076	0.305	0.128	0.299	0.14
60	0.198	0.091	0.258	0.12	0.137	0.164	0.27	0.076	0.302	0.129	0.296	0.14
61	0.192	0.092	0.254	0.12	0.133	0.168	0.266	0.077	0.3	0.129	0.293	0.14
62	0.187	0.094	0.25	0.121	0.13	0.173	0.264	0.078	0.297	0.129	0.289	0.14
63	0.182	0.096	0.247	0.121	0.128	0.178	0.26	0.078	0.294	0.13	0.287	0.141
64	0.178	0.1	0.245	0.121	0.125	0.182	0.256	0.078	0.292	0.131	0.284	0.141
65	0.173	0.102	0.242	0.121	0.123	0.186	0.254	0.078	0.289	0.131	0.281	0.141
66	0.171	0.104	0.238	0.121	0.12	0.19	0.25	0.079	0.286	0.132	0.278	0.141
67	0.167	0.105	0.236	0.121	0.118	0.194	0.246	0.08	0.283	0.132	0.275	0.142
68	0.165	0.105	0.235	0.122	0.116	0.198	0.241	0.081	0.281	0.132	0.273	0.142
69	0.161	0.105	0.231	0.122	0.114	0.201	0.238	0.081	0.277	0.133	0.27	0.142
70	0.158	0.105	0.228	0.123	0.111	0.204	0.234	0.082	0.274	0.133	0.267	0.143
71	0.157	0.104	0.225	0.123	0.109	0.208	0.231	0.083	0.271	0.134	0.263	0.143
72	0.154	0.105	0.222	0.123	0.106	0.212	0.228	0.084	0.268	0.134	0.26	0.143
73	0.151	0.107	0.219	0.124	0.103	0.216	0.225	0.086	0.265	0.135	0.257	0.143
74	0.147	0.111	0.215	0.124	0.101	0.22	0.223	0.087	0.26	0.136	0.255	0.143
75	0.145	0.112	0.213	0.125	0.099	0.223	0.221	0.089	0.257	0.136	0.253	0.144
76	0.141	0.115	0.209	0.125	0.097	0.227	0.217	0.09	0.253	0.137	0.251	0.144
77	0.138	0.118	0.206	0.126	0.094	0.23	0.213	0.093	0.251	0.137	0.248	0.144

Point/ N°	T=0.5s		T=0.7s		T=0.81s		T=1s		T=1.6s		T=2s	
	X	Y	X	Y	X	Y	X	Y	X	Y	X	Y
78	0.134	0.122	0.205	0.127	0.092	0.233	0.211	0.095	0.249	0.137	0.246	0.144
79	0.131	0.124	0.201	0.127	0.089	0.238	0.209	0.096	0.247	0.137	0.244	0.144
80	0.129	0.127	0.198	0.127	0.086	0.242	0.206	0.098	0.244	0.138	0.241	0.144
81	0.126	0.13	0.196	0.128	0.084	0.246	0.205	0.1	0.24	0.139	0.239	0.145
82	0.122	0.133	0.194	0.129	0.082	0.25	0.201	0.102	0.238	0.14	0.236	0.145
83	0.118	0.136	0.191	0.13	0.079	0.254	0.2	0.105	0.234	0.14	0.234	0.145
84	0.116	0.139	0.19	0.13	0.078	0.258	0.196	0.107	0.232	0.141	0.231	0.145
85	0.114	0.143	0.188	0.131	0.076	0.261	0.194	0.11	0.228	0.141	0.228	0.146
86	0.111	0.146	0.186	0.131	0.074	0.264	0.191	0.113	0.225	0.142	0.224	0.146
87	0.108	0.15	0.184	0.132	0.071	0.267	0.189	0.115	0.223	0.142	0.222	0.146
88	0.105	0.153	0.181	0.133	0.068	0.272	0.186	0.117	0.22	0.143	0.218	0.147
89	0.102	0.156	0.177	0.134	0.065	0.276	0.184	0.12	0.218	0.143	0.216	0.147
90	0.099	0.161	0.174	0.135	0.063	0.281	0.182	0.123	0.214	0.143	0.215	0.147
91	0.096	0.164	0.17	0.136	0.058	0.285	0.18	0.125	0.212	0.145	0.212	0.147
92	0.093	0.166	0.166	0.137	0.055	0.291	0.177	0.128	0.213	0.144	0.211	0.148
93	0.09	0.169	0.161	0.138	0.052	0.296	0.175	0.131	0.21	0.145	0.209	0.148
94	0.087	0.172	0.157	0.139	0.05	0.301	0.172	0.133	0.208	0.145	0.206	0.148
95	0.084	0.176	0.154	0.14	0.047	0.307	0.171	0.135	0.206	0.146	0.204	0.149
96	0.079	0.181	0.151	0.141	0.045	0.314	0.169	0.138	0.204	0.147	0.202	0.149
97	0.074	0.186	0.148	0.142	0.042	0.32	0.167	0.139	0.201	0.147	0.199	0.149
98	0.07	0.192	0.145	0.143	0.04	0.325	0.165	0.141	0.198	0.148	0.197	0.15
99	0.07	0.195	0.142	0.144	0.037	0.332	0.162	0.143	0.197	0.149	0.195	0.15
100	0.068	0.199	0.139	0.145	0.035	0.34	0.16	0.145	0.194	0.149	0.193	0.15
101	0.065	0.203	0.135	0.147	0.033	0.348	0.158	0.148	0.193	0.15	0.191	0.15
102	0.064	0.207	0.136	0.146	0.033	0.352	0.156	0.15	0.191	0.151	0.188	0.151
103	0.063	0.211	0.133	0.148	0.032	0.36	0.154	0.152	0.19	0.151	0.186	0.152
104	0.064	0.217	0.131	0.149	0.03	0.365	0.152	0.154	0.187	0.152	0.182	0.152

Point/ N°	T=0.5s		T=0.7s		T=0.81s		T=1s		T=1.6s		T=2s	
	X	Y	X	Y	X	Y	X	Y	X	Y	X	Y
105	0.065	0.224	0.128	0.15	0.029	0.372	0.15	0.156	0.185	0.152	0.179	0.153
106	0.067	0.229	0.127	0.151	0.027	0.377	0.147	0.158	0.183	0.152	0.177	0.153
107	0.07	0.233	0.124	0.153	0.024	0.382	0.146	0.16	0.183	0.154	0.175	0.153
108	0.074	0.236	0.122	0.155	0.019	0.386	0.144	0.163	0.18	0.154	0.174	0.154
109	0.076	0.238	0.121	0.156	0.016	0.389	0.141	0.166	0.178	0.154	0.17	0.154
110	0.08	0.24	0.12	0.158	0.011	0.392	0.139	0.17	0.175	0.154	0.168	0.156
111	0.083	0.243	0.119	0.159	0.007	0.393	0.137	0.172	0.173	0.155	0.166	0.156
112	0.086	0.245	0.117	0.162	0.004	0.394	0.134	0.175	0.173	0.156	0.161	0.157
113	0.09	0.246	0.116	0.165	6.34E-05	0.395	0.131	0.178	0.171	0.156	0.16	0.157
114	0.093	0.249	0.113	0.166	Max (Y)=	0.395	0.13	0.181	0.169	0.156	0.157	0.157
115	0.098	0.251	0.113	0.169			0.126	0.186	0.167	0.157	0.154	0.158
116	0.101	0.251	0.113	0.172			0.122	0.19	0.165	0.158	0.188	0.151
117	0.105	0.252	0.113	0.175			0.121	0.193	0.162	0.158	0.172	0.154
118	0.107	0.254	0.112	0.178			0.12	0.195	0.16	0.159	0.164	0.157
119	0.11	0.255	0.111	0.179			0.118	0.199	0.158	0.16	0.152	0.158
120	0.114	0.257	0.11	0.182			0.116	0.202	0.156	0.16	0.15	0.158
121	0.116	0.258	0.108	0.184			0.114	0.204	0.154	0.161	0.149	0.159
122	0.119	0.259	0.107	0.188			0.114	0.207	0.153	0.161	0.147	0.159
123	0.121	0.26	0.105	0.189			0.112	0.209	0.151	0.162	0.146	0.159
124	0.123	0.261	0.104	0.191			0.11	0.213	0.15	0.163	0.144	0.161
125	0.125	0.261	0.102	0.193			0.107	0.217	0.148	0.163	0.142	0.16
126	0.129	0.262	0.102	0.195			0.106	0.219	0.147	0.164	0.14	0.161
127	0.133	0.262	0.099	0.196			0.105	0.223	0.146	0.164	0.137	0.161
128	0.139	0.262	0.097	0.199			0.102	0.226	0.144	0.165	0.134	0.161
129	0.144	0.262	0.094	0.202			0.101	0.229	0.142	0.166	0.132	0.162
130	0.147	0.262	0.092	0.204			0.1	0.232	0.141	0.166	0.13	0.162
131	0.151	0.262	0.089	0.207			0.098	0.235	0.14	0.167	0.128	0.162

Point /N°	T=0.5s		T=0.7s		T=0.81s		T=1s		T=1.6s		T=2s	
	X	Y	X	Y	X	Y	X	Y	X	Y	X	Y
132	0.158	0.261	0.087	0.21			0.097	0.238	0.138	0.168	0.126	0.162
133	0.165	0.261	0.085	0.212			0.095	0.241	0.136	0.168	0.123	0.163
134	0.171	0.261	0.084	0.216			0.093	0.245	0.133	0.168	0.121	0.163
135	0.175	0.262	0.081	0.218			0.092	0.25	0.131	0.17	0.118	0.164
136	0.179	0.264	0.079	0.221			0.09	0.254	0.129	0.171	0.116	0.164
137	0.182	0.267	0.078	0.223			0.088	0.258	0.127	0.172	0.113	0.165
138	0.179	0.269	0.075	0.226			0.086	0.261	0.125	0.172	0.111	0.165
139	0.177	0.271	0.074	0.23			0.084	0.266	0.124	0.173	0.107	0.166
140	0.175	0.273	0.072	0.233			0.083	0.267	0.121	0.174	0.104	0.166
141	0.173	0.274	0.072	0.234			0.082	0.269	0.118	0.175	0.102	0.166
142	0.171	0.275	0.07	0.237			0.08	0.272	0.116	0.175	0.1	0.166
143	0.168	0.278	0.069	0.24			0.079	0.276	0.115	0.177	0.097	0.166
144	0.165	0.281	0.068	0.243			0.078	0.279	0.114	0.178	0.095	0.167
145	0.161	0.284	0.067	0.244			0.076	0.282	0.112	0.179	0.092	0.167
146	0.155	0.285	0.065	0.247			0.075	0.286	0.111	0.179	0.09	0.168
147	0.151	0.288	0.064	0.25			0.074	0.289	0.11	0.18	0.087	0.169
148	0.147	0.29	0.062	0.252			0.073	0.292	0.108	0.18	0.085	0.169
149	0.141	0.293	0.061	0.255			0.071	0.296	0.106	0.181	0.081	0.17
150	0.136	0.294	0.059	0.259			0.071	0.3	0.104	0.182	0.078	0.17
151	0.131	0.295	0.058	0.262			0.071	0.303	0.102	0.183	0.075	0.171
152	0.124	0.295	0.056	0.264			0.071	0.306	0.1	0.184	0.074	0.171
153	0.118	0.297	0.054	0.268			0.071	0.309	0.099	0.183	0.071	0.172
154	0.112	0.298	0.054	0.271			0.07	0.311	0.097	0.184	0.069	0.173
155	0.108	0.298	0.052	0.274			0.07	0.314	0.096	0.185	0.067	0.173
156	0.103	0.298	0.052	0.276			0.069	0.316	0.093	0.186	0.064	0.174
157	0.097	0.296	0.05	0.278			0.069	0.319	0.092	0.186	0.061	0.175
158	0.093	0.294	0.049	0.281			0.068	0.321	0.09	0.186	0.058	0.176

Point /N°	T=0.5s		T=0.7s		T=0.81s		T=1s		T=1.6s		T=2s	
	X	Y	X	Y	X	Y	X	Y	X	Y	X	Y
159	0.086	0.294	0.047	0.284			0.066	0.325	0.089	0.186	0.055	0.177
160	0.082	0.293	0.047	0.286			0.065	0.328	0.088	0.187	0.053	0.178
161	0.077	0.291	0.045	0.289			0.063	0.33	0.086	0.187	0.05	0.179
162	0.071	0.291	0.043	0.293			0.061	0.334	0.085	0.188	0.047	0.181
163	0.067	0.29	0.042	0.296			0.06	0.337	0.083	0.189	0.044	0.181
164	0.062	0.289	0.04	0.298			0.058	0.34	0.081	0.189	0.041	0.183
165	0.055	0.288	0.039	0.301			0.056	0.343	0.079	0.188	0.038	0.184
166	0.051	0.287	0.038	0.303			0.053	0.346	0.077	0.188	0.035	0.185
167	0.045	0.286	0.036	0.306			0.052	0.35	0.076	0.189	0.033	0.186
168	0.042	0.285	0.036	0.308			0.05	0.353	0.074	0.19	0.031	0.187
169	0.039	0.284	0.035	0.311			0.048	0.356	0.073	0.191	0.029	0.188
170	0.036	0.283	0.035	0.313			0.046	0.36	0.071	0.192	0.027	0.189
171	0.032	0.28	0.034	0.315			0.044	0.363	0.069	0.193	0.025	0.19
172	0.03	0.279	0.034	0.316			0.043	0.366	0.068	0.194	0.023	0.191
173	0.027	0.277	0.034	0.317			0.041	0.369	0.066	0.194	0.02	0.192
174	0.025	0.276	0.034	0.32			0.039	0.372	0.063	0.195	0.019	0.192
175	0.022	0.274	0.034	0.323			0.038	0.375	0.061	0.196	0.017	0.193
176	0.02	0.273	0.034	0.324			0.038	0.377	0.058	0.198	0.015	0.194
177	0.015	0.271	0.034	0.328			0.037	0.38	0.056	0.198	0.014	0.194
178	0.01	0.27	0.034	0.331			0.036	0.384	0.052	0.2	0.011	0.195
179	0.008	0.27	0.035	0.335			0.037	0.388	0.05	0.201	0.009	0.195
180	0.005	0.27	0.035	0.34			0.04	0.39	0.049	0.202	0.007	0.195
181	0.002	0.27	0.036	0.342			0.041	0.393	0.047	0.203	0.005	0.195
182	Max(Y)=	0.298	0.037	0.344			0.042	0.395	0.045	0.205	0.003	0.195
183			0.037	0.347			0.043	0.401	0.043	0.206	0.002	0.195
184			0.038	0.349			0.043	0.404	0.041	0.208	2.41E-04	0.195
185			0.039	0.352			0.043	0.407	0.039	0.209	Max(Y)=	0.195

Point /N°	T=0.5s		T=0.7s		T=0.81s		T=1s		T=1.6s		T=2s	
	X	Y	X	Y	X	Y	X	Y	X	Y	X	Y
186			0.04	0.355			0.042	0.41	0.038	0.211		
187			0.041	0.357			0.042	0.414	0.035	0.212		
188			0.043	0.361			0.042	0.418	0.034	0.213		
189			0.045	0.365			0.041	0.42	0.031	0.215		
190			0.046	0.368			0.041	0.424	0.03	0.216		
191			0.047	0.37			0.04	0.427	0.028	0.219		
192			0.048	0.373			0.04	0.43	0.026	0.22		
193			0.05	0.375			0.039	0.435	0.025	0.222		
194			0.052	0.377			0.039	0.436	0.023	0.223		
195			0.053	0.379			0.039	0.439	0.021	0.225		
196			0.054	0.381			0.039	0.443	0.019	0.226		
197			0.055	0.385			0.039	0.447	0.016	0.226		
198			0.057	0.388			0.039	0.449	0.014	0.227		
199			0.058	0.392			0.041	0.45	0.013	0.229		
200			0.061	0.393			0.042	0.453	0.011	0.23		
201			0.063	0.396			0.043	0.456	0.009	0.23		
202			0.064	0.398			0.043	0.459	0.008	0.231		
203			0.066	0.402			0.046	0.46	0.005	0.231		
204			0.068	0.405			0.047	0.461	0.004	0.231		
205			0.069	0.407			0.048	0.463	0.003	0.232		
206			0.07	0.409			0.051	0.466	0.001	0.233		
207			0.071	0.41			0.052	0.467	6.74E-04	0.233		
208			0.072	0.411			0.053	0.468	1.62E-04	0.233		
209			0.072	0.415			0.054	0.469				
210			0.074	0.417			0.054	0.47	Max(Y)=	0.233		
211			0.074	0.42			Max(Y)=	0.47				

Point/ N°	T=0.5s		T=0.7s		T=0.81s		T=1s		T=1.6s		T=2s	
	X	Y	X	Y	X	Y	X	Y	X	Y	X	Y
212			0.074	0.427								
213			0.072	0.429								
214			0.07	0.432								
215			0.069	0.434								
216			0.065	0.437								
217			0.064	0.437								
218			0.061	0.439								
219			0.059	0.441								
220			0.056	0.441								
221			0.053	0.442								
222			0.049	0.443								
223			0.046	0.444								
224			0.043	0.444								
225			0.039	0.444								
226			0.036	0.445								
227			0.033	0.446								
228			0.03	0.447								
229			0.027	0.447								
230			0.024	0.448								
231			0.022	0.45								
232			0.019	0.451								
233			0.016	0.453								
234			0.014	0.455								
235			0.013	0.455								
236			0.009	0.455								
237			0.006	0.456								
238			0.003	0.456								

Point/ N°	T=0.5s		T=0.7s		T=0.81s		T=1s		T=1.6s		T=2s	
	X	Y	X	Y	X	Y	X	Y	X	Y	X	Y
239			0.002	0.457								
240			4.36E-04	0.457								
241			Max(Y)=	0.457								

Appendix E

The Fundamental Equations of Fluid Flow

The governing equations are called flow equations and are described below:

◆ Continuity Equation:

$$\frac{\partial \rho}{\partial t} + \frac{\partial (\rho u)}{\partial x} + \frac{\partial (\rho v)}{\partial y} + \frac{\partial (\rho w)}{\partial z} = 0; \qquad \text{E1}$$

Mass of fluid entering the volume = Mass of fluid leaving the volume (mass balance) where $\partial/\partial t, \partial/\partial x, \partial/\partial y \; and \; \partial/\partial z$ are respectively the partial derivative with respect to time, to x, to y and to z, and (x, y, z) is the coordinate of fluids particle at time t

◆ Momentum Equation:

This equation is derived by M. Navier and G.Stokes. It is based on Newton's second law of motion (Equation E2)

$$(F = m * a) \qquad \text{E2}$$

The force on the fluid element = its mass times the acceleration of the element. It is also an extension of the Euler equations, which include the effects of the viscosity of the flows. It describes the velocity, the temperature, the pressure, and the density of fluids in motion in general conditions (three dimensional space and unsteady form).

1) Momentum Equation in x direction:

$$\rho\left(\frac{\partial u}{\partial t} + u\frac{\partial u}{\partial x} + v\frac{\partial u}{\partial y} + w\frac{\partial u}{\partial z}\right) = \rho g_x - \frac{\partial p}{\partial x} + \mu\left(\frac{\partial^2 (u)}{\partial x^2} + \frac{\partial^2 (u)}{\partial y^2} + \frac{\partial^2 (u)}{\partial z^2}\right) \qquad 4.3$$

2) Momentum Equation in y direction:

$$\rho\left(\frac{\partial v}{\partial t} + u\frac{\partial v}{\partial x} + v\frac{\partial v}{\partial y} + w\frac{\partial v}{\partial z}\right) = \rho g_y - \frac{\partial p}{\partial y} + \mu\left(\frac{\partial^2 (v)}{\partial x^2} + \frac{\partial^2 (v)}{\partial y^2} + \frac{\partial^2 (v)}{\partial z^2}\right) \qquad 4.4$$

3) Momentum Equation in z direction:

$$\rho\left(\frac{\partial w}{\partial t}+u\frac{\partial w}{\partial x}+v\frac{\partial w}{\partial y}+w\frac{\partial w}{\partial z}\right)=\rho g_z-\frac{\partial p}{\partial z}+\mu\left(\frac{\partial^2(w)}{\partial x^2}+\frac{\partial^2(w)}{\partial y^2}+\frac{\partial^2(w)}{\partial z^2}\right) \quad 4.5$$

◆ The conservation of energy Equation:

$$\frac{\partial}{\partial t}\left[\rho\left(e+\frac{1}{2}v^2\right)\right]+\frac{\partial}{\partial x}\left[\rho u\left(e+\frac{1}{2}v^2\right)\right]+\frac{\partial}{\partial y}\left[\rho v\left(e+\frac{1}{2}v^2\right)\right]+\frac{\partial}{\partial z}\left[\rho w\left(e+\frac{1}{2}v^2\right)\right]$$
$$=-\frac{\partial q_x}{\partial x}-\frac{\partial q_y}{\partial y}-\frac{\partial q_z}{\partial z}+\frac{\partial}{\partial x}\left(u\sigma_{xx}+v\sigma_{xy}+w\sigma_{xz}\right)+\frac{\partial}{\partial y}\left(u\sigma_{yx}+v\sigma_{yy}+w\sigma_{yz}\right)$$
$$+\frac{\partial}{\partial z}\left(u\sigma_{zx}+v\sigma_{zy}+w\sigma_{zz}\right)+\rho u g_x+\rho v g_y+\rho w g_z \quad 4.6$$

This equation can be used if the flow is compressible (density ρ is not constant). It presents the conservation of energy of the moving flow.

[Rate of change of energy of the fluid within the element (or control volume)] = [The net thermal energy (Heat) into the element] + [Rate of work done on the element by external forces (body and surface forces)].

Appendix F

2.3.4. Snapshots of the CFD simulation of the maximum sloshing height of the water surface

T=0.5s

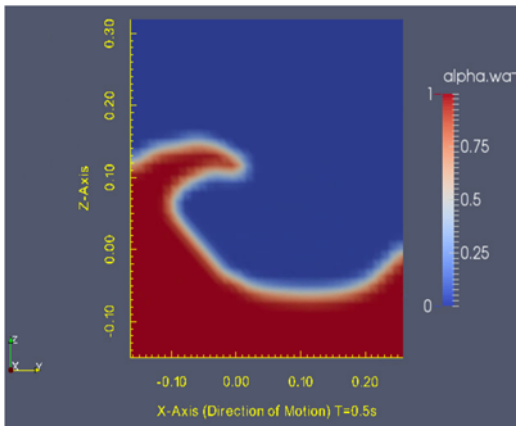

T=0.7s

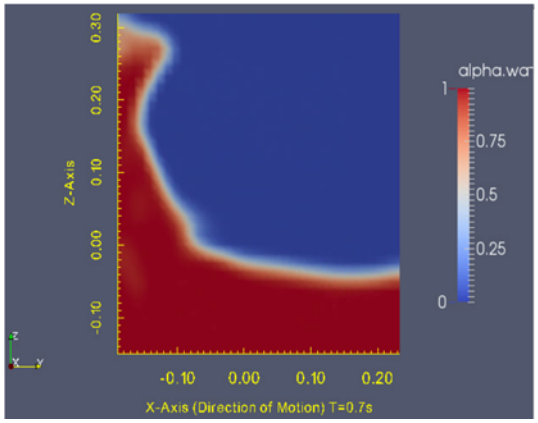

T=0.81s

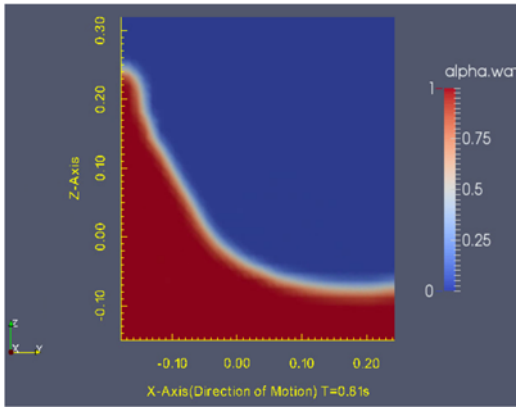

T=1s

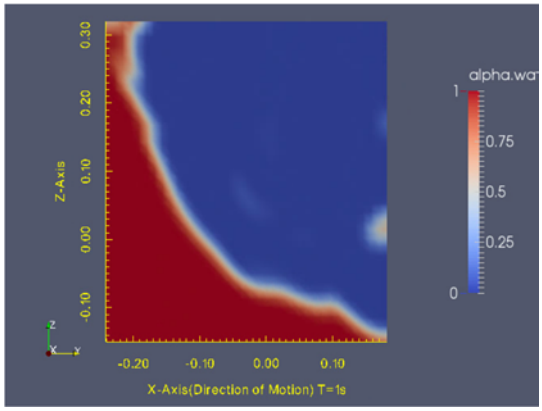

T=1.6s

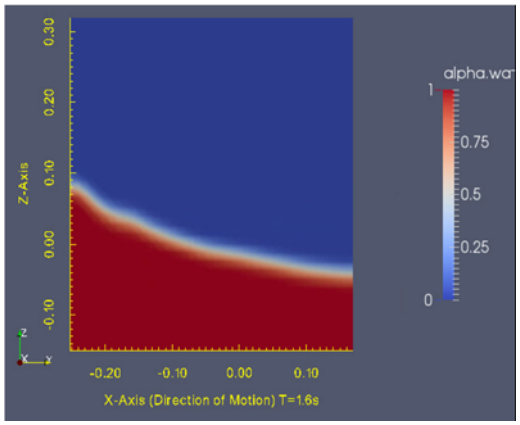

T=2s

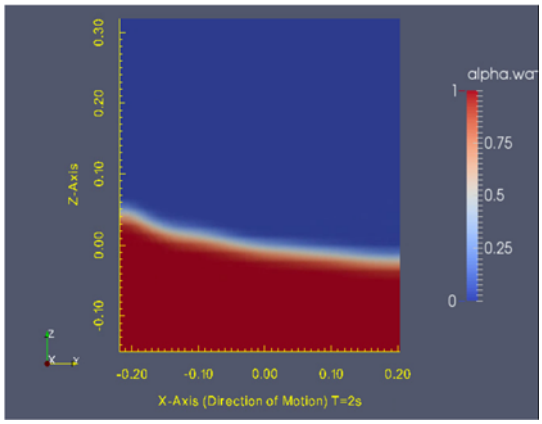

Appendix G
OpenFoam files

FILE : blockMeshDict (Page1/2)

```
/*--------------------------------*- C++ -*----------------------------------*\
| =========                 |                                                 |
| \\      /  F ield         | OpenFOAM: The Open Source CFD Toolbox           |
|  \\    /   O peration     | Version:  2.4.0                                 |
|   \\  /    A nd           | Web:      www.OpenFOAM.org                      |
|    \\/     M anipulation  |                                                 |
\*---------------------------------------------------------------------------*/
FoamFile
{
    version     2.0;
    format      ascii;
    class       dictionary;
    object      blockMeshDict;
}
// * * * * * * * * * * * * * * * * * * * * * * * * * * * * * * * * * * * * //
// General m4 macros
// * * * * * * * * * * * * * * * * * * * * * * * * * * * * * * * * * * * * //
// User-defined parameters
convertToMeters 0.01;
      // Length of tank (x-direction)
      // Breadth of tank (y-direction)
      // Depth of tank (z-direction)
     // Depth to the top (height) of lower chamfer
    // Height of upper chamfer
 // Angle of lower chamfer to the horizontal
 // Angle of upper chamfer to the horizontal
  // Centre of gravity in y-direction
        // Centre of gravity in z-direction
     // Number of cells in the length (1 for 2D)
     // Number of cells in the breadth
    // Number of cells in the height of the lower champfer
     // Number of cells in the height between the chamfers
   // Number of cells in the height of the upper champfer
// * * * * * * * * * * * * * * * * * * * * * * * * * * * * * * * * * * * * //
// Derived parameters
 // Breadth to the top (height) of lower chamfer
 // Breadth of upper chamfer
FILE : blockMeshDict (Page2/2)
// * * * * * * * * * * * * * * * * * * * * * * * * * * * * * * * * * * * * //
```

```
// Parametric description
 vertices (
    (-21.1 -21.1 -15) // Vertex bllcb = 0
    (-21.1 -21.1 -14)  // Vertex bllc = 1
    (-21.1 -21.1 31)  // Vertex bluc = 2
    (-21.1 -21.1 32) // Vertex bluct = 3
    (-21.1 21.1 -15) // Vertex brlcb = 4
```

FILE : blockMeshDict (Page2/2)

```
    (-21.1 21.1 -14)  // Vertex brlc = 5
    (-21.1 21.1 31)  // Vertex bruc = 6
    (-21.1 21.1 32) // Vertex bruct = 7
    (21.1 -21.1 -15) // Vertex fllcb = 8
    (21.1 -21.1 -14)  // Vertex fllc = 9
    (21.1 -21.1 31)  // Vertex fluc = 10
    (21.1 -21.1 32) // Vertex fluct = 11
    (21.1 21.1 -15) // Vertex frlcb = 12
    (21.1 21.1 -14)  // Vertex frlc = 13
    (21.1 21.1 31)  // Vertex fruc = 14
    (21.1 21.1 32) // Vertex fruct = 15
);
blocks
(
    // block0
    hex (0 4 5 1 8 12 13 9)
    (35 1 35)
    simpleGrading (1 1 1)
    // block1
    hex (1 5 6 2 9 13 14 10)
    (35 35 35)
    simpleGrading (1 1 1)
    // block2
    hex (2 6 7 3 10 14 15 11)
    (35 1 35)
    simpleGrading (1 1 1)
);
patches
(
    patch walls
    (
        (0 4 12 8)
        (4 5 13 12)
        (5 6 14 13)
        (6 7 15 14)
        (7 3 11 15)
        (3 2 10 11)
        (2 1 9 10)
        (1 0 8 9)
        (8 12 13 9)
        (9 13 14 10)
        (10 14 15 11)
        (0 1 5 4)
        (1 2 6 5)
        (2 3 7 6)
  )    );    // ************************************************************************* //
```

FILE : blockMeshDict4 (1/3)

```
/*--------------------------------*- C++ -*----------------------------------*\
| =========                 |                                                 |
| \\      /  F ield         | OpenFOAM: The Open Source CFD Toolbox           |
|  \\    /   O peration     | Version:  2.4.0                                 |
|   \\  /    A nd           | Web:      www.OpenFOAM.org                      |
|    \\/     M anipulation  |                                                 |
\*---------------------------------------------------------------------------*/
FoamFile
{
    version     2.0;
    `format'      ascii;
    class       dictionary;
    object      blockMeshDict;
}
// * * * * * * * * * * * * * * * * * * * * * * * * * * * * * * * * * * * * * //
// General m4 macros
changecom(//)changequote([,]) dnl>
define(calc, [esyscmd(perl -e 'use Math::Trig; print ($1)')]) dnl>
define(VCOUNT, 0)
define(vlabel, [[// ]Vertex $1 = VCOUNT define($1, VCOUNT)define([VCOUNT],
incr(VCOUNT))])
define(hex2D, hex (b$1 b$2 b$3 b$4 f$1 f$2 f$3 f$4))
define(quad2D, (b$1 b$2 f$2 f$1))
define(frontQuad, (f$1 f$2 f$3 f$4))
define(backQuad, (b$1 b$4 b$3 b$2))
// * * * * * * * * * * * * * * * * * * * * * * * * * * * * * * * * * * * * * //
// User-defined parameters
convertToMeters 0.01;
define(l, 42.2)       // Length of tank (x-direction)
define(b, 42.2)       // Breadth of tank (y-direction)
define(h, 47)       // Depth of tank (z-direction)
define(hlc, 1)      // Depth to the top (height) of lower chamfer
define(huc, 1)      // Height of upper chamfer
define(thetalc, 90) // Angle of lower chamfer to the horizontal
define(thetauc, 90) // Angle of upper chamfer to the horizontal
define(CofGy, calc(b/2.0))  // Centre of gravity in y-direction
define(CofGz, 15)         // Centre of gravity in z-direction
define(Nl, 35)      // Number of cells in the length (1 for 2D)
define(Nb, 35)      // Number of cells in the breadth
define(Nhlc, 1)     // Number of cells in the height of the lower champfer
define(Nh, 35)      // Number of cells in the height between the chamfers
```

FILE : blockMeshDict4 (2/3)

```
define(Nhuc, 1)    // Number of cells in the height of the upper champfer
// * * * * * * * * * * * * * * * * * * * * * * * * * * * * * * * * * * * * * * * * //
// Derived parameters
define(blc, calc(hlc/tan(deg2rad(thetalc)))) // Breadth to the top (height) of lower chamfer
define(buc, calc(huc/tan(deg2rad(thetauc)))) // Breadth of upper chamfer
define(Yl, -CofGy)
define(Yllc, calc(Yl + blc))
define(Yluc, calc(Yl + buc))
define(Yr, calc(Yl + b))
define(Yrlc, calc(Yr - blc))
define(Yruc, calc(Yr - buc))
define(Zb, -CofGz)
define(Zlc, calc(Zb + hlc))
define(Zt, calc(Zb + h))
define(Zuc, calc(Zt - huc))

define(Xf, calc(l/2.0))
define(Xb, calc(Xf - l))

// * * * * * * * * * * * * * * * * * * * * * * * * * * * * * * * * * * * * * * * * //
// Parametric description

vertices
(
    (Xb Yllc Zb) vlabel(bllcb)
    (Xb Yl Zlc)  vlabel(bllc)
    (Xb Yl Zuc)  vlabel(bluc)
    (Xb Yluc Zt) vlabel(bluct)
    (Xb Yrlc Zb) vlabel(brlcb)
    (Xb Yr Zlc)  vlabel(brlc)
    (Xb Yr Zuc)  vlabel(bruc)
    (Xb Yruc Zt) vlabel(bruct)
    (Xf Yllc Zb) vlabel(fllcb)
    (Xf Yl Zlc)  vlabel(fllc)
    (Xf Yl Zuc)  vlabel(fluc)
    (Xf Yluc Zt) vlabel(fluct)
    (Xf Yrlc Zb) vlabel(frlcb)
    (Xf Yr Zlc)  vlabel(frlc)
    (Xf Yr Zuc)  vlabel(fruc)
    (Xf Yruc Zt) vlabel(fruct)
);
blocks
(
```

FILE : blockMeshDict4 (3/3)

```
// block0
  hex2D(llcb, rlcb, rlc, llc)

   FILE : blockMeshDict4 (3/3)
(Nb Nhlc Nl)
    simpleGrading (1 1 1)

    // block1
    hex2D(llc, rlc, ruc, luc)
    (Nb Nh Nl)
    simpleGrading (1 1 1)

    // block2
    hex2D(luc, ruc, ruct, luct)
    (Nb Nhuc Nl)
    simpleGrading (1 1 1)
);

patches
(
    patch walls
    (
        quad2D(llcb, rlcb)
        quad2D(rlcb, rlc)
        quad2D(rlc, ruc)
        quad2D(ruc, ruct)
        quad2D(ruct, luct)
        quad2D(luct, luc)
        quad2D(luc, llc)
        quad2D(llc, llcb)
        frontQuad(llcb, rlcb, rlc, llc)
        frontQuad(llc, rlc, ruc, luc)
        frontQuad(luc, ruc, ruct, luct)
        backQuad(llcb, rlcb, rlc, llc)
        backQuad(llc, rlc, ruc, luc)
        backQuad(luc, ruc, ruct, luct)
    )
);

// ************************************************************************* //
```

FILE : boundary

```
/*--------------------------------*- C++ -*----------------------------------*\
| =========                 |                                                 |
| \\      /  F ield         | OpenFOAM: The Open Source CFD Toolbox           |
|  \\    /   O peration     | Version:  2.4.0                                 |
|   \\  /    A nd           | Web:      www.OpenFOAM.org                      |
|    \\/     M anipulation  |                                                 |
\*---------------------------------------------------------------------------*/
FoamFile
{
    version     2.0;
    format      ascii;
    class       polyBoundaryMesh;
    location    "constant/polyMesh";
    object      boundary;
}
// * * * * * * * * * * * * * * * * * * * * * * * * * * * * * * * * * * * * * * * //

1
(
    walls
    {
        type            patch;
        nFaces          7630;
        startFace       132160;
    }
)

// ************************************************************************* //
```

FILE : dynamicMeshDict

```
/*--------------------------------*- C++ -*----------------------------------*\
| =========                 |                                                 |
| \\      /  F ield         | OpenFOAM: The Open Source CFD Toolbox           |
|  \\    /   O peration     | Version:  2.4.0                                 |
|   \\  /    A nd           | Web:      www.OpenFOAM.org                      |
|    \\/     M anipulation  |                                                 |
\*---------------------------------------------------------------------------*/
FoamFile
{
    version     2.0;
    format      ascii;
    class       dictionary;
    location    "constant";
    object      dynamicMeshDict;
}
// * * * * * * * * * * * * * * * * * * * * * * * * * * * * * * * * * * * * * //

dynamicFvMesh   solidBodyMotionFvMesh;

solidBodyMotionFvMeshCoeffs
{
    /*solidBodyMotionFunction SDA;
    SDACoeffs
    {
        CofG          ( 0 0 0 );
        lamda         50;
        rollAmax       0.22654;
        rollAmin       0.10472;
        heaveA         3.79;
        swayA          2.34;
        Q             2;
        Tp            13.93;
        Tpn            11.93;
        dTi           0.059;
        dTp           -0.001;
    }*/
solidBodyMotionFunction oscillatingLinearMotion;
oscillatingLinearMotionCoeffs
{
amplitude (0 0.05 0);
omega 7.76;
}
}
// ************************************************************************* /
```

FILE : RASProperties

```
 /*--------------------------------*- C++ -*----------------------------------*\
| =========                 |                                                 |
| \\      /  F ield         | OpenFOAM: The Open Source CFD Toolbox           |
|  \\    /   O peration     | Version:  2.4.0                                 |
|   \\  /    A nd           | Web:      www.OpenFOAM.org                      |
|    \\/     M anipulation  |                                                 |
\*---------------------------------------------------------------------------*/
FoamFile
{
    version     2.0;
    format      ascii;
    class       dictionary;
    location    "constant";
    object      RASProperties;
}
// * * * * * * * * * * * * * * * * * * * * * * * * * * * * * * * * * * * * * * * //

RASModel        laminar;

turbulence      off;

printCoeffs     on;


// ************************************************************************* //
```

FILE : transportProperties

```
/*--------------------------------*- C++ -*----------------------------------*\
| =========                 |                                                 |
| \\      /  F ield         | OpenFOAM: The Open Source CFD Toolbox           |
|  \\    /   O peration     | Version:  2.4.0                                 |
|   \\  /    A nd           | Web:      www.OpenFOAM.org                      |
|    \\/     M anipulation  |                                                 |
\*---------------------------------------------------------------------------*/
FoamFile
{
    version     2.0;
    format      ascii;
    class       dictionary;
    location    "constant";
    object      transportProperties;
}
// * * * * * * * * * * * * * * * * * * * * * * * * * * * * * * * * * * * * * //

phases (water-air);

water
{
    transportModel  Newtonian;
    nu              nu [ 0 2 -1 0 0 0 0 ] 1e-06;
    rho             rho [ 1 -3 0 0 0 0 0 ] 998.2;
}

air
{
    transportModel  Newtonian;
    nu              nu [ 0 2 -1 0 0 0 0 ] 1.48e-05;
    rho             rho [ 1 -3 0 0 0 0 0 ] 1;
}

sigma           sigma [ 1 0 -2 0 0 0 0 ] 0;

// ************************************************************************* /
```

FILE : turbulenceProperties

```
/*--------------------------------*- C++ -*----------------------------------*\
| =========                 |                                                 |
| \\      /  F ield         | OpenFOAM: The Open Source CFD Toolbox           |
|  \\    /   O peration     | Version:  2.4.0                                 |
|   \\  /    A nd           | Web:      www.OpenFOAM.org                      |
|    \\/     M anipulation  |                                                 |
\*---------------------------------------------------------------------------*/
FoamFile
{
    version     2.0;
    format      ascii;
    class       dictionary;
    location    "constant";
    object      turbulenceProperties;
}
// * * * * * * * * * * * * * * * * * * * * * * * * * * * * * * * * * * * * * //

simulationType  laminar;


// ************************************************************************* //
```

FILE : controlDict (1/2)

```
/*--------------------------------*- C++ -*----------------------------------*\
| =========                 |                                                 |
| \\      /  F ield         | OpenFOAM: The Open Source CFD Toolbox           |
|  \\    /   O peration     | Version:  2.4.0                                 |
|   \\  /    A nd           | Web:      www.OpenFOAM.org                      |
|    \\/     M anipulation  |                                                 |
\*---------------------------------------------------------------------------*/
FoamFile
{
    version     2.0;
    format      ascii;
    class       dictionary;
    location    "system";
    object      controlDict;
}
// * * * * * * * * * * * * * * * * * * * * * * * * * * * * * * * * * * * * //
application     interDyMFoam;
startFrom       startTime;
startTime       0;
stopAt          endTime;
endTime         5;
deltaT          0.05;
writeControl    adjustableRunTime;
writeInterval   0.05;
purgeWrite      0;
writeFormat     ascii;
writePrecision  6;
writeCompression compressed;
timeFormat      general;
timePrecision   6;
runTimeModifiable yes;
adjustTimeStep  yes;
maxCo           0.5;
maxAlphaCo      0.5;
maxDeltaT       1;
functions
/*{
    probes
    {
        type          probes;
        functionObjectLibs ("libsampling.so");
        outputControl   timeStep;
        outputInterval  1;
        probeLocations
        (
            ( 0 9.95 19.77 )
            ( 0 -9.95 19.77 )
        );
```

FILE : controlDict (2/2)

```
        fixedLocations  false;
        fields
        (
            p
        );
    }
}*/
{
wallPressure
{
type surfaces;
functionObjectLibs ("libsampling.so");
outputControl outputTime;
outputInterval 1;
surfaceFormat raw;
interpolationScheme cell;
fields ( alpha1
p
);
surfaces
(
leftwalls
{
type patch;
patches (leftWall);
interpolate true;
triangulate false;
}
rightwalls
{
type patch;
patches (rightWall);
interpolate true;
triangulate false;
}
);

} // end functions
// ************************************************************************* //
```

FILE : decomposeParDict

```
/*--------------------------------*- C++ -*----------------------------------*\
| =========                 |                                                 |
| \\      /  F ield         | OpenFOAM: The Open Source CFD Toolbox           |
|  \\    /   O peration     | Version:  2.4.0                                 |
|   \\  /    A nd           | Web:      www.OpenFOAM.org                      |
|    \\/     M anipulation  |                                                 |
\*---------------------------------------------------------------------------*/
FoamFile
{
    version     2.0;
    format      ascii;
    class       dictionary;
    location    "system";
    object      decomposeParDict;
}
// * * * * * * * * * * * * * * * * * * * * * * * * * * * * * * * * * * * * * * * //

numberOfSubdomains 16;

method          hierarchical;

simpleCoeffs
{
    n           ( 2 2 1 );
    delta       0.001;
}

hierarchicalCoeffs
{
    n           ( 4 2 2 );
    delta       0.001;
    order       xyz;
}

manualCoeffs
{
    dataFile        "";
}

distributed     no;
roots           ( );
// ************************************************************************* //
```

FILE : fvScheme

```
/*--------------------------------*- C++ -*----------------------------------*\
| =========                 |                                                 |
| \\      /  F ield         | OpenFOAM: The Open Source CFD Toolbox           |
|  \\    /   O peration     | Version:  2.4.0                                 |
|   \\  /    A nd           | Web:      www.OpenFOAM.org                      |
|    \\/     M anipulation  |                                                 |
\*---------------------------------------------------------------------------*/
FoamFile
{
    version     2.0;
    format      ascii;
    class       dictionary;
    location    "system";
    object      fvSchemes;
}
// * * * * * * * * * * * * * * * * * * * * * * * * * * * * * * * * * * * * * //
ddtSchemes
{
    default         Euler;
}
gradSchemes
{
    default         Gauss linear;
}
divSchemes
{
    div(rhoPhi,U)  Gauss vanLeerV;
    div(phi,alpha)  Gauss vanLeer;
    div(phirb,alpha) Gauss vanLeer;
    div((muEff*dev(T(grad(U))))) Gauss linear;
}
laplacianSchemes
{
    default         Gauss linear corrected;
}
interpolationSchemes
{
    default         linear;
}
snGradSchemes
{
    default         corrected;
}
```

```
fluxRequired
{
    default         no;
    p_rgh;
    pcorr;
}
// ************************************************************************* //
```

FILE : fvSolution (1/3)

```
/*--------------------------------*- C++ -*----------------------------------*\
| =========                 |                                                 |
| \\      /  F ield         | OpenFOAM: The Open Source CFD Toolbox           |
|  \\    /   O peration     | Version:  2.4.0                                 |
|   \\  /    A nd           | Web:      www.OpenFOAM.org                      |
|    \\/     M anipulation  |                                                 |
\*---------------------------------------------------------------------------*/
FoamFile
{
    version     2.0;
    format      ascii;
    class       dictionary;
    location    "system";
    object      fvSolution;
}
// * * * * * * * * * * * * * * * * * * * * * * * * * * * * * * * * * * * * * //
solvers
{
    alpha.water
    {
        nAlphaCorr      1;
        nAlphaSubCycles 3;
        cAlpha          1.5;
    }
    pcorr
    {
        solver          PCG;
        preconditioner
        {
            preconditioner  GAMG;
            tolerance       1e-05;
            relTol          0;
            smoother        DICGaussSeidel;
            nPreSweeps      0;
            nPostSweeps     2;
            nFinestSweeps   2;
            cacheAgglomeration false;
            nCellsInCoarsestLevel 10;
            agglomerator    faceAreaPair;
            mergeLevels     1;
        }
        tolerance       1e-05;
        relTol          0;
```

```
    maxIter         100;
}
p_rgh
{
    solver          GAMG;
```

FILE : fvSolution (2/3)

```
    tolerance       1e-08;
    relTol          0.01;
    smoother        DIC;
    nPreSweeps      0;
    nPostSweeps     2;
    nFinestSweeps   2;
    cacheAgglomeration true;
    nCellsInCoarsestLevel 10;
    agglomerator    faceAreaPair;
    mergeLevels     1;
}
p_rghFinal
{
    solver          PCG;
    preconditioner
    {
        preconditioner  GAMG;
        tolerance       2e-09;
        relTol          0;
        nVcycles        2;
        smoother        DICGaussSeidel;
        nPreSweeps      2;
        nPostSweeps     2;
        nFinestSweeps   2;
        cacheAgglomeration true;
        nCellsInCoarsestLevel 10;
        agglomerator    faceAreaPair;
        mergeLevels     1;
    }
    tolerance       2e-09;
    relTol          0;
    maxIter         20;
}

U
{
```

```
        solver          smoothSolver;
        smoother        GaussSeidel;
        tolerance       1e-06;
        relTol          0;
        nSweeps         1;
    }
}

PIMPLE
{
    momentumPredictor no;
```

FILE : fvSolution (3/3)

```
    nCorrectors     2;
    nNonOrthogonalCorrectors 0;
    correctPhi      no;
    pRefPoint       (0 0 0.15);
    pRefValue       1e5;
}
relaxationFactors
{
    fields
    {
    }
    equations
    {
        "U.*"           1;
    }
}
// ************************************************************************* //
```

FILE : setFieldsDict

```
/*--------------------------------*- C++ -*----------------------------------*\
| =========                 |                                                 |
| \\      /  F ield         | OpenFOAM: The Open Source CFD Toolbox           |
|  \\    /   O peration     | Version:  2.4.0                                 |
|   \\  /    A nd           | Web:      www.OpenFOAM.org                      |
|    \\/     M anipulation  |                                                 |
\*---------------------------------------------------------------------------*/
FoamFile
{
    version     2.0;
    format      ascii;
    class       dictionary;
    location    "system";
    object      setFieldsDict;
}
// * * * * * * * * * * * * * * * * * * * * * * * * * * * * * * * * * * * * * * * //

defaultFieldValues
(
    volScalarFieldValue alpha.water 0
);

regions
(
    boxToCell
    {
        box ( -100 -100 -100 ) ( 100 100 0 );
        fieldValues
        (
            volScalarFieldValue alpha.water 1
        );
    }
);


// ************************************************************************* //
```

FILE : log.blockMesh (1/2)

```
/*---------------------------------------------------------------------------*\
| =========                 |                                                 |
| \\      /  F ield         | OpenFOAM: The Open Source CFD Toolbox           |
|  \\    /   O peration     | Version:  2.4.0                                 |
|   \\  /    A nd           | Web:      www.OpenFOAM.org                      |
|    \\/     M anipulation  |                                                 |
\*---------------------------------------------------------------------------*/
Build  : 2.4.0-f0842aea0e77
Exec   : blockMesh
Date   : Jun 12 2015
Time   : 14:16:00
Host   : "adel-Inspiron-3847"
PID    : 7054
Case   : /home/adel/Desktop/SloshingTank5T=0.81s
nProcs : 1
sigFpe : Enabling floating point exception trapping (FOAM_SIGFPE).
fileModificationChecking : Monitoring run-time modified files using timeStampMaster
allowSystemOperations : Allowing user-supplied system call operations

// * * * * * * * * * * * * * * * * * * * * * * * * * * * * * * * * * * * * * * * * * * * * //
Create time
Creating block mesh from

"/home/adel/Desktop/SloshingTank5T=0.81s/sloshingTankiman/constant/polyMesh/blockMesh
Dict"
No nonlinear edges defined
Creating topology blocks
Creating topology patches
Reading patches section
Creating block mesh topology
Reading physicalType from existing boundary file
Default patch type set to empty
Check topology
        Basic statistics
                Number of internal faces : 2
                Number of boundary faces : 14
                Number of defined boundary faces : 14
                Number of undefined boundary faces : 0
        Checking patch -> block consistency
Creating block offsets
Creating merge list.
```

FILE : log.blockMesh (2/2)

```
Creating polyMesh from blockMesh
Creating patches
Creating cells
Creating points with scale 0.01
    Block 0 cell size :
        i : 0.0120571.. 0.0120571
        j : 0.01.. 0.01
        k : 0.0120571.. 0.0120571

    Block 1 cell size :
        i : 0.0120571.. 0.0120571
        j : 0.0128571.. 0.0128571
        k : 0.0120571.. 0.0120571

    Block 2 cell size :
        i : 0.0120571.. 0.0120571
        j : 0.01.. 0.01
        k : 0.0120571.. 0.0120571

There are no merge patch pairs edges

Writing polyMesh
----------------
Mesh Information
----------------
  boundingBox: (-0.211 -0.211 -0.15) (0.211 0.211 0.32)
  nPoints: 49248
  nCells: 45325
  nFaces: 139790
  nInternalFaces: 132160
----------------
Patches
----------------
  patch 0 (start: 132160 size: 7630) name: walls

End
```